Dissertation

submitted to the
Combined Faculty for the Natural Sciences and Mathematics
of the Ruperto Carola University Heidelberg, Germany
for the degree of

Doctor of Natural Sciences

Presented by

M.Sc. Karol Andrea Granados Blanco

born in: San Jose, Costa Rica

Oral examination: 05.12.2019

Partial reprogramming - a model for melanoma targeted therapy resistance

Referees: Prof. Dr. Viktor Umansky

Prof. Dr. Jochen Utikal

Declarations according to § 8 (3) b) and c) of the doctoral degree regulations:

b) I hereby declare that I have written the submitted dissertation myself and, in this process, have used no other sources or materials than those expressly indicated,

c) I hereby declare that I have not applied to be examined at any other institution, nor have I used the dissertation in this or any other form at any other institution as an examination paper, nor submitted it to any other faculty as a dissertation.

Heidelberg, 19.09.2019

(Karol Andrea Granados Blanco)

This Thesis is dedicated to my parents and my sisters,
for all their unconditional love and support.

Parts of this thesis have been published in:

Conferences and workshop presentations

- Karol Granados, Laura Hüser, Sachindra Sachindra, Aniello Federico, Viktor Umansky, Jochen Utikal. Poster presentation: “Partial reprogramming – a model for melanoma targeted therapy resistance” Summer School in translational cancer research, June 2017, Albufeira, Portugal.

- Karol Granados, Laura Hüser, Sachindra Sachindra, Aniello Federico, Viktor Umansky, Jochen Utikal. Poster presentation: “Partial reprogramming – a model for melanoma targeted therapy resistance” Hallmarks of Skin Cancer Conference, November 2017, Heidelberg, Germany.

- Karol Granados, Laura Hüser, Sachindra Sachindra, Aniello Federico, Gretchen Wolff, Viktor Umansky, Jochen Utikal. Poster presentation: “Partial reprogramming of melanoma cells confers drug resistance and increased vulnerability to channel antagonists” DKFZ PhD poster presentation, November 2018, Heidelberg, Germany.

- Karol Granados, Laura Hüser, Sachindra Sachindra, Aniello Federico, Gretchen Wolff, Viktor Umansky, Jochen Utikal. Poster presentation: “Partial reprogramming of melanoma cells confers drug resistance and increased vulnerability to calcium channel antagonists” 1st German Cancer Research Congress (GCRC), February 2019, Heidelberg, Germany.

- Karol Granados, Laura Hüser, Sachindra Sachindra, Aniello Federico, Gretchen Wolff, Viktor Umansky, Jochen Utikal. Poster presentation: “Partial reprogramming of melanoma cells confers drug resistance and increased vulnerability to channel antagonists” AACR Annual meeting 2019, April 2019, Atlanta, Georgia, USA.

Within the thesis, works from the following publications were included:

Karol Granados, Laura Hüser, Aniello Federico, Sachindra Sachindra, Gretchen Wolff, Thomas Hielscher, Daniel Novak, Verónica Madrigal-Gamboa, Qian Sun, Marlene Vierthaler, Lionel Larribère, Viktor Umansky, Jochen Utikal. T-type calcium channel inhibition restores sensitivity to MAPK inhibitors in dedifferentiated and resistant melanoma cells. Manuscript under review.

Table of Contents

Abstract

Background: Understanding the development of resistance to treatments remains as one of the major challenges in melanoma therapy. It is well known that tumor cells undergo phenotype switching during melanoma progression, increasing plasticity and resistance to mitogen-activated protein kinase inhibitors (MAPKi). Therefore, studying melanoma phenotype switching could reveal new targets that could be used to overcome therapy resistance. **Methods:** A model of partial reprogramming was established to susceptibility of dedifferentiated melanoma cells to treatment with MAPKi in order to find new targets to overcome the resistance to MAPKi. **Results:** The results of this study show that partially reprogrammed C790 and 4434 cells were less proliferative, more invasive and more dedifferentiated cell population, expressing a gene signature associated with stemness and suppressing melanocyte-specific markers. To investigate the development of resistance to MAPKi, murine and human melanoma cells were exposed to BRAF and MEK inhibitors. Dedifferentiated cells were less sensitive to MAPKi, indicated by increased cell viability and decreased apoptosis. Furthermore, T-type calcium channels were overexpressed in partially reprogrammed C790 and 4434 cells, as well as in human adaptive resistant melanoma cells. Treatment with the calcium channel blocker mibefradil induced cell death, differentiation and susceptibility to MAPKi *in vitro* and *in vivo* in human adaptive resistant melanoma cells. **Conclusions:** The results of this study indicate that partial reprogramming represents an innovative model to study melanoma progression and the development of resistance to MAPKi. Moreover, the use of a calcium channel antagonist, such as mibefradil, enhances the effect of MAPKi, by restoring the sensitivity of resistant melanoma cells.

Zusammenfassung

Hintergrund: Die Aufklärung der Mechanismen, die eine Entwicklung von Resistenzen gegen gängige Behandlungen bewirken, bleibt eine der größten Herausforderungen der Melanomtherapie. Es ist bekannt, dass Tumorzellen während der Melanomprogression einen phänotypischen Wechsel durchlaufen, welcher ihre Plastizität und auch die Resistenz gegen Mitogen-aktivierte Protein Kinase Inhibitoren (MAPKi) erhöht. Die Erforschung des Phänotypwechsels bei Melanomzellen könnte somit neue Angriffspunkte enthüllen, welche dazu genutzt werden könnten, um Resistenzmechanismen zu überwinden. **Methoden:** Ein Modell für partielle Reprogrammierung wurde entwickelt, um die Sensitivität von Melanomzellen mit unterschiedlichen Differenzierungszuständen gegenüber MAPKi-Behandlung zu untersuchen, um damit neue Ziele zur Überwindung von MAPKi-Resistenz zu finden. **Ergebnisse:** Die Ergebnisse dieser Untersuchung haben gezeigt, dass partiell reprogrammierte C790- und 4434-Zellen weniger proliferativ und invasiv sowie stärker dedifferenziert sind, als die parentalen Zellen. Sie weisen eine stammzellspezifische Gensignatur auf und exprimieren keine melanozytenspezifischen Marker mehr. Um die Resistenzentwicklung gegen MAPKi zu untersuchen, wurden murine und humane Melanomzellen BRAF- und MEK-Inhibitoren ausgesetzt. Dedifferenzierte Zellen waren weniger empfindlich gegenüber MAPKi, was sich in erhöhter Viabilität und verringerter Apoptose äußerte. Darüber hinaus wurden T-Typ Kalziumkanäle in partiell reprogrammierten C790- und 4434-Zellen sowie in humanen adaptiv resistenten Melanomzellen überexprimiert. Die Behandlung mit dem Kalziumkanalblocker Mibefradil induzierte in humanen adaptiv resistenten Melanomzellen den Zelltod, Differenzierung und die Empfindlichkeit gegenüber MAPKi *in vitro* und *in vivo*. **Fazit:** Die Ergebnisse dieser Untersuchung zeigen, dass partielle Reprogrammierung ein innovatives Model zur Untersuchung von Melanomprogression und Resistenzentwicklung gegen MAPKi darstellt. Darüber hinaus wird durch die Verwendung eines Kalziumkanal-Antagonisten wie Mibefradil die Wirkung von MAPKi verstärkt, indem die Empfindlichkeit von resistenten Melanomzellen wiederhergestellt wird.

List of Figures

List of Supplementary Figures

List of Supplementary Tables

Abbreviations

%	percentage
°C	degree Celsius
µM	micromolar
18S	18S ribosomal RNA
ACT	adoptive cell therapy
AIRD2	AT-rich interactive domain 2
AKT	v-akt murine thymoma viral oncogene
ANOVA	analysis of variance
ATCC	American type culture collection
AXL	AXL Receptor Tyrosine Kinase
B7-1	Activation B7-1 Antigen
B7-2	Activation B7-2 Antigen
BRAF	B-Raf Proto-Oncogene, Serine/Threonine Kinase
BRAFi	BRAF inhibitor
BSA	Bovine serum albumin
CACNA1H	Calcium Voltage-Gated Channel Subunit Alpha1 H
CARs	chimeric antigen receptors
CAV3.1	Calcium Voltage-Gated Channel 3.1
CAV3.2	Calcium Voltage-Gated Channel 3.2
CCND1	kinase cyclin-dependent kinase 4 (CDK4)/Cyclin D1
CD27	Surface Glycoprotein Cluster of Differentiation 27
CD28	Surface Glycoprotein Cluster of Differentiation 28
CDK4	cyclin-dependent kinase 4
CDKN2A	Cyclin Dependent Kinase Inhibitor 2
cm	centimeter
CNS	central nervous system
CRAF	C-Raf Proto-Oncogene, Serine/Threonine Kinase
c-Fos	Fos Proto-Oncogene
c-MYC	Proto-Oncogene C-Myc
C02	carbon dioxide
COT	Proto-Oncogene C-Cot
CSC	Cancer stem cells
Ct	cycle threshold
CTLA-4	Cytotoxic T lymphocyte antigen 4
DDX3X	DEAD-Box Helicase 3 X-Linked
DKFZ	Deutsches Krebsforschungszentrum

DMEM	Dulbecco's modified eagle's medium
DMSO	dimethylsulfoxide
DNA	deoxyribonucleic acid
DOX	Doxycycline
E	Glutamic acid
EDTA	ethylenediaminetetraacetic acid
EGFR	Epidermal Growth Factor Receptor
EMT	Epithelial-to-Mesenchymal Transition
ERK	Extracellular Signal Regulated Kinase
ERBB3	v-erb-b2 avian erythroblastic leukemia viral oncogene homolog 3 receptor
ESC	Embryonic stem cells
ESRRB	Estrogen Related Receptor Beta
et al.	et alteri
FC	fold change
FCS	fetal calf serum
FDA	Food and Drug Administration
FOXD3	Forkhead Box D3
GAPDH	Glyceraldehyde 3-phosphate dehydrogenase
GM-CSF	granulocyte macrophage colony-stimulating factor
GTP	Guanosine triphosphate
HGF	hepatocyte growth factor
HRAS	Harvey Ras viral oncogene homolog
HRP	Horseradish peroxidase
HOXD8	Homeobox D8
ID1	Inhibitor of DNA Binding 1
ID3	Inhibitor of DNA Binding 3
IDH1	Isocitrate Dehydrogenase (NADP (+)) 1
IDO	Indoleamine 2,3-Dioxygenase 1
IC50	half maximal inhibitory concentration
IEG	intermediated early genes
IL-2	Interleukin 2
IL-10	Interleukin 10
INF- α	Interferon alpha
iPSC	Induced pluripotent stem cells
iPCCs	Induced pluripotent cancer cells
IPA	Ingenuity pathway analysis

K	Lysine
KD	knockdown
kDa	kiloDalton
KIT	tyrosine protein kinase kit
KLF4	Kruppel Like Factor 4
KRAS	Kirsten Ras viral oncogene homolog
LB	Lysogeny broth
Lin28	Lin-28 Homolog A
log	logarithm
log2	binary logarithm
LNGFR	low-affinity nerve growth factor receptor
Lys	Lysine
M	molar
mm	millimeters
MAPK	Mitogen-activated protein kinase
MAPKi	MAPK inhibitor
MAP2K1	Dual specificity mitogen-Activated Protein Kinase Kinase 1
MEF	Mouse Embryonic Fibroblasts
MEK	Mitogen Activated Protein Kinase
MEKi	MEK inhibitor
mibe	Mibefradil
MDM2	murine-double-minute− 2
MHC	major histocompatibility complex
min	minutes
MITF	Microphthalmia-Associated Transcription Factor
ml	milliliter
MLANA	melan-A
mRNA	messenger Ribonucleic Acid
mTOR	Mechanistic Target of Rapamycin Kinase
MYOD1	Myogenic Differentiation 1
g	grams
NANOG	Nanog Homeobox
NEAA	non-essential amino acids
NF1	neurofibromin 1
NFkB	Nuclear Factor Kappa B Subunit 1
ng	nanogram
nM	nanomolar

NOD/SCID	Nonobese Diabetic/Severe Combined Immunodeficient
NRAS	Neuroblastoma RAS Viral Oncogene Homolog
ns	non-significant
Oct4	Octamer-Binding Protein 4
OS	overall survival
p	p value
PBS	phosphate buffered saline
PCR	polymerase chain reaction
PDGFR	platelet derived growth factor receptor
PDK1	3-phosphoinositide-dependent kinase 1
PD-1	Programmed death 1
PD-L1	PD-ligand 1
PFA	paraformaldehyde
PFS	progression-free survival
PH	pleckstrin homology
PI3K	Phosphatidylinositol-4,5-bisphospahte 3-kinase
PIP2	Phosphatidylinositol bi-phosphate
PIP3	Phosphatidylinositol tri-phosphate
PKA	Protein kinase A
PMEL	pre-melanosomal protein
POU5F1	POU Class 5 Homeobox 1
PP	Protein phosphatases
PPP6C	Protein Phosphatase 6 Catalytic Subunit
PTEN	Phosphatase and tensin homolog
PVDF	polyvinylidenfluorid
qPCR	quantitative real-time polymerase chain reaction
RAC1	Rac Family Small GTPase 1
RAF	Rat fibrosarcoma
RAS	Rat sarcoma
RB1	Retinoblastoma1
RFU	relative fluorescence unit
RIPA	radioimmunoprecipitation assay buffer
RNA	ribonucleic acid
rpm	revolutions per minute
RSK	ribosomal S6 kinase
RT	room temperature
RTK	Receptor tyrosine kinase

S	Serine
S2	Biosafety level 2 laboratory
SALL4	Spalt Like Transcription Factor 4
SCG2	Secretogranin 2
SDS	sodium dodecyl sulfate
shRNA	short hairpin RNA
SNX31	Sorting Nexin 31
SOX	SRY (sex determining region Y)-box
SOX2	SRY-Box 2
Ssea-1	Stage specific embryonic antigen 1
STK19	Serine/Threonine Kinase 19
T	Threonin
TACC1	Transforming Acidic Coiled-Coil Containing Protein 1
TCF	ternary complex factor
TCGA	The Cancer Genome Atlas
TCR	T cell receptor
TERT	telomerase reverse transcriptase
TF	transcription factor
TILs	tumor-infiltrating lymphocytes
TP53	Tumor protein p53
Tra	trametinib
TRP1	Tyrosinase-related protein 1
TRP2	Tyrosinase-related protein 2
T-VEC	talimogen laherparepvec
TYR	Tyrosinase
UV	ultraviolet radiation
V	Valine
Vem	vemurafenib
VS	versus
WB	Western Blot
WNT	Wingless/Integrated
WT	wild type
µg	microgram
µl	microliter

1. Introduction

Malignant melanoma is an aggressive type of skin cancer with survival rates and treatments that vary depending on tumor stages. While early stages have a good prognosis, unresectable stage III and IV melanomas are often fatal and therapy resistance is a major challenge. Around 50% of melanoma patients carry mutations in the BRAF gene and around 30% of patients in the NRAS gene resulting in an aberrant activation of the mitogen-activated protein kinase (MAPK) pathway[1], making this signaling cascade one of the most important targets for melanoma therapy[2,3].

The clinical use of BRAF inhibitors (vemurafenib, dabrafenib, encorafenib), MEK inhibitors (trametinib, cobimetinib, binimetinib) or their combinations significantly increases progression-free (PFS) and overall survival (OS) of patients[4]. Unfortunately, most patients develop resistance to these inhibitors soon after the start of the therapy[5,6] because of different factors including tumor heterogeneity and plasticity[7].

The high cellular heterogeneity of melanomas is partially due to a degree of phenotypic plasticity. Melanoma cells switch between proliferative/differentiated and invasive/dedifferentiated phenotypes during metastasis progression, mimicking the epithelial-to-mesenchymal transition, which facilitates invasion to secondary tumor sites[8–10]. Indeed, induction of phenotype switching towards a dedifferentiated state is likely one of the most common mechanisms underlying the development of resistance to therapies in melanoma patients[9].

Drug resistance in melanoma has been classified as intrinsic, adaptive or acquired, depending on whether the resistance is present already before treatment or it develops either shortly or longer time upon beginning of treatment[2,11]. Several mechanisms have been reported to promote resistance in melanoma. These include reactivation of extracellular-signal regulated kinase (ERK) signaling or activation of alternative pathways[2,5].In this study, partial reprogramming of melanoma cells was used[12] to investigate the connection between de-differentiation and development of therapy resistance.

1.1 General aspects of melanoma

1.1.1 Causes, incidence and Mortality

Melanoma is a type of skin cancer that arises from melanin-producing cells called melanocytes. The primary cause of melanoma is the ultraviolet (UV) radiation from the sun or other sources[13], but also age, gender and family history are risk factors[14,15]. Melanoma not only emerges on skin exposed to sun but also from mucosa or skin that has not been exposed to sunlight. The incidence of melanoma has increased over the last decades and 132.000 new cases are reported each year worldwide. Additionally, it is estimated that 4.500 additional cases occur due to the decrease in ozone levels every year[14,16,17].

The classification of skin cancers includes non-melanoma skin cancers and melanoma. Non-melanoma skin cancers comprise basal cell carcinomas and squamous cells carcinomas. These carcinomas are frequent in body areas commonly exposed to sun, are rarely lethal, easy to treat, and their incidence increases with a decrease in latitude[14].

On the other hand, malignant melanoma is less frequent but is the main cause of deaths from skin cancers. The risk of developing melanoma correlates mainly with genetic characteristics, as well as UV exposure[14,15]. Caucasian populations have a higher risk of non-melanoma and melanoma skin cancers due to their reduced skin pigmentation. Persons with pale or freckled skin, red hair or blue eyes show the highest risk. However, regardless of these characteristics, excessive sun exposure can damage all types of skin[15].

Melanoma causes 9.000 deaths each year in the United States[13] and is the fifth most common cancer in men and the seventh most common in women. Around the world, malignant melanoma is responsible for 75% of all deaths related to skin cancers[15], and survival rates of melanoma patients highly depend on early detection and treatment. If melanoma is detected at an early stage, the prognosis is more favorable in comparison to melanoma that has already metastasized to other parts of the body[14].

1.1.2 Mutations

As mentioned before, most of the melanoma cases are due to a certain degree (low/high) of exposure to UV radiation. UV light causes direct or indirect damage to

DNA of the cells and induce pyrimidine dimers (thymine or cytosine), which disturb the DNA structure and cause mutations during DNA replication or repair processes[18,19]. Mutations in proto-oncogenes (gain-of-function mutation) or tumor suppressor genes (loss-of-function mutations) alter their functions and initiate malignant transformation of normal cells[19].

One of the most common somatic mutation in melanoma occur in the B-raf proto-oncogene serine/threonine kinase (BRAF), particularly the amino acid exchange V600E, where valine (V) at position 600 is substitute with glutamic acid (E). BRAF is critical for regulation of the MAPK signaling that promotes proliferation, differentiation and survival. BRAF mutations are found in approximately 60% of melanomas, from which V600E mutation represents 80%[20] and promotes cancer progression by constitutively activating MAPK signaling (Figure 1). Mutations leading to different substitutions, such as V600K or V600R, are less frequent and represent only 20% and 7% of the BRAF mutations, respectively[20]. Importantly, the BRAF V600E mutation is also present in 80% of non-malignant lesions (benign nevi), suggesting that BRAF mutations alone are not enough to drive carcinogenesis[21].

Among other somatic mutations that have been reported to promote melanoma progression are neurofibromin 1 (NF1), neuroblastoma rat sarcoma viral oncogene homolog (NRAS), tumor protein 53 (TP53), ras-related C3 botulinum toxin substrate 1 (RAC1), phosphatase and tensin homolog (PTEN), tyrosine protein kinase kit (KIT), and cyclin-dependent kinase 4 (CDK4)[21–23](Figure 1).

NRAS belongs to the RAS family of G-regulatory proteins that regulate normal cell growth through the MAPK and PI3K/AKT/mTOR pathway. NRAS mutations at codons 12,13 and 61 constitute the second most common driver mutations in melanoma (20%) and are associated with an increment in tumor aggressiveness and poor prognosis[5,24]. The RAS family also includes two more proto-oncogenes called Harvey Ras viral oncogene homolog (HRAS) and Kirsten Ras viral oncogene homolog (KRAS), but mutations in these genes are rare in melanomas[21].

Although melanomas often harbor several somatic mutations, also familial cases harboring a germline mutation in the cyclin-dependent kinase inhibitor 2A (CDKN2A) gene have been described in caucasian populations [25]. CDKN2A is a tumor suppressor gene that encodes two proteins: $p16^{INK4A}$ and $p14^{ARF}$, both proteins control the cell cycle progression. $p16^{INK4A}$ blocks the cyclin-dependent kinase 4 (CDK4)/Cyclin D1 (CCND1) while $p14^{ARF}$ affects the murine-double-minute− 2 (MDM2) protein,

preventing the degradation of p53[23,25]. Therefore, CDKN2A mutations lead to uncontrolled cell-cycle progression, contributing to melanoma progression. The frequency of CDKN2A mutation is higher in malignant melanoma patients with a family history of melanoma compared to those without[21,25].

Finally, some melanomas also show mutations of the telomerase reverse transcriptase (TERT) promoter, increasing the expression of the enzyme telomerase. As a result, cells are able to evade senescence and keep undergoing cellular division, growing for long periods of time, which is known as cell immortalization[21]. Mutations in the TERT promoter region have been found in melanoma (29%) and in other types of cancer of the central nervous system (43%), the thyroid (10%) and the bladder (59%)[26].

Over the last years, new significant mutations have been discovered in melanomas affecting a plethora of genes: AIRD2, PPP6C, SNX31, TACC1, STK19 MAP2K1, IDH1, RB1 and DDX3X[22,23,27]. The identification of important mutations in melanoma has improved the efficacy of treatments by increasing survival rates in patients. Considering the variety of the genes that are mutated in melanoma, knowing the mutational status of melanoma patients is indeed essential for an appropriate selection of a therapy.

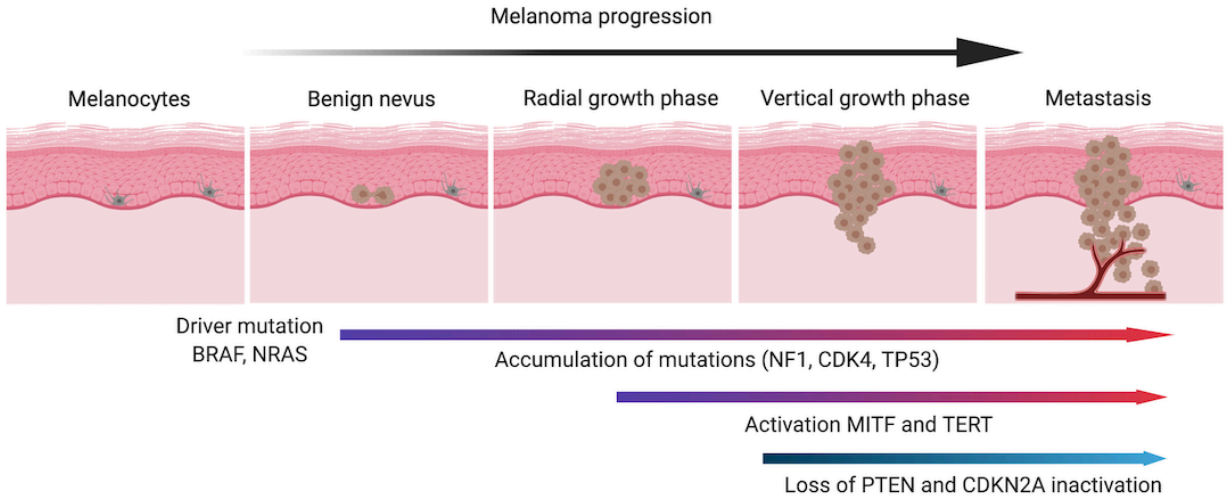

Figure 1. The most frequent genetic alterations during melanoma progression. Initial malignant transformation of melanocytes is driven by mutations on BRAF and NRAS. However, accumulation of additional mutations must occur to support the tumorigenesis (e.g. CDK4, NF1, TP53, PTEN, CDKN2A). Adapted from Vultur & Herlyn 2013, *Cancer Cell* [28].

1.1.3 Deregulated pathways

Under physiological conditions, cell proliferation is tightly controlled and closely connected with apoptosis in order to maintain an appropriated number of healthy cells, eliminate unwanted or damaged cells and with this assure tissue homeostasis. Alterations in either one of these processes usually lead to uncontrolled growth and tumor formation[29].

The MAPK and PI3K/AKT/mTOR pathways regulate cell proliferation, survival, migration, differentiation and metabolism. In cancer, these pathways are constitutively activated and both cascades can interact to promote growth and survival of malignant cells[30,31].

MAPK pathway is activated by growth factors, hormones, chemokines and other molecules, which bind to catalytic receptors like receptor tyrosine kinase (RTK), G protein-coupled receptors, or direct activation of protein kinase C[30]. MAPK signaling initiates with activation of the Ras-family GTPases. Once active, GTP-bound Ras activates a cascade of serine/threonine protein kinases starting with the protein kinase RAF (MAPKKK), which has three isoforms: ARAF, BRAF and CRAF. RAF is responsible for the phosphorylation and activation of the protein kinase MEK1 and MEK2 (MAPKK) which in turn phosphorylate and activate the effector protein kinases ERK1 and ERK2 (MAPK)[29,31] (Figure 2).

ERK constitutes the main protein kinase in this pathway due to its final cellular functions. Activated ERK can phosphorylate cytoplasmic proteins like the ribosomal S6 kinase (RSK), or translocate to the nucleus and phosphorylate transcription factors including the ternary complex factor (TCF) which induce expression of immediate early genes (IEG). The IEG products (c-MYC, c-Fos) induce expression of late-response genes that promote cell division, motility and cell survival[29–31].

Melanoma like other types of cancer arises from accumulation of mutations that constitutively activate pro-proliferative and pro-survival pathways[30]. Most of the patients carrying BRAF mutations show an over-activation of MAPK signaling, making this pathway one of the most important targets for melanoma therapy. Mutations in components of the PI3K/AKT/mTOR pathway and the tumor suppressor gene PTEN in melanoma have also been reported, but at a lower frequency[5] (Figure 2).

The PI3K/AKT/mTOR pathway is also activated by growth factors that bind to catalytic receptors RTK or can be induced by GTP-bound RAS protein. RTK activation recruits the phosphatidylinositol 3-Kinase (PI3K) heterodimer to the plasma membrane. PI3K

belongs to a family of lipid kinases that phosphorylate specific substrates. PI3K phosphorylates the substrate PIP_2 to produce PIP_3. Importantly, PTEN promotes dephosphorylation of PIP_3 to PIP_2, negatively regulating the PI3K/AKT/mTOR pathway.

PIP_3 recruits and activates proteins with pleckstrin homology (PH) domains, among the proteins containing PH domains are the AKT and 3-phosphoinositide-dependent kinase 1 (PDK1). AKT kinase is recruited to the plasma membrane by PIP_3 and then activated by PDK1. Once active, AKT can phosphorylate different proteins to activate (mTOR, NFkB, MDM2) or inactivate (IKKα or pro-apoptotic proteins) them, in order to promote cellular survival[29,30].

There is evidence that the MAPK and PI3K/AKT/mTOR pathways are interconnected by different mechanisms of cross-activation, cross-inhibition and convergence[31]. For instance, ERK can inactivate mTOR complex 1 and 2 by dissociation of their dimers, impairing the role of mTOR complex 2 to inhibit mTOR signaling[30]. Inhibition of one of these pathways often leads to the activation of the other signaling cascade, therefore, blockage of both pathways is considered as a good strategy to eliminate cancer cells[29].

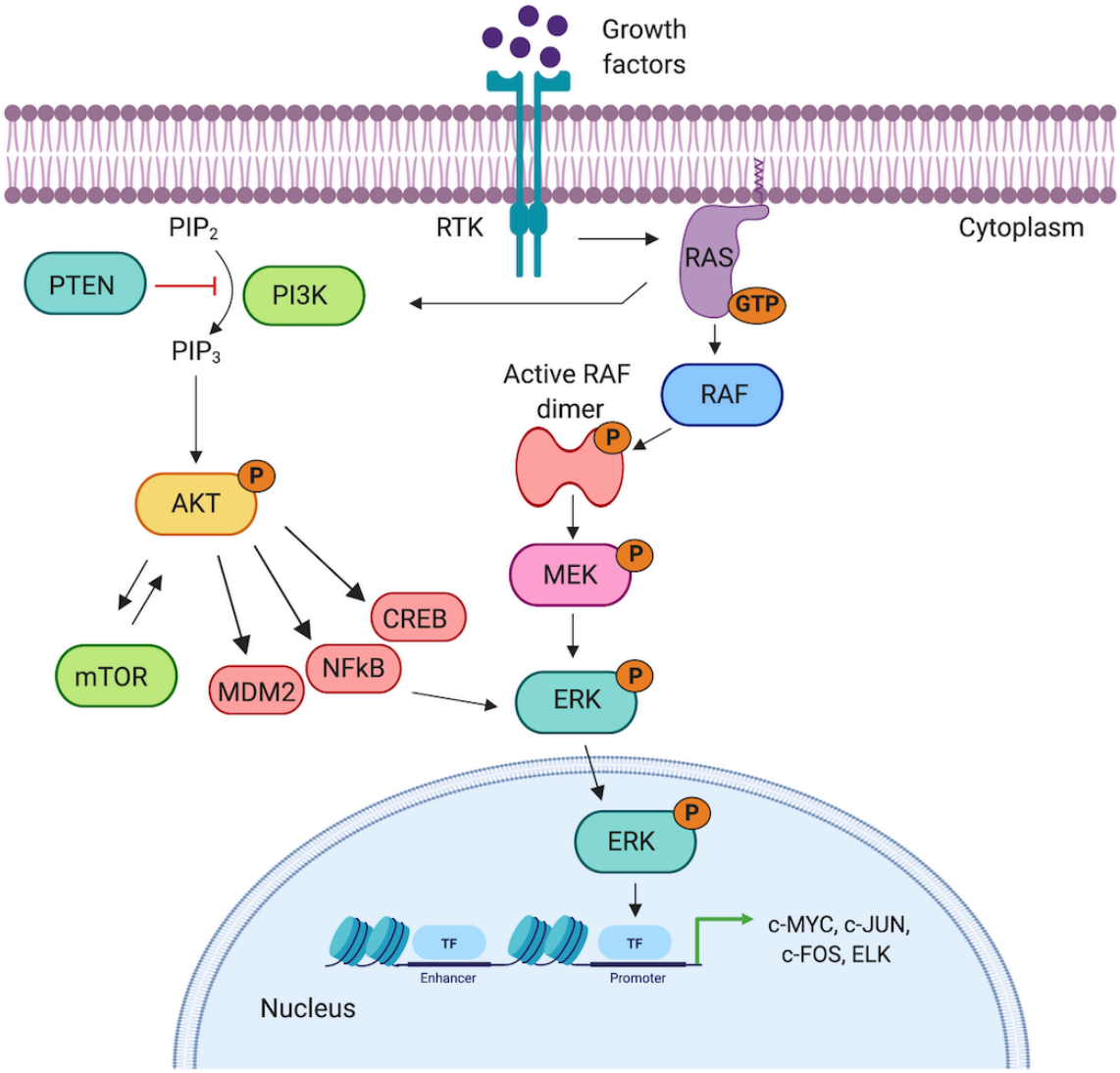

Figure 2. Most common deregulated pathways in melanoma. Extracellular signals like growth factors can lead to activation of MAPK and PI3K/AKT/mTOR pathways through membrane receptors RTK. RTK phosphorylate Ras protein, which initiates the activation of the cascade of kinases RAF, MEK and ERK. Ras protein can also activate PI3K that transforms PIP_2 to PIP_3, activating AKT kinase. AKT has several targets like mTOR, MDM2 and NFkB. Activation of these pathways induces transcription of specific genes that increase cell proliferation and survival. Adapted from Vultur & Herlyn 2013, *Cancer Cell* [28].

1.1.4 Phenotype switching

Melanoma is a tumor with high heterogeneity that shows phenotypic plasticity as a consequence of genetic mutations, micro environmental signals, and reversible epigenetic changes[32]. Melanoma cells can switch between proliferative/differentiated

and invasive/dedifferentiated phenotypes during metastasis progression, in a similar way to epithelial-to-mesenchymal transition (EMT), which facilitates dissemination from a primary tumor to distant sites through the transition into an invasive phenotype[8–10]. Besides cell-intrinsic proliferation and migration factors, tumor micro environmental conditions such as hypoxia[32–34] and inflammatory signals can also promote melanoma phenotype switching (Figure 3).

In order to induce the switch between proliferative and invasive phenotypes different cellular events must occur. For instance, invasive capacity of BRAF mutant melanoma cells has been associated with a switch in expression of cadherin proteins[35]. During metastasis, there is a progressive loss of E-cadherin and an increase in levels of N-cadherin. This switch from E-cadherin to N-cadherin promotes survival and migration of melanoma cells[9,32,35]. In addition, Bettum and collaborators (2015) demonstrated that the transformation into the invasive phenotype in melanoma facilitates de-differentiation and a metabolic switch from mitochondrial oxidation to glycolysis, which is beneficial for survival and growth of cancer cells during phenotypic transition.

Regardless, the central factor involved in melanoma phenotype switching is the microphthalmia-associated transcription factor (MITF), which regulates the expression of melanocyte differentiation and pigmentation genes and is responsible for reversible and functional reprogramming of signaling pathways in melanoma[36,37]. MITF is a lineage-specific oncogene highly expressed in human melanomas that contributes to tumorigenesis[38,39].

Goding and collaborators (2011) proposed that the level of MITF activity correlates to the phenotype switching in melanoma tumor cells. According to the “MITF rheostat” model, a high level of MITF activity promotes differentiation, mid-level activity promotes proliferation, and low-level activity promotes an invasive, stem cell-like phenotype, and the absence of MITF activity causes senescence or cell death[40] (Figure 3).

Moreover, reduction of MITF expression in melanoma cells has been related to increased plasticity and therapy resistance, supporting that induction of phenotypic switching toward a more dedifferentiated state drastically determines the aggressiveness of the tumor and constitutes an important mechanism underlying the development of resistance to therapies in melanoma patients[41–43].

In addition, expression of MITF and other genes involved in phenotype switching and metastasis permits to discriminate between BRAFi-sensitive and BRAFi-resistant melanoma cells, based on their RNA expression signatures. Sensitive melanoma cells

show high activity of MITF and downstream differentiation markers including tyrosinase-related protein1 (TYRP1), melan-A (MLANA) and pre-melanosomal protein (PMEL), whereas resistant cells show low MITF activity but high expression of NFkB, Wnt5 and the receptor tyrosine kinase AXL[36,39,44]. Furthermore, expression of MITF and AXL has been reported in several melanoma cells and the ratio MITF/AXL has been used to describe early resistance in melanoma[44].

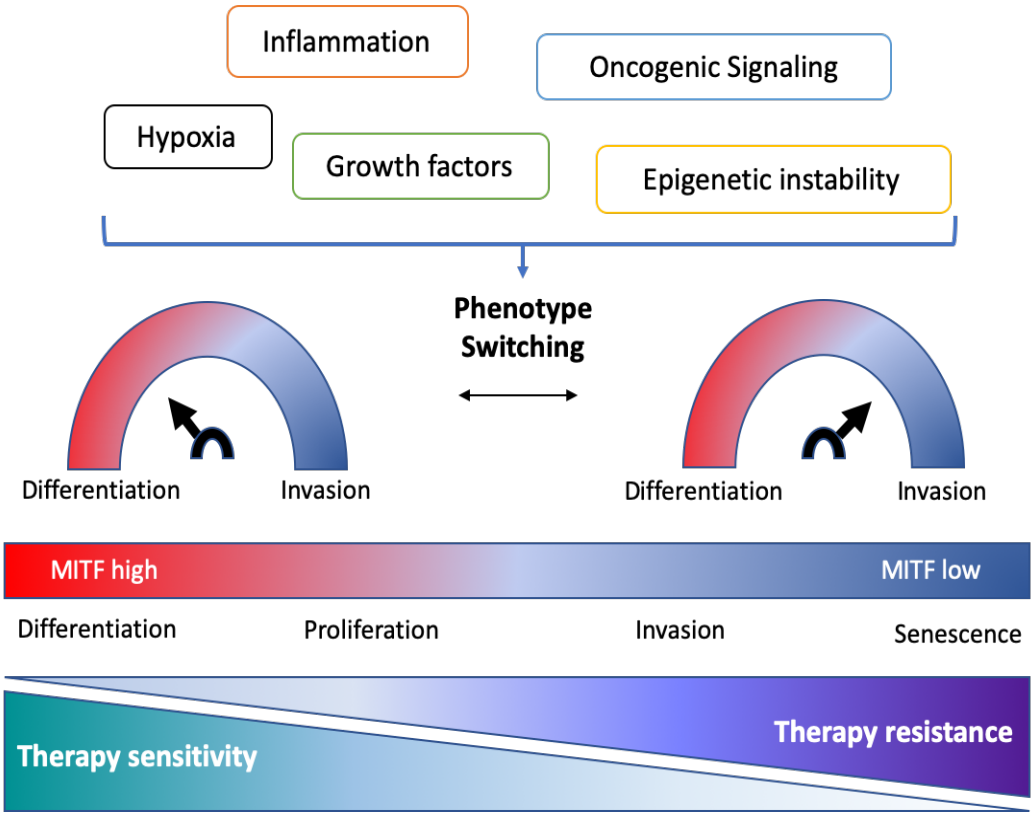

Figure 3. Characteristics of phenotype switching in melanoma. There are several factors that promote phenotype switching, including hypoxia, growth factors, epigenetic changes, and others. Melanoma cells can switch between a proliferative and an invasive phenotype, inducing a more dedifferentiated status and poor response to treatments. MITF is the main factor that drives melanoma phenotype switching and its expression correlates with each specific phenotype and the therapy response. Adapted from Vandame & Berx 2014, *Frontiers in Oncology* [8].

1.2 Treatments for melanoma

1.2.1 Surgery and chemotherapy

Current therapeutic options for melanoma patients involve surgical excision, chemotherapy, immunotherapy and targeted therapy (Figure 4). Generally, surgery is one of the first options for patients at early and intermediate-stages of the disease, with high rate of success. However, for patients in stage IV, the main option of treatment consists of systemic therapies including chemotherapy, immunotherapy or combinatorial approaches. Although melanoma is considered to be relatively radioresistant to radiotherapy, it is frequently used for the treatment of patients with metastases in the central nervous system (CNS) due to limited penetration of systemic drugs into the CNS[45].

Regardless of all the latest advances in treatment options, chemotherapy together with high dose interleukin-2 (IL-2) has been extensively used for the treatment of advanced stages of melanoma for several decades. Although chemotherapy is no longer a frontline therapy in advanced-stage melanoma, it still is a suitable treatment for melanomas that do not show somatic mutations that can be targeted with specific inhibitors. In these cases, usually after receiving immunotherapy, the next line of treatment is chemotherapy[46] (Figure 4).

Several chemotherapeutic agents have been used as single-agent chemotherapy or in combination for the treatment of advanced melanoma, including dacarbazine, temozolomide, nitrosoureas (carmustine and lomustine), carboplatin, cisplatin and taxanes (paclitaxel and docetaxel)[46].

Dacarbazine is an alkylating agent that forms DNA adducts, inducing DNA damage and cytotoxic effects in the cells[45]. Dacarbazine was approved by the FDA in 1975 for melanoma treatment and since then is considered the standard chemotherapy for patients with metastatic melanoma. Doses and side effects (nausea and vomiting) of dacarbazine vary but it is tolerated quite well in general.

Another alkylating agent used for treatment of advanced melanoma is temozolomide, an analog of dacarbazine that is also approved for glioblastoma treatment. Temozolomide is administered orally and can cross the blood-brain barrier thus causing headache, nausea and vomiting as main side effects[45]. Studies have shown no differences in the efficacy of temozolomide and dacarbazine, bringing the possibility of using both agents interchangeably[46]. Nitrosoureas are also alkylating agents that

have been used in combination, in most of the cases, for the treatment of advanced melanoma.

The platinum analogs cisplatin and carboplatin are used against several solid tumors. Patients with metastatic melanoma treated with carboplatin have shown a positive but more moderate effect compared to dacarbazine[47]. Finally, taxanes are antimicrotubular agents that affect tubulin polymerization and microtubule formation, resulting in dysfunctional mitotic spindle complexes and cell death. Paclitaxel specifically inhibits the microtubule disassembly and has shown a modest effect as single or in combinatorial treatment in patients with metastatic melanoma, while docetaxel has shown a more potent outcome. Combination of platinum analogs and taxanes have also been tested for treating of advanced stages of melanoma with positive results[46,47].

Additional combinations of chemotherapy along with immunotherapy have been evaluated (biochemotherapy). For instance, combination with interferon alpha (INF-α) and IL-2 have been extensively tested on advanced-stage melanoma patients with response rates between 10-20 % and 15-20 %, respectively. However, severe toxicity is usually observed in this biochemotherapy regimen and the results are not translated into an OS benefit. Therefore, this approach is not considered anymore as a standard treatment for patients with advanced melanoma[46].

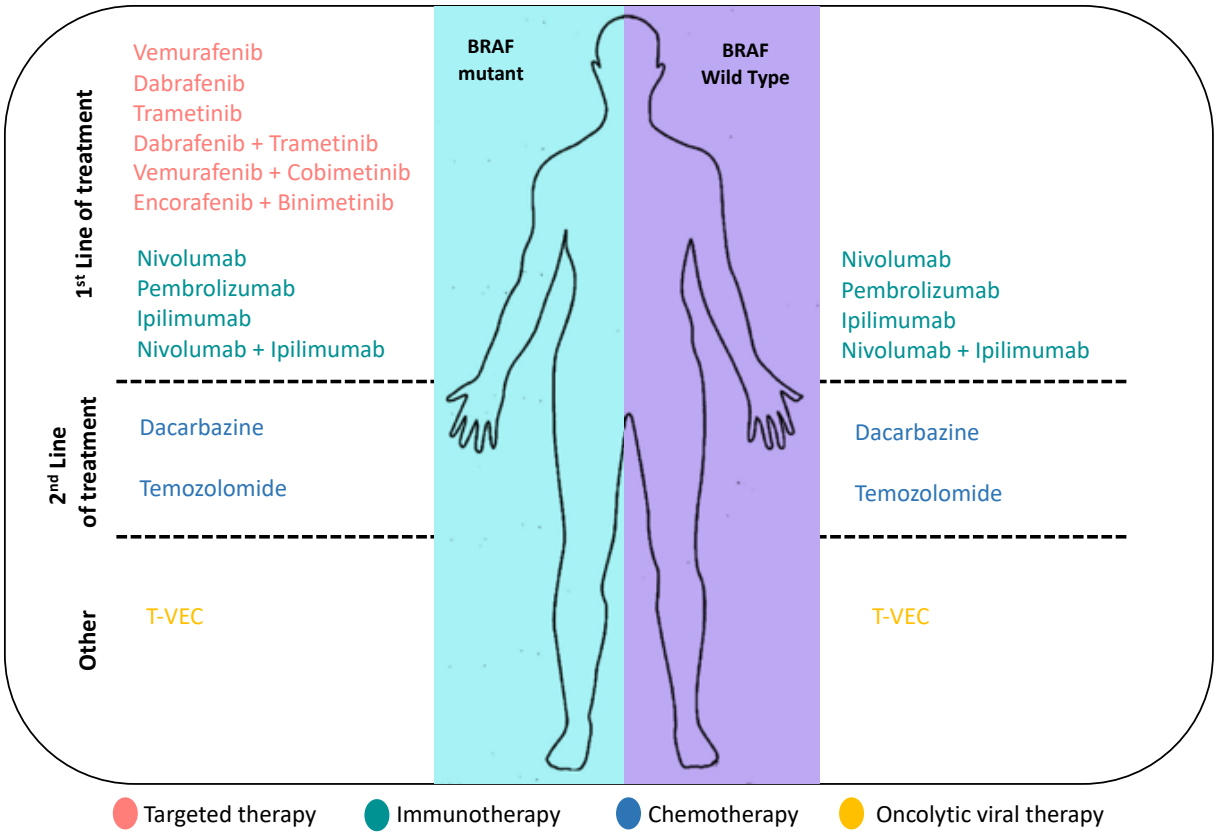

Figure 4. Current systemic treatments approved for patients with unresectable metastatic melanoma. First line of treatment varies depending on the mutation status of the patient and how fast the disease progresses. Patients with BRAF-mutant melanoma receive targeted therapies or immunotherapies as first line of treatment, because immunotherapy may take longer, BRAFi monotherapy or the combination with MEKi is preferred. If there is no response, patients then can receive immunotherapies as second line of treatment. Patients with BRAF-wild type tumors receive immunotherapies as first line of treatment. Moreover, chemotherapy is also administered as a second line of treatments and some cases can be treated locally using oncolytic virus-based therapy. Adapted from Kozar *et al* 2019, *Reviews on Cancer* [48].

1.2.2 Targeted therapy

Targeted therapy specifically eliminates cancer cells that harbor targets that are exclusively expressed by these cells. Since BRAF mutations were described as the most frequent mutations in melanoma, development of BRAF inhibitors (BRAFi) and MAPK inhibitors (MAPKi) has increased (Figure 5).

Inhibitors of RAF protein include type I inhibitors that selectively inhibit the activated RAF kinase, like vemurafenib and dabrafenib, and the type II inhibitors, which inhibit

the resting RAF protein, like sorafenib. Although melanoma cells carrying BRAF mutations are sensitive to both types of inhibitors, type I inhibitors have demonstrated better results compared to type II inhibitors in the treatment of BRAF-mutant metastatic melanoma [46].

During initial trials in 2010, targeted therapy generated significant results in several patients with metastatic melanoma, producing a partial or complete tumor regression. Vemurafenib was the first FDA-approved BRAF V600E inhibitor and improved OS (6 months survival rate, 84% vs 64%) and PFS (5.3 vs 1.6 months) compared to the traditional chemotherapy with dacarbazine[49]. Unfortunately, long-term follow-up studies reported limited OS up to 16 months among patients treated with vemurafenib monotherapy.

Importantly, not all BRAF-mutant patients respond to inhibition with vemurafenib or dabrafenib and usually resistance to these monotherapies appears in most patients, a few months later[46]. In addition, treatment of melanoma cells with wild-type BRAF with RAF inhibitors leads to a paradoxical increase of the MAPK pathway and ERK activity. This because the inhibition of BRAF in these wild type BRAF cells enhances signaling through CRAF and as a result the pathway remains activated[50].

Due to the constant MAPK pathway activation, even after development of resistance to BRAF inhibitors, several clinical trials have evaluated MEKi alone or in combination with type I RAF inhibitors. MEK inhibitors inhibits the kinases MEK1 and MEK2 of the MAPK pathway and have been used for treatment in some cancers, especially BRAF-mutant melanoma[51] (Figure 5).

In 2013, the FDA approved the use of trametinib for the treatment of BRAF-mutant melanoma, after results of clinical trials that evaluated the efficacy of trametinib monotherapy showed a significantly increased 6-month OS rate (81% vs 61%) compared to chemotherapy[51].

Moreover, the combination of BRAFi (dabrafenib) and MEKi (trametinib) for treating BRAF-mutant metastatic melanoma has shown an improvement of PFS (9.4 vs 4.8 months), OS and the rate of partial or complete response (76% vs 54%) compared to dabrafenib monotherapy[52]. In addition, combination of vemurafenib with the MEKi cobimetinib significantly increased the PFS compared to vemurafenib monotherapy plus placebo (9.9 vs 6.2 months)[53,54].

Furthermore, preclinical studies on NRAS-mutant melanomas demonstrated that these tumors are relatively insensitive to vemurafenib treatment. However, according to a

phase II study that reported 20% of partial response, the treatment with MEKi binimetinib may be effective against NRAS-mutant melanomas. Additionally, new MEK inhibitors are under clinical investigation as single treatments or in combination, including TAK733 and selumetinib for advanced metastatic melanoma[46].

Finally, as mentioned before, PIK3/AKT/mTOR signaling is an important pathway that drives tumorigenesis and resistance in melanoma. Preclinical studies have reported the utility of inhibition of PIK3/AKT/mTOR in melanomas with resistance to vemurafenib and dabrafenib[55,56]. However, clinical trials using combination of these inhibitors are still ongoing and involve c-Kit inhibitors (sunitinib, imatinib, dasatinib) and mTOR inhibitors (temsirolimus and everolimus)[57] (Figure 5).

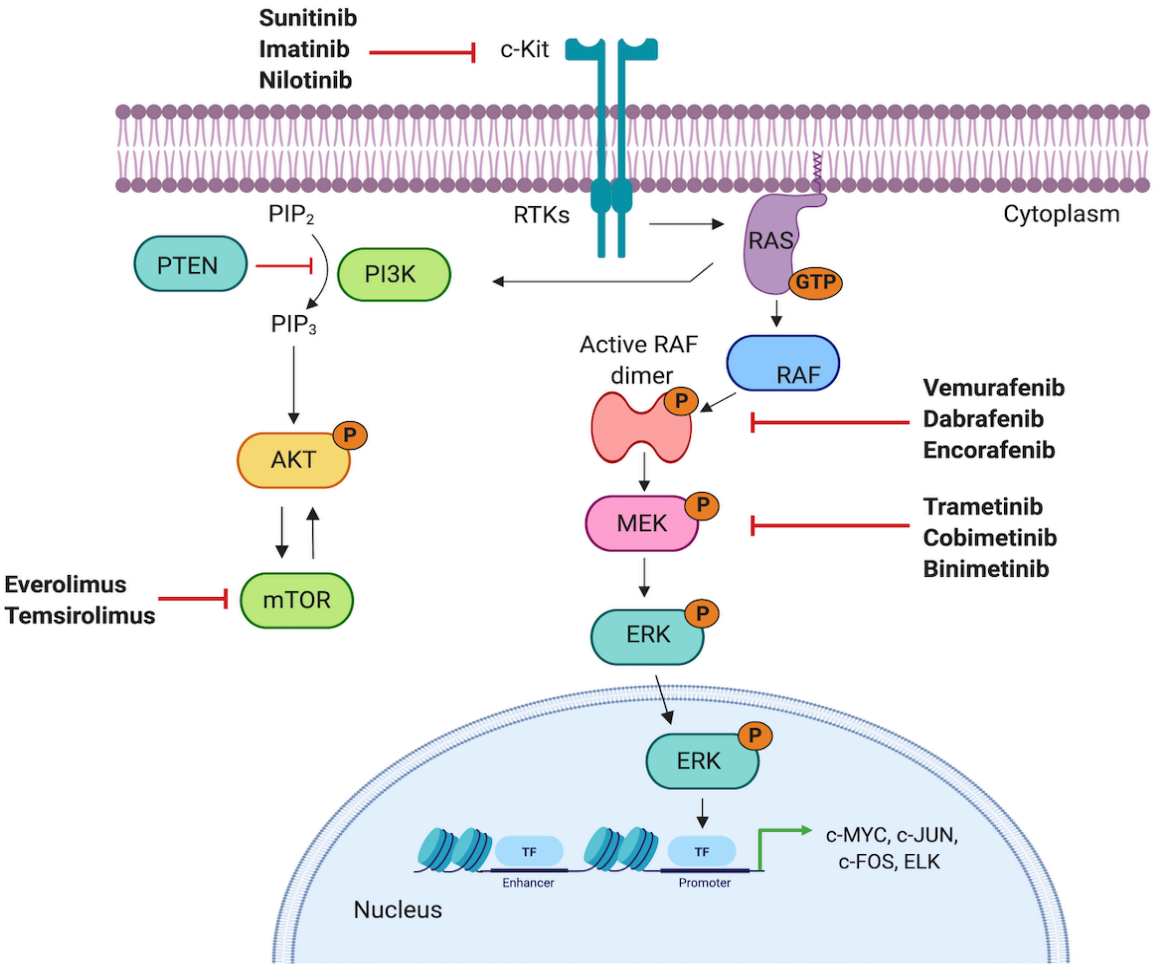

Figure 5. Therapeutic targets in the MAPK and PI3K/AKT/mTOR cascades developed for targeted therapy of melanoma. Several inhibitors have been developed to inhibit the main pathways aberrantly activated in melanoma. BRAF, MEK, mTOR and RTKs are the main therapeutic targets for melanoma treatment. Adapted from Tran *et al* 2016, *Drug design, Development and Therapy*[58] .

1.2.2 Immune checkpoints inhibitors

Long-term survival rates for patients with metastatic melanoma are a very low percentage but, with the latest advances in treatments with immune checkpoints inhibition and targeted therapy, the clinical outcome of the patients has improved.

Tumor cells can escape immune recognition and elimination by selection of clones able to evade the immune system (immunoediting), by downregulating factors that make them vulnerable such as tumor antigens or MHC class I or by activating negative feedback mechanisms that prevent immunopathology. These mechanisms include the secretion of inhibitory cytokines (IL-10), recruiting inhibitory cell types (T-regs, B-regs and MDSC), and producing metabolic modulators (IDO) and inhibitory receptors like PD1 and CTLA-4, also known as immune checkpoint molecules[59].

The FDA-approved immunotherapies for the treatment of metastatic melanomas including the cytotoxic T lymphocyte-associated antigen (CTLA-4) antibody called ipilimumab, and the programmed cell death 1 (PD-1) receptor antibodies called nivolumab or pembrolizumab. These three immune checkpoint inhibitors have been used as first or second line of treatment for advanced melanomas, as single treatment or in combination (nivolumab + ipilimumab) with promising results[60] (Figure 4).

CTLA-4 belongs to the B7/CD28 family and is constitutively expressed on regulatory T cells, contributing to their inhibitory functions. CLTA-4 is also expressed on T lymphocytes upon activation and acts like a negative regulator of T-cell activation. CTLA-4 counteracts positive stimulatory signals by binding to B7-1 and B7-2 receptors and competing with CD28, a co-stimulatory molecule[59]. Due to the inhibitory role of CTLA-4 during T-cell activation, Leach and collaborators (1996) tested the hypothesis that blockage of CTLA-4 could increase immune response against tumor cells. The study showed a rejection of tumor after CTLA-4 administration *in vivo*, supporting that blockage of inhibitory functions of CTLA-4 enhances anti-tumor immune response[61].

CLTA-4 was the first FDA-approved immune checkpoint inhibitor for the treatment of cancer patients. Clinical trials on patients with advanced melanoma patients reported an improvement of OS using ipilimumab (10 months) compared to peptide vaccines (6.4 months)[62]. Moreover, treatment with ipilimumab alone compared to dacarbazine showed an increment in survival (47.3% vs 36.3%) after 1 year of initial treatment[63].

Strategies that block other immune checkpoint molecules have also demonstrated positive results in melanoma patients. This was the case for the anti-PD 1 drugs nivolumab and pembrolizumab. PD-1 negatively regulates T-cell activity by interacting

with its ligands PD-L1 and PD-L2. Once PD-1/PD-L1 pathway is activated, PD-1 inhibits the kinase cascade responsible for T cell activation. PD-L1 is also expressed on regulatory T cells, enhancing their immunosuppressive functions as well[59,64].

Phase I studies on patients with advanced melanoma have shown long response rates (40%) with minimal toxicity after treatment with nivolumab[65]. Other studies have demonstrated a higher response rate for nivolumab compared to dacarbazine[66]. Pembrolizumab also have showed similar efficacy to nivolumab with regard to tumor responses. More importantly, pembrolizumab was approved to be used in patients previously treated with ipilimumab or BRAF inhibitors[67]. Some of these studies are currently under process.

In the case of immunotherapy using antibodies against PD-L1, this seems to be a promising approach but clinical studies are still ongoing. PD-L1 also inhibits T cell activity by binding to B7 ligand. However, targeting PD-L1 may result in a different immune response than targeting PD-1 [46]. Antibodies that block PD-L1 do not prevent PD-1 from interacting with PD-L2.

1.2.3 Other treatments

Considering the latest scientific advances in therapeutic strategies for advanced melanoma, patients now have access to more effective and personalized therapies. Among these therapies are adoptive cell therapy (ACT), CAR modified T cells, and oncolytic viral therapy.

ACT involves the collection of lymphocytes from patients, either peripheral or tumor-infiltrating lymphocytes (TILs), then selection, expansion and activation *in vitro,* followed by transfusion of the processed lymphocytes back into the patient to induce a specific immune response against cancer cells[45]. Several studies have evaluated efficacy of adoptive T-cell transfer. Hunder and collaborators (2008) showed that isolation and expansion of autologous CD4+ T cells with specificity for the melanoma-associated antigen NY-ESO-1 successfully induced a durable anti-tumor response in patients with refractory metastatic melanoma, after CD4+ T cells were transfused back into the patient[68].

Furthermore, by using gene therapy to introduce TCRs or chimeric antigen receptors (CARs), T cells that target any antigen of interest can be generate. The CAR receptors combine a high-affinity antigen recognition domain with the efficient killing machinery

of T cells. This is possible by creating a molecule that links the variable domains of an antibody to the intracellular signaling domains of the TCR complex, in this way, the recognition by CARs is HLA-independent and is directed to a specific protein expressed on tumor cells[46]. Because initial studies did not show the expected results, for the next generations of CARs, intracellular domains of costimulatory molecules (CD27, CD28, CD19) were added, improving the clinical benefit especially in leukemias[69]. Currently, second and third generation of CAR T cells are the most effective effector T cells in use, however, their efficacy is limited to hematological malignancies than solid tumors. Preclinical studies with CAR T cells in melanoma are still under investigation[70].

On the other hand, oncolytic viral therapy using the genetically modified virus talimogen laherparepvec (T-VEC) has shown promising results for melanoma treatment (Figure 4). T-VEC can target tumor cells and induce anti-tumor immune response. T-VEC carries the gene for granulocyte macrophage colony-stimulating factor (GM-CSF) and has tumor selectivity[64,71]. A phase III study showed clinical benefits and durable response in patients with unresectable melanoma in comparison to patients treated with subcutaneous injections of GM-CSF [72].

1.3 Resistance to targeted therapy in melanoma

1.3.1 Types of resistances

Regardless the great variety of therapeutic options for the treatment of metastatic melanoma, the efficacy of treatments remains unsatisfactory due to the development of resistance followed by recurrence of the disease.

With the discovery and initial administration of the combination therapy with BRAF and MEK inhibitors, the PFS and OS improved in metastatic melanoma patients. About 90% of the patients showed some improvement or tumor regression, achieving partial or complete responses. These responses although promising were limited, with only few long-term and durable responses[49]. Unfortunately, about 50% of patients that show initial improvement, usually relapse within 7 months of treatment, a condition referred to as acquired resistance. Moreover, there are approximately 10% of patients that do not respond to targeted inhibition at all, showing an intrinsic or primary resistance to targeted therapy[73].

Hence, resistance to BRAF inhibitors can be caused by the presence of mutations in melanoma cells before start of the treatment (intrinsic resistance) or by the acquisition of new mutations in melanoma cells upon treatment (acquired resistance) (Figure 6). Recently, different studies have reported a type of adaptive resistance in melanoma cells[74–76] that involves initial cellular adjustments that allow melanoma cells to adapt, proliferate and survive shortly after starting the treatment. This mechanism of resistance may underlie the development of acquired resistance by providing time to melanoma cells to develop additional mutations[76].

1.3.2 Mechanisms of resistance to BRAF inhibitors

Among the mechanisms driving intrinsic or primary resistance are: amplification and overexpression of cyclin D1, RAC1 and HOXD8, alterations in the PTEN tumor suppressor gene, loss of NF1, microenvironmental factors like secretion of hepatocyte growth factor (HGF) by stromal cells with the subsequent activation of c-Met receptor, and reactivation of MAPK and PI3K/AKT/mTOR signaling[2,5] (Figure 6).

Moreover, reactivation of MAPK pathway is the most frequent cause of acquired or secondary resistance to BRAF and MEK inhibitors and can be divided into two main groups: MAPK-dependent and MAPK-independent mechanisms[2] (Figure 6). MAPK-independent mechanisms include activation of alternative pathways like PI3K/AKT/mTOR signaling, loss of PTEN and amplification of AKT protein, whereas MAPK-dependent mechanisms involve alternative splicing or amplification of BRAF, NRAS mutations, mutations in the kinase MEK1/2, overexpression of COT, alterations in MITF expression, upregulation of RTKs and reactivation of ERK[2,5,77] (Figure 7). Together, these mechanisms provide melanoma cells with a survival advantage towards BRAF and MEK inhibitors treatment, by enhancing proliferative pathways and inhibiting cell death.

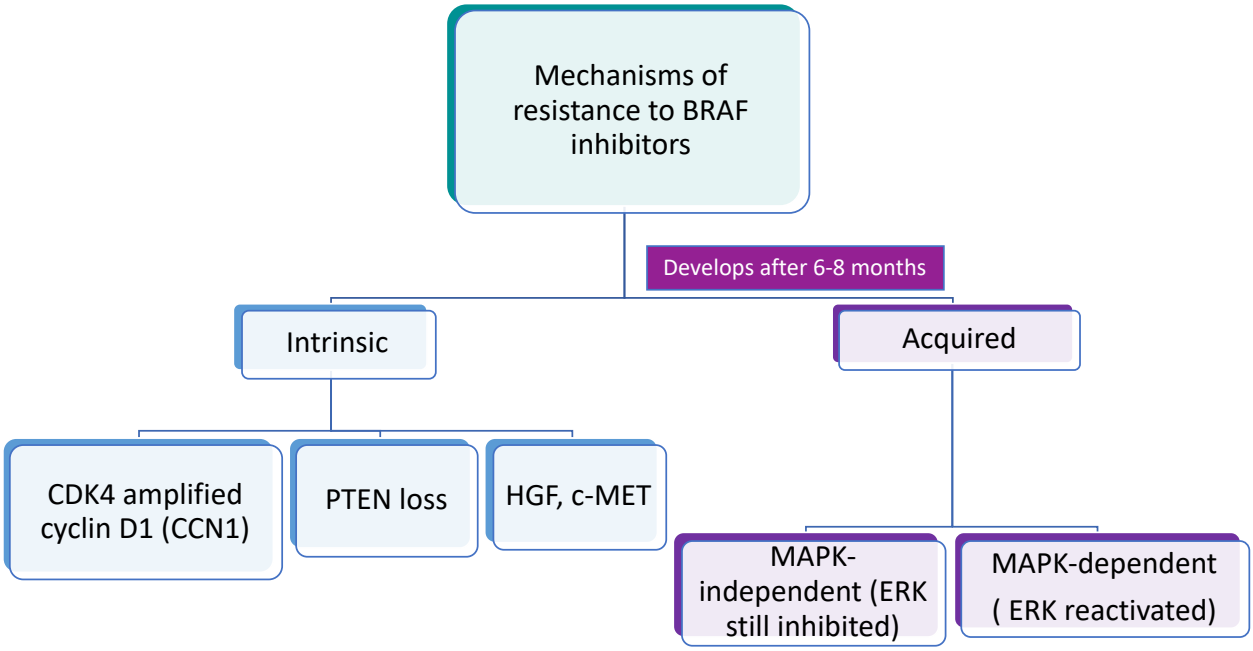

Figure 6. Mechanisms associated with the different types of resistance to BRAF inhibitors in melanoma. Intrinsic resistance is driven mainly by pre-existing mutations before the start of the treatment. Acquired resistance develops after approximately 6-8 months and involves either mechanisms associated with ERK reactivation or alternative pathways independent of MAPK reactivation. Adapted from Muñoz-Consuelo *et al* 2015, *Ann Transl Med*[2].

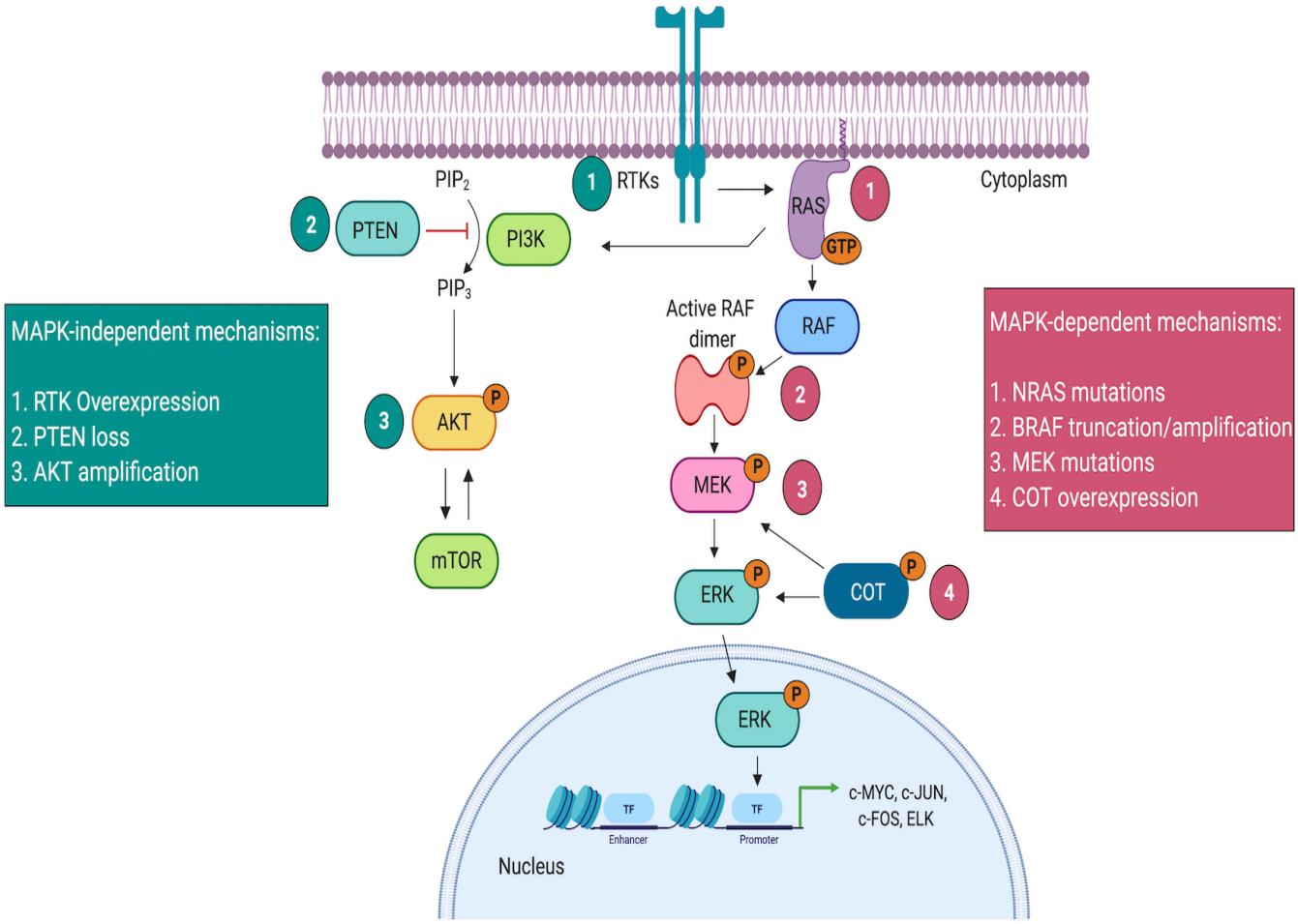

Figure 7. Mechanisms associated with acquired resistance to BRAF inhibitors in melanoma. The mechanisms behind acquired resistance are divided into MAPK-dependent and MAPK-independent mechanisms. However, the main cause of acquired resistance is the reactivation of MAPK pathway. Adapted from Muñoz-Consuelo *et al* 2015 *a*nd Manzano *et al* 2016, *Ann Transl Med*[2,5].

Unlike acquired resistance, the mechanisms driving adaptive resistance to BRAF inhibitors are rapid responses that occur just a few hours upon treatment. Drug withdrawal can reset the compensatory mechanisms during the adaptive response that usually involve an increase in pro-survival pathways, stablishing the preliminary set up for the acquired resistance[76,78].

Adaptive resistance mechanism can be subdivided into three groups: re-setting ERK1/2 protein, overexpression of RTKs with activation of PIK3/AKT/mTOR, and changes in metabolic pathways. Re-setting of ERK signaling has been reported in

some BRAF mutant melanoma cells after treatment with BRAFi, mainly due to a reduction of negative feedback regulators[79].

Among all the RTKs involved in resistance, the v-erb-b2 avian erythroblastic leukemia viral oncogene homolog 3 (ERBB3) receptor and the platelet derived growth factor receptor (PDGFR) are both upregulated during adaptive response to BRAFi[76]. ERBB3 is a member of the epidermal growth factor family of RTKs and exhibits low kinase activity in comparison with other members. Abel and collaborators (2013) reported and upregulation of ERBB3 just a few hours after treatment with vemurafenib in melanoma cells that depends on FOXD3 activity. This effect was reversible upon drug removal[80].

Although differences between adaptive and acquired resistance mechanisms seem minor, identification of early factors involved in adaptive response to BRAF inhibitors is essential to develop combinatorial treatments that enhance current efficacy of target therapies in metastatic melanoma.

1.4 Cellular reprogramming

1.4.1 De-differentiation, reprogramming and transdifferentiation

According to Waddington's epigenetic landscape model, cells develop from a progenitor stem cell to a mature, fully differentiated and functional cell. In this model, cells are depicted as balls rolling down through the epigenetic landscape and falling into deeper valleys that determinate their fate during normal cell development and maintenance[81]. Although this process was thought to be unidirectional, research on different cellular phenomena such as dedifferentiation, transdifferentiation and reprogramming has shown that the process can be reversed[82] (Figure 8).

The term dedifferentiation describes the conversion of a fully differentiated cell into a more primitive and less differentiated cell type. The complete dedifferentiation towards a pluripotent stage is called reprogramming, while transdifferentiation refers to the conversion of one differentiated cell type into another[83]. Although the terms de-differentiation and reprogramming are usually used interchangeably, reprogramming implies completed dedifferentiation into a pluripotent state, while dedifferentiation itself does not necessarily end in pluripotency but involves intermediated stages that are reversible[83].

Cancer progression resembles the process of cellular reprogramming. Transformed cells can display features of pluripotent-like cells losing their original cell identity and

expressing transcription factors that are commonly expressed in embryonic stem cells (ESC)[84,85]. Therefore, molecular mechanisms responsible for cell fate maintenance and self-renewal of progenitor cells might also be involved in the development and progression of cancer.

Tumor cells that show self-renewal capacity and that give rise to heterogeneous progeny of cancer cells within the tumor are defined as cancer stem cells (CSC), a unique subpopulation of cells that can self-replicate indefinitely and is insensitive to anticancer therapies[84].

The CSC model suggests that the CSCs maintain the malignant growth through their ability to self-renew and their capacity to give rise to a progeny with limited proliferative capacity. This suggest a hierarchy where CSC are responsible to generate all the different types of cells within a tumor and increasing tumor heterogeneity[84]. Several studies have shown that this hierarchical CSC model can be bidirectional in some tumors, reporting that non-CSC dedifferentiate and acquire CSC-like features under certain conditions, causing tumor cell plasticity[85,86](Figure 8).

A better understanding of the changes that occur during cellular reprogramming might provide new insights into cancer initiation, progression and recurrence. The development of alternative models to study cancer plasticity and generation of CSC is essential to improve the efficacy of current cancer treatments and escape therapy resistance.

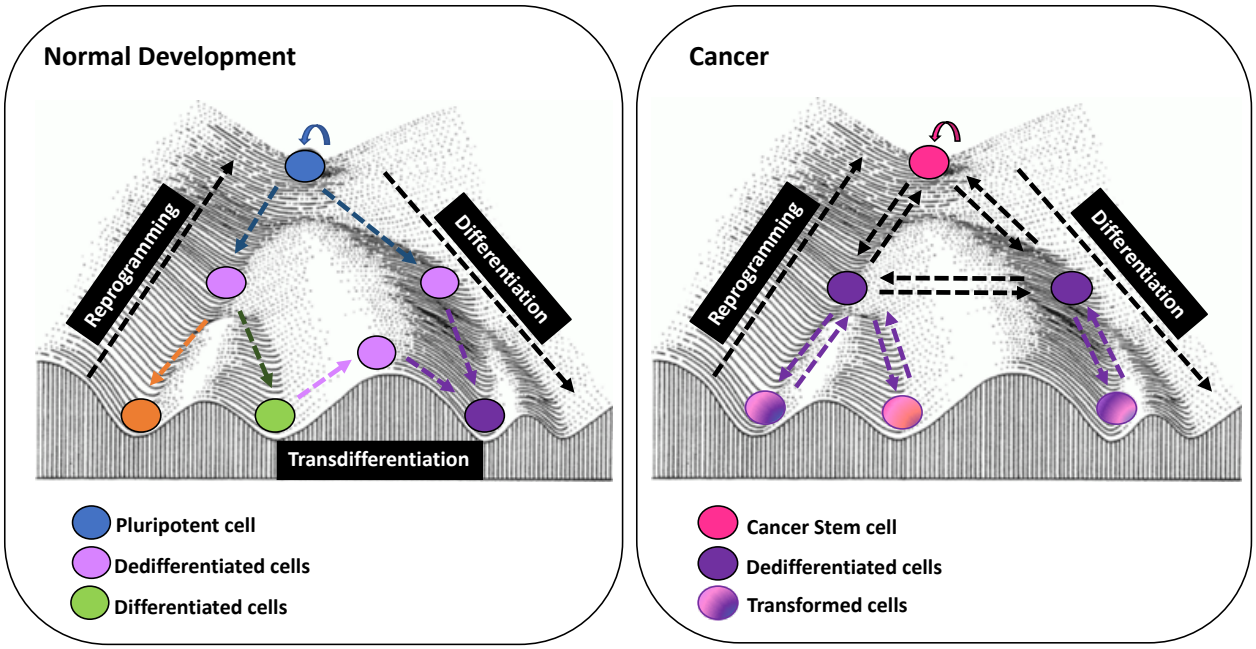

Figure 8. Comparison between normal development and cancer, using a representation of the epigenetic landscape described by Waddington. Pluripotent cells can differentiate into cells from different lineages. The opposite process is known as reprogramming, where pluripotency state is induced. Additionally, differentiated cells can switch between lineages, a process known as transdifferentiation. In cancer, cancer stem cells can generate differentiated and transformed cells within the tumor, increasing the tumor heterogeneity and prolonging tumor growth. Adapted from Waddington, C.H. (1957). *The Strategy of the Genes*[81].

1.4.2 Stem cells and iPSCs

Stem cells are undifferentiated cells that can self-renew and that have the potency to differentiate into different specialized cell types. Based on their differentiation potential, stem cells can be classified as totipotent, pluripotent, multipotent or unipotent [87,88]. Totipotent cells are the only cells able to produce a fertile adult individual. The zygote and early blastomeres are totipotent.

Pluripotent cells include ESCs, perinatal stem cells, and induced pluripotent stem cells (iPSCs). ESCs can be isolated from the inner cell mass of the blastocyst and can give rise to every cell type from the three embryonic germ layers (ectoderm, mesoderm and endoderm), but not the extraembryonic tissue like placenta and umbilical cordon[89]. Indeed, ESCs and iPSCs both can form teratomas, encapsulated tumors consisting of different differentiated cells from all three embryonic germ layers.

iPSCs share many properties with ESCs and have been derived from many types of somatic cells by a process called cellular reprogramming. In order to produce iPSCs, either the genome, the environment or both have to be manipulated to successfully reprogram somatic cells.

As mentioned earlier, reprogramming is a cellular process in which a fully differentiated cell reverts to a pluripotent state with the potential to differentiate into all cell types of the three germ layers. The concept of cellular reprogramming was first investigated by John Gurdon in 1958, when he and his collaborators successfully transferred a nucleus from an embryonic cell into an enucleated and unfertilized egg and thereby initiating nuclear reprogramming of a differentiated cell[90].

Later, iPSCs were successfully generated by direct reprogramming using a combination of only four transcription factors: Oct4, Sox2, Klf4 and c-Myc (OSKM)[91] that were ectopically expressed in somatic cells. Since then, different combinations of transcription factors including Nanog or Lin28 have been utilized to successfully produce iPSCs *in vitro* and *in vivo* from somatic cells in different organisms[92–94]. Other strategies for reprogramming involve cell fusion, transfection with miRNAs, and even the use of small molecules that can enhance reprogramming of somatic cells, including vitamin C, valproic acid (histone deacetylase inhibitor) or 5-azacytidine (DNA methyltransferase inhibitor)[95,96].

Although reprogramming seems a stochastic process at the beginning, where genes are repressed or activated apparently without a specific pattern, it is well known that there are specific genetic programs that must unlock as well as particular epigenetic changes that must occur (DNA methylation and histone modifications) to facilitate reprogramming[97]. During the initial phase of reprogramming, transcription factors Oct4, Sox2, Klf4 but not c-Myc, can access chromatin at distal elements and activate silent genes such as ESRRB and Sall4 that are required to induce pluripotency. Particularly, Oct4 has an essential role during reprogramming by binding to the enhancer elements of the Nanog, POU5F1 and MYOD1 genes. Moreover, c-Myc can co-bind to OSK at the distal elements, which promotes open chromatin and access to promoters, resulting in amplification of gene expression[98].

Later, induction of ectopic expression of c-Myc leads to an increase in proliferation through upregulation of several pathways. At the same time, transcription factors can induce metabolic switch from oxidative phosphorylation to glycolysis, which enhances

the efficiency of cellular reprogramming. These features are commonly seen in pluripotent cells, adult stem cells and cancer cells[99,100].

For successful reprogramming, active expression of endogenous stemness related genes like Oct4, Nanog and Sox2 is indispensable to maintain pluripotency independently of the expression of exogenous transcription factors. Oct4 and Nanog are key regulators of reprogramming in cooperation with Sox2 due to their role in embryogenesis[101]. Studies show that these three transcription factors bind to pluripotency-specific genes forming a regulatory loop that maintains their own expression as well as the expression of other key genes. Moreover, a complete repression of lineage-specifying genes is necessary to activate self-renewal and other properties of pluripotent cells[101].

In contrast to pluripotent stem cells, somatic or adult stem cells are tissue-restricted and can only differentiated into a few cell types within one particular lineage (multipotent) or into only one type (unipotent) depending on their differentiation potential. In general, adult stem cells can regenerate the cell types from the specific tissue or organ where they reside[87–89]. For instance, hematopoietic stem cells in the bone marrow can generate all types of red blood cells, white blood cells and platelets but not liver or brain cells.

1.4.3 Cellular reprogramming and cancer

Due to all the genetic and epigenetic alterations that occur during the process of de-differentiation, one of the numerous applications for cellular reprogramming is disease modeling, including cancer. De-differentiation has been established as a hallmark of cancer progression and contributes to the acquisition of plasticity and therapy resistance in tumor cells[43,86]. Different studies have reported that poorly differentiated tumors possess an embryonic stem-like gene signature, expressing different stem cell-related factors like Oct4, Nanog and Sox2[85,86].

Typically, cellular reprogramming is associated with tissue regeneration[102–104]. However, this process has also been related to cancer initiation, progression and recurrence. Certainly, reprogramming of cancer cells can explain the phenotypic and functional heterogeneity observed among cancer cells[105].

Cancer cell subpopulations are organized in a hierarchical fashion, with the CSCs at the top. CSCs display stemness features, tumor initiation capacity in several types of

cancer, and are usually quiescent which allows them to survive the toxic effects of many anti-cancer treatments[105]. Somatic stem cells and CSCs use common regulatory mechanisms including Notch, Wnt and Hedgehog pathways, as well as stemness-related transcription factors. Indeed, each of the transcription factors used for cellular reprogramming also plays a role in tumorigenesis, including Oct4, Sox2, Nanog, Klf4 and Lin28[84,85].

Based on the theory that CSCs arise from normal stem cells or from a specific population of progenitor cells with self-renewal and unlimited proliferation capacity, many cancers might originate from somatic stem cells under pathological conditions where genetic and epigenetic changes induce cellular reprogramming of somatic stem cells, producing CSCs as a result (Figure 9). It is well established that CSCs are involved in acquisition of drug resistance, metastasis and disease relapse. CSC populations can support long-term tumor growth due to their self-renewal capacity, telomerase activity and upregulation of multidrug resistance pathways[106,107]. Currently, many investigations aim at identifying and eliminating cancer initiating cells or CSCs, selectively, in order to overcome drug resistance and tumor relapse.

To investigate the dedifferentiation of cancer cells and the generation of CSCs, different protocols for the generation of iPSCs, *in vitro* and *in vivo*, have been implemented for several types of cancer cells[108]. However, the molecular mechanisms that participate during this process are not fully understood. Dedifferentiating cancer cells by ectopically expressing the reprogramming transcription factors such as OSKM, have been reported in melanoma[12,109], Leukemia[110], gastrointestinal cancer[111], osteosarcoma[112], colorectal cancer[111], and pancreatic ductal adenocarcinoma[113].

As a consequence of reprogramming, induced pluripotent cancer cells (iPCCs) are less tumorigenic and have the potential to differentiate into different type cell[108,109] (Figure 9). One advantages of reprogramming cancer cells is the possibility to produce a significant number of CSCs to explore their properties and the molecular mechanisms that increase therapy resistance. In addition, iPCCs can be used for pharmacological screenings in order to discover new therapeutic targets in CSCs.

Finally, because reprogramming of cancer cells can mimic the heterogeneity of tumors, this model represents a suitable platform to study features of tumor progression and to identify key factors that are involved in the development of resistance to cancer therapies, which remains one of the main problems during treatment of melanoma and other types of cancer.

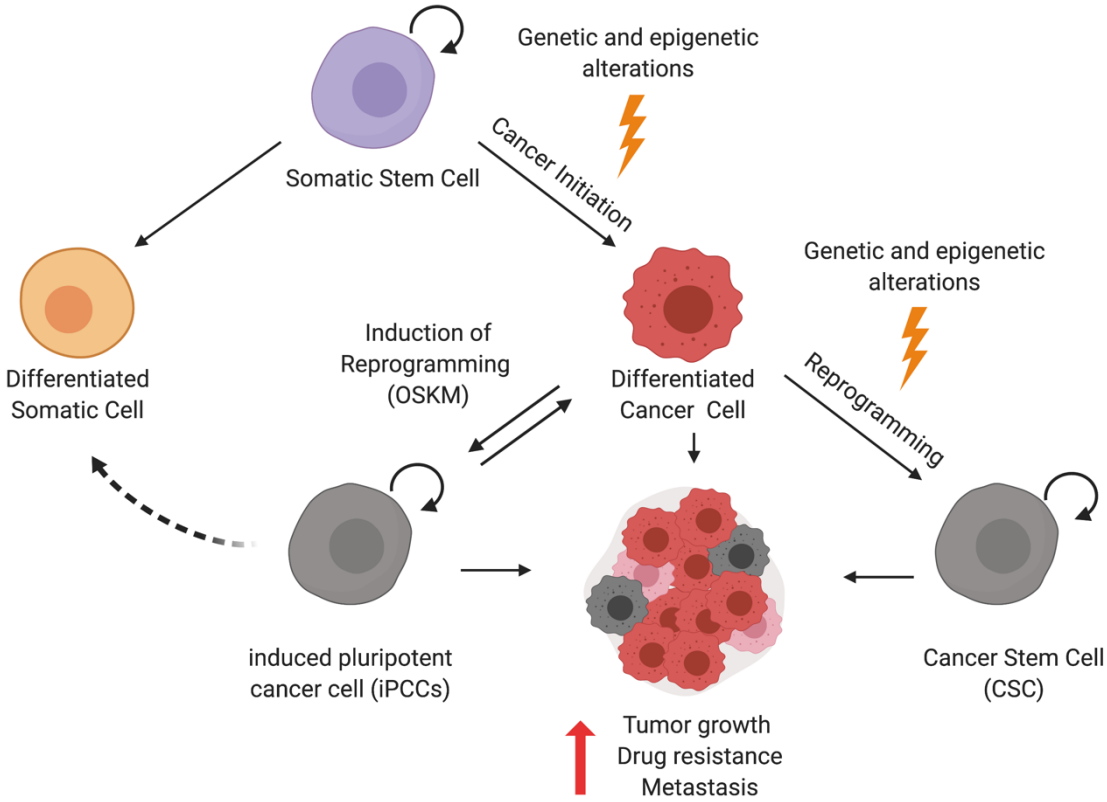

Figure 9. Generation of CSC and reprogramming of cancer cells. Genetics and epigenetic changes induce somatic stem cells to differentiate into transformed cells. These cells can go under reprogramming until CSC and support tumor growth, drug resistance and metastasis. Additionally, differentiated cancer cells can be reprogrammed into induced pluripotent cancer cells (iPCCs), which can also differentiate into a different cell type. Adapted from Xiong *et al* 2019 *Trends in Cell Biology,* Bernhardt *et al* 2017 *Stem Cell Reports,* and Câmara *et al* 2016 *Journal of Cancer*[105,108,109].

2. Aims of the thesis

The main aim of this work was to investigate the phenotypic and genetic changes that occur during melanoma progression, using partial reprogramming of melanoma cells as a model for de-differentiation and resistance to MAPK inhibitors. Additionally, identify new suitable candidate molecules that can be used as targets in order to overcome resistance to MAPK inhibitors.

The specifics aim of this thesis are:

2.1. Partially reprogram murine melanoma cells using an *in vitro* model to study phenotype switching in melanoma by inducing de-differentiation.

2.2 Evaluate the effect of BRAF and MEK inhibitors on partially reprogrammed melanoma cells in order to study therapy resistance.

2.3 Analyze the characteristics of MAPKi-resistant cells to find new candidates that can be targeted in order to eliminate or sensitize MAPKi-resistant melanoma cells.

3. Materials and Methods

3.1 Materials

3.1.1 Reagents and Kits

Product	Company	Catalog No.
Agarose NEEO Ultra Qualität	Carl Roth	2267.4
Alamar Blue®	Invitrogen	DAL1100
Ampicillin	Carl Roth	HP62.1
Ammonium Persulfate (APS)	Carl Roth	9592
BioCoat™ Tumor Cell Invasion Systems	Corning	354165
BSA-Powder, Albumin Fraction V	Carl Roth	8076.2
Complete Mini Protease Inhibitor Cocktail	Roche Diagnostics	4693159001
DH5α Competent Cells	Thermo Fisher Scientific	18265017
Endofree Plasmid Maxi Kit	Qiagen	12362
FITC-Annexin V apoptosis Kit	BD Biosciences	556547
High Performance Chemiluminescence Film	GE healthcare	28906836
MouseRef-8 v2.0 Expression BeadChips	Illumina	BD-202-0202
GeneChip® Mouse Genome 430 2.0 Array	Affymetrix	900595
Immobilon PVDF membrane, 0.45µM	Merck Millipore	IPVH00010
Luminata Forte Western HRP Substrate	Merck Millipore	WBLUF0500
MicroAmp Optical 96well Plate qPCR	Thermo Fisher Scientific	N8010560
NuPAGE™ Novex™ 3-8% Tris-Acetate Protein Gels	Thermo Fisher Scientific	EA03752BOX
NuPAGE™ LDS Sample Buffer (4X)	Thermo Fisher Scientific	NP0008
NuPAGE™ Reducing Agent (10X)	Thermo Fisher Scientific	NP0004
PageRuler Plus Prestained Protein Ladder	Life Technologies	26619
Paraformaldehyde	Sigma Aldrich	P6148-1KG
Pierce BCA Protein Assay Kit	Thermo Fisher Scientific	23225
Qiaprep Spin Miniprep Kit	Qiagen	27106

RevertAid First strand cDNA Synthesis Kit	Thermo Fisher Scientific	K1622
Rnase-Free Dnase Set	Qiagen	79254
RNeasy Plus Mini Kit	Qiagen	74136
Skim milk powder	Gerbu Biotechnik	16021000
SYBR Green PCR Master Mix	Applied Biosystems	4309155
TEMED	Carl Roth	2367,3
TritonX-100	Carl Roth	3051,4
Tween® 20	Applichem	A13890500
Venor Gem Classic Myco PCR Kit	Minerva Biolabs	11-1100
X-treme GENE® 9 DNA Transfection Reagent	Roche Diagnostics	6365787001

3.1.2 Reagents for cell culture

Product	Company	Catalog No.
2-Mercaptoethanol	Gibco®Life Technologies	31350010
Blasticidin	Sigma Aldrich	15205
Calcein AM Fluorescent Dye	Corning	354217
DMSO	Carl Roth	A994.2
Doxycycline	Sigma-Aldrich	D1822
Dulbecco's Modified Eagle's Medium (DMEM)	Thermo Fisher Scientific	10569010
Embryonic Stem Cells Serum (ES-FCS)	Thermo Fisher Scientific	16141079
Fetal Calf Serum (FCS)	Biochrom	S0115
L-Glutamine	Thermo Fisher Scientific	25030081
Knockout™DMEM	Thermo Fisher Scientific	10829018
Murine LIF	Sigma-Aldrich	L5158
Non-essential amino acids	Sigma-Aldrich	M7145
PBS	Sigma-Aldrich	D8537
Penicillin/Streptomycin	Sigma-Aldrich	P4333
Polybrene Infection / Transfection Reagent	Sigma Aldrich	TR-1003-G
Puromycin	Carl Roth	240,1
Trypan blue solution	Sigma-Aldrich	93595
Trypsin -EDTA solution	Sigma-Aldrich	T3924

3.1.3 Human cell lines

Cell Line	Source	Cell type	Mutation
A375	ATCC	Melanoma cell line	BRAF V600E
HT144	ATCC	Melanoma cell line	BRAF V600E
SK-MEL-28	ATCC	Melanoma cell line	BRAF V600E
HEK293T	ATCC	embryonic kidney cells	WT
4434	Obtained from Dr. Richard Marais (University of Manchester, UK)	Melanoma cells	BRAF V600E
C790	Obtained from Dr. Richard Marais (University of Manchester, UK)	Melanoma cells	NRAS

3.1.4 Antibodies

Specificity	Source	Company	Catalog No.
Anti-rabbit IgG, HRP-linked	Goat	Cell signaling	7074S
Anti-mouse IgG, HRP-linked	Horse	Cell signaling	7076
T-type Ca++ Cav3.2	mouse	Santa Cruz	sc-377510
Caspase 3	Rabbit	Cell signaling	9662
ERK	Rabbit	Cell signaling	4695
GAPDH	Rabbit	Cell signaling	CST2118
SOX2	Rabbit	Cell signaling	23064S
pERK (T202/Y204)	Mouse	Cell signaling	9106S

3.1.5 Inhibitors

Product	Company	Catalog No.
Lomerizine	Sigma-Aldrich	L6295
Mibefradil	Sigma-Aldrich	M5441
Trametinib (GSK1120212)	Selleckchem	S2673
Vemurafenib (PLX4032)	Selleckchem	S1267

3.1.6 Plasmids

Name	Source
CAV3.2 shRNA 1	TRCN0000044212
CAV3.2 shRNA 2	TRCN0000044210
pCMV-dR8.91 (Packaging)	Konrad Hochedlinger (Harvard, Boston, USA)
pCMV-VSV-G (Packaging)	Addgene #8454
pLU-EF1aL-rtTA3-iCherry	Wistar Institute
pLKO.1- puro scrambled	Addgene # 1864

3.1.7 Primers

Mouse qPCR primers		
Amplification target	Forward Sequence	Reverse Sequence
Gapdh	AGGTCGGTGTGAACGGATTTG	TGTAGACCATGTAGTTGAGGTCA
Sox2	TTAACGCAAAAACCGTGATG	GAAGCGCCTAACGTACCACT
Oct4 endogenous	AGTTGGCGTGGAGACTTTGC	CAGGGCTTTCATGTCCTGG
Ssea1	ACGGATAAGGCGCTGGTACTA	GGAAGCCATAGGGCACGAA
Mitf	CCAACAGCCCTATGGCTATGC	CTGGGCACTCACTCTCTGC
Pmel	CCTTGGGCAGGCTCCCTTGC	TCCACTGAGGAGCGGGCTGT
Cacna1h	CGGCCCTACTACGCA	ATCCTCGCTGCATTC
CD271	TGCCGATGCTCCTATGGCTA	CTGGGCACTCTTCACACACTG
Human qPCR primers		
18S	GAGGATGAGGTGGAACGTGT	TCTTCAGTCGCTCCAGGTCT
SOX2	GCCGAGTGGAAACTTTTGTCG	GGCAGCGTGTACTTATCCTTCT
ID1	CTGCTCTACGACATG	GAAGGTCCCTGATGT
ID3	GCTTGCTGGACGACA	GCGCTGTAGGATTTC
CAV3.1	GCTCCGGCACAAGTA	C CACAATGAGCAGGAA
CAV3.2	TCGAGGAGGACTTCC	TGCATCCAGGAATGG

3.1.8 Solutions and Buffers

Transfer buffer (pH 8.3) 25mM Glycine 190mM Tris 20% SDS 20% Methanol dH_2O	Running buffer (pH8.3) 25mM Glycine 190mM Tris 0.1% SDS dH_2O
TBS 10X (pH 7.6) 150mM NaCl 50mM Tris dH_2O	Washing buffer (TBST) 0.02% Tween® 20 1X TBS
Blocking buffer (milk) 5% Skim milk powder 1x TBS	Blocking buffer (BSA) 5% BSA 1x TBS
RIPA buffer 4M NaCl 1% IGEPAL (Sigma-Aldrich) 10% Sodium deoxycholate 10% SDS 1M Tris, pH 8 dH_2O	TEB buffer 0.5% Triton X 100 2mM phenylmethylsulfonyl fluoride 0.02% Sodium Azide dH_2O
SOC Outgrowth Medium New England BioLabs (B9020S)	LB Medium 20g LB-Medium (Carl Roth, X964.2) 1l H_2O
Cell freezing medium 80% FCS 20% DMSO	Cell freezing medium for reprogramming 80% ECS 20% DMSO
Crystal violet solution 0.5% Crystal violet 20% Methanol dH_2O	HPMC solution 20%HPMC 1% Tween 20 dH_2O

3.1.9 Equipment

Product	Company
12 Well Multiwell Plates	Grenier Bio-One
2100 Bioanalyzer Instrument	Agilent
6 Well Multiwell Plates	Grenier Bio-One
AB 7500 Real-Time PCR Machine	Applied Biosytems
CELLSTAR® Cell Culture Flasks	Grenier Bio-One
ChemiDoc™ Touch Imaging System	Bio-Rad
Culture-inserts 2 well	Ibidi
FACSCanto II	BD Biosciences

Haemocytometry	Neubauer
Leica DM LS light microscope	Leica
MicroAmp Optical 96well Plate qPCR	Thermo Fisher Scientific
Microplates 24-well	Falcon
Microplates 96-well	Falcon
Nanodrop Spectophotometer ND-1000	Peqlab Biotechnologie GmbH
Nikon Eclipse Ti Fluorescence Microscope	Nikon
Nunc™ Cell Culture Cryogenic Tubes	Thermo Fisher Scientific
Rotilabo®-syringe filters, 0,22 µm	Carl Roth
Rotilabo®-syringe filters, 0,45 µm	Carl Roth
Tecan Infinite F200 PRO	Tecan
Veriti™ 96-Well Thermal Cycler	Thermo Fisher Scientific

3.1.10 Software tools

Software name	Source
7500 Software v2.0.5	Applied Biosystems
Chipster	Chipster Open source
FlowJo 7.2.2	FlowJo License
GraphPad PRISM 8	GraphPad License
iControl 1.10	TECAN
Image J	NIH
Image Lab 6.0.1	Bio-Rad
Ingenuity® Pathway Analysis (IPA®)	QIAGEN Bioinformatics
NIS-Element	Nikon
Primer-BLAST	https://www.ncbi.nlm.nih.gov/tools/primer-blast/
TScratch	CSElab
Software R 3.5	https://www.r-project.org/

3.2 Methods

3.2.1 Cell Culture

All cells were maintained under optimal conditions in 5 % CO_2 atmosphere and 37°C. Human melanoma cell lines A375, HT144, and SK-mel-28 were obtained from ATCC (Virginia, USA) and mouse melanoma cells C790 (Nras mutant) and 4434 (BrafV600E mutant) were kindly provided by Professor Richard Marais (University of Manchester, UK). All cells were cultured in DMEM medium (Thermo Fisher Scientific) supplemented with 10 % FCS, 1 % nonessential amino acids, 0.75 % 2-mercaptoethanol, 100

units/mL penicillin and 100 µg/mL streptomycin. Cell culture stocks were stored in liquid nitrogen at low passages. All cell lines were tested and free of mycoplasma contamination.

Reprogramming experiments were performed using KnockOut™ DMEM medium (Thermo Fisher Scientific), supplemented with 10 % ES-FCS (Thermo Fisher Scientific), 1 % glutamine, 1 % penicillin/streptomycin, 1 % nonessential amino acids, and 100 U/ mL mouse Leukemia Inhibitory Factor.

3.2.2 Partial reprogramming

The partial reprogramming model was established using mouse melanoma cells C790 and 4434, based on a previous method describe by Knappe *et al* 2016[12]. Briefly, cells were transduced with a doxycycline-inducible polycistronic lentiviral vector encoding for Oct4, Sox2, Klf4 and a blasticidin resistance gene, in combination with a lentiviral vector pLU-EF1aL-rtTA3-iCherry (The Wistar Institute) encoding for the constitutively active reversed tetracycline-controller trans activator (rtTA) coupled to mCherry. After transduction cells were maintained in reprogramming medium containing doxycycline (1 µg/ mL) in order to induce transgene expression. At day three, cells were selected with Blasticidin (10 µg/mL) and maintained in culture for twenty days.

3.2.3 Lentiviral vector production

Production of lentiviral vector was performed using human HEK293T cells. HEK293T were cultured in DMEM medium (Thermo Fisher Scientific) supplemented with 10 % FCS, 1 % nonessential amino acids, 0.75 % 2-mercaptoethanol, 100 units/mL penicillin and 100 µg/mL streptomycin. Briefly, 11 µg of each construct of interest is mixed with 8.25 µg of pCMV-dR8.91 and 5.5 µg of pCMV-VSV-G, lentiviral packaging constructs, along with 50 µl of X-tremeGENE™ 9 DNA transfection reagent (Roche Diagnostics). After 30 minutes incubation, the mixture was added on HEK293T cells (70 % confluent) and cells were incubated in 5 % CO_2 atmosphere and 37°C in a biosafety level II laboratory S2. After 12 hours, cell medium was discarded and fresh medium was added. Subsequently, supernatant was collected at defined time points (24, 36 and 48 hours). All supernatants were filtered using Rotilabo®-syringe filters, 0,45 µm (Carl

Roth) and used for cell transduction immediately or ultracentrifuged and stored at -80°C.

For the cell transduction, target cells were harvested 2 days before in 6-well plates at low density. On day 1, cells were infected with filtered virus in fresh medium (1:2), along with 2 µg/mL polybrene (Sigma-Aldrich) to increase the transduction efficiency (optional). After 24 hours, cells were re-infected (filtered virus and fresh medium,1:2). On day 4, cells were washed twice with PBS and fresh medium was added. Cells were incubated in 5 % CO_2 atmosphere and 37°C in a biosafety level I laboratory. After 24 hours, cells were selected during 3 – 5 days using the respective selection antibiotic based on the vector used (1-3 µg/mL of puromycin, Carl Roth; or 8-20 µg/mL of blasticidin, Sigma-Aldrich). Knockdown of CACNA1H was performed by using the method previously described and shRNA against CACNA1H (TRCN0000044212) and (TRCN0000044210) (Sigma-Aldrich), while a scramble shRNA vector (Addgene) was used as control.

3.2.4 Bacterial transformation

In order to obtain amplified plasmid DNA of interest, competent E. coli bacteria were transformed. Briefly, competent bacterial cells (DH5α, Sigma-Aldrich) from E. coli were thawed on ice, mixed with approximately 100 ng of plasmid DNA and incubated for 40 min. Next, bacteria suffered heat-shock for 3 min at 42 °C followed by 1 min cool down on ice. Next, SOC medium was added to the bacteria-DNA mixture, followed by 1h incubation at 37°C and constant shaking. Finally, bacteria were plated on agar plates containing the antibiotic ampicillin (100 µg/mL) for selection. After incubation overnight at 37°C, growing colonies on agar plates were picked and allowed to grow in LB medium containing ampicillin, overnight under constant agitation. Afterwards, plasmid was isolated using Qiaprep Spin Miniprep Kit (Qiagen) and analyzed with restriction digestion in order to confirm that the plasmid was correct. Then, bacteria carrying the correct plasmid were cultured in 200 mL of LB medium containing ampicillin, overnight at 37°C and under constant agitation. Finally, Endofree Plasmid Maxi Kit (Qiagen) was used to isolate the plasmid of interest, following the instructions of the manufacturer. DNA plasmid concentration was determinate using Nanodrop ND-1000 and DNA plasmid sequence was confirmed by DNA sequencing (LGC Genomics).

3.2.5 Inhibitors

The following inhibitors were used: trametinib (GSK1120212) (Selleckchem), vemurafenib (PLX4032) (Selleckchem), lomerizine dihydrichloride (Sigma-Aldrich), and mibefradil dihydrochloride hydrates (Sigma-Aldrich). All drugs were dissolved in DMSO to desired final concentration, aliquoted and stored according to the manufacturers' guidelines.

3.2.6 RNA Isolation

Total RNA was isolated using RNeasy Mini Kit (Qiagen) and DNase I digestion for 15 minutes at RT to remove genomic DNA. Protocol was performed according to the manufacturers' guidelines. RNA concentration and quality were evaluated by spectrophotometry using NanoDrop ND1000 device. RNA was used immediately or stored at -80°C.

3.2.7 cDNA synthesis

cDNA was synthesized using cDNA Reverse Transcription kit (Thermo Fisher Scientific) according to the manufacturers' guidelines. First, RNA was dilute with 1 µL of Oligo- $(dT)_{18}$ primer and dH_2O up to 12 µL, for a final concentration of 500 ng/µL. This mixture was centrifuged and incubate at 65°C for 5 minutes, chilled on ice and spun down. Master mix was prepared using 4 µL of 5X Binding Buffer, 1 µL of RiboLock RNase inhibitor (20 U/ µL), 2 µL of 10mM dNTP mix and 1 µL of RevertAid M MuL-V-RT enzyme (200 U/ µL). Afterwards, 8 µL of master mix was added to each reaction tube and tubes were incubate for 60 minutes at 42°C, followed by 5 minutes at 70°C. cDNA was used immediately or stored at -20°C.

3.2.8 Quantitative real-time PCR

Quantitative RT-PCR was performed using Applied Biosystems 7500 Real-Time PCR Systems (Applied Biosystems) and SYBR Green PCR master mix (Thermo Fisher Scientific), according to the manufacturers' guidelines. All reactions were performed at least in triplicates and the amplification signal from the target gene was normalized to

GAPDH for mouse samples or 18S for human samples. PCR conditions were: 50°C 2 minutes, 95°C 10 minutes, 40× cycles of 95 °C 15 seconds, 60°C 1 minute and 72°C 7 seconds. Primer sequences are listed in the section 3.1.7.

3.2.9 Protein isolation

Cells were harvested and washed twice with PBS, cell pellets were collected and stored at -80°C before protein extraction. Protein isolation was performed using RIPA buffer in presence of phosphatase inhibitors. Briefly, cell pellets were disrupted with RIPA buffer, mixed and chilled on ice. Protein lysates were centrifuged for at least 30 minutes at 4°C. Supernatants were collected and quantified.
Protein quantification was performed using Pierce BCA Protein Assay Kit (Thermo Fisher Scientific). First, samples were diluted in buffer (1:10) and standards were prepared based on manufacturers' guidelines. Then, 25 µL of sample or standard were mixed with 200 µL of BCA reagent in 96-well plates and incubated for 30 minutes at 37°C. Finally, after incubation, absorbance was obtained using a reader plate (TECAN) and protein concentration was calculated based on standard curve.

3.2.10 Western Blot

Protein samples (20-30 µg) were run on SDS-PAGE gels (at 100V for 2 hours) and transferred into PVDF membranes (at 90V for 1 hour). Once transfer was completed, membranes were blocked using 5% skim milk or 5% BSA in TBS buffer (1X) for at least 30 minutes at RT. After blockage, membranes were probed first with the primary antibody overnight at 4°C followed by an incubation with the respective secondary antibody (1:10000) for 1 hour at RT. Luminata Forte Western HRP Substrate and chemiluminescence films were used for detection. The complete list of antibodies used can be found in the section 3.1.4. All antibodies were diluted and maintained according to manufacturers' guidelines.

3.2.11 Cell viability assay

Cells were harvested and seeded in 96-well plates in triplicates, at a density of 1×10^3 - 1×10^5 cells. After 24 hours, treatments were added using a range of concentrations between 0,0001 µM and 10 µM for 24, 48 or 72 hours. Cell viability was determined using Alamar Blue solution (Invitrogen), according to manufacturers' guidelines. Briefly, 10 % of Alamar Blue solution was added to 96-well plates and incubated for 4 hours at 37°C. Afterwards, fluorescence was measured at 590 nm using a microplate reader (Tecan). Cell viability and IC50 values were calculated.

3.2.12 EdU incorporation assay

Cell proliferation and cell cycle were determined using Click-iT EdU Cell Proliferation Kit according to the manufacturer's instructions (Invitrogen). Cells were seeded in 6-well plates at low density. After 24 hours, EdU compound (10 µM) was added to the medium for 2 hours. Cells were harvested, washed and fixed for 15 minutes at RT in the dark. After fixation cells were washed again and stained with Click-iT™ Plus reaction cocktail containing Alexa Fluor™ 647, for 30 minutes in the dark. Finally, cells were treated with Ribonuclease A, stained with PI (50 µg/mL) and analyzed by flow cytometry. Data were analyzed using the FlowJo Software.

3.2.13 Apoptosis assay

Detection of apoptosis was performed using FITC Annexin V Apoptosis Detection Kit I (RUO) (DB Biosciences). Cells were seeded at a concentration of 1 x 10^5 cells/mL in 6-well plates. Treatments were added to the medium the following day, concentration used was calculated based on IC50 values. After 24, 48 or 72 hours, supernatants were collected, cells were washed twice with PBS and resuspended in 1X Binding Buffer to final concentration of 1 x 10^6 cells/mL. Later, cell suspension (100 µL) was stained with 5 µl of FITC Annexin V and 5 µL of PI. Cells were incubated for 15 minutes at RT in the dark. Then, 400 µL of 1X Binding Buffer was added to each tube and then analyzed by flow cytometry. Doxorubicin (0.003 µM) was used as a positive control to induce apoptosis for 72 hours. Data were analyzed using the FlowJo Software.

3.2.14 Invasion assay

To assess invasion, BioCoat™ Tumor Invasion 24-Multiwell Plates containing FluoroBlok™ PET membrane (Corning) were used. First, plates were rehydrated for 2 hours at 37°C. Then, 500 µL of cell suspension (3×10^4 cells/mL) was added to the apical chambers and 750 µL of chemoattractant (10% FCS in DMEM) to basal chambers. Plate was incubated for 22 hours at 37°C and 5 % CO_2. After incubation, calcein solution (4 µg/mL) was added to a second 24-well plate and incubated for 1hour at 37°C and 5 % CO_2. Finally, calcein solution was removed and fluorescence was read for invading cells at 517 nm, using a microplate reader (Tecan). Data were expressed as relative fluorescent units (RFU) of invaded cells.

3.2.15 Migration assay

Migration assay was performed using Culture-Insert 2 Well in µ-Dish 35 mm (Ibidi). Briefly, cell suspension (3×10^5 cells/mL) was prepared as usual. Inserts were placed into the plates and 70 µL of cell suspension was added into each well of the insert. The plate was incubated for 24 hours at 37°C, 5% CO_2. After incubation, inserts were removed and 500 µL of fresh medium was added. Progress of migration was checked with a microscope every 12 hours starting from time 0 until 48 hours or when the gap was completely closed. Microscope pictures were analyzed using TScratch software. Data were expressed as percentage of migration.

3.2.16 Clonogenic assay

Colony formation assay was performed following the method described by Franken and coworkers [114]. First, cells were harvested, counted and seeded in 6-well plates (1:500) for 24 hours. After cells were attached, treatments were added accordingly with the IC50 values, for another 24 hours. Treatments were withdrawn and fresh medium was added to cells every 3 - 5 days. After 10 -15 days, colonies were fixed and stained with crystal violet solution (0.5%). Colony area was calculated using ImageJ software.

3.2.17 *In vivo* experiments

In vivo experiments were assessed using NSG xenograft mouse model. Four to six-week-old female mice were injected subcutaneously (SC) with 100 µL PBS containing 1 x 10^6 A375 cells or 5 x 10^6 HT144 cells, both after 24 hours treatment with vemurafenib. Tumor-bearing mice (100-300 mm3) were randomly distributed to four groups (n= 40) and treated in one of the following ways: 1) mibefradil (0.25 mg/mL) in drinking water for 5 days; 2) vemurafenib (100 mg/kg) dissolved in HPMC solution (0.5%) by oral gavage once a day for 5 days; 3) sequential treatment: vemurafenib by oral gavage once a day for 5 days and mibefradil in drinking water on the next 5 days; and 4) vehicle: 0.5 % HPMC solution by oral gavage once a day for 5 days. Animals were treated in 2 cycles. Tumor volume, animal weight (18-20 Kg) and welfare were monitored daily. Tumor measurements were conducted using a caliper and tumor volume was calculated using the following formula = (length x width2) x 0.5. Animals were sacrificed by cervical dislocation once the tumor volume reached 1000 mm^3. Drug administration or euthanasia did not require the use of anesthesia. Animals were maintained in the animal house facility under optimal conditions and with food and water ad libitum. All animal experiments were performed according to procedures approved by the German authorities.

3.2.18 Whole Genome microarray analysis

Total RNA was isolated as it is described in section 3.2.5. Afterwards, RNA was labeled and hybridized to GeneChip® Mouse Genome 430 2.0 Array (Affymetrix, Santa Clara, CA, USA) by DKFZ Genomics and Proteomics Core Facility. After normalization using RMA method, fold change and p value of differentially expressed genes between + dox vs - dox cells were derived from the CEL files, using Chipster software. Additional samples were hybridized to Illumina MouseRef-8 v2.0 Expression BeadChips by DKFZ Genomics and Proteomics Core Facility. Enrichment analyses were made using Ingenuity Pathway Analysis (IPA) (Ingenuity® Systems, CA, USA, www.ingenuity.com) in order to identify upstream pathways, regulators and predictors. The RNA sequencing data can be downloaded with the GEO accession number: GSE122399, GSE122402 and GSE122763.

Additionally, RNA-Seq data for 459 melanoma patients with follow-up information was downloaded from the TCGA-SKCM project (https://portal.gdc.cancer.gov/projects/TCGA-SKCM), including 357 metastatic samples and 102 primary tumor samples. Recursive partitioning[115] based on tissue type and log2-transformed FPKM expression values for CACNA1H was performed by Dr. Thomas Hielscher from DKFZ biostatistics division, to identify risk groups for overall survival. P-value was adjusted for multiple testing using Bonferroni correction. Software R 3.5 including add-on packages TCGAbiolinks[116] and partykit were used for analysis.

3.2.19 Statistical analysis

All results are expressed as mean ± SEM from at least three or more independent experiments. Differences were analyzed using one-way ANOVA followed by post-hoc test Bonferroni or Tukey. Data analyses and graphs were made with GraphPad Prism (GraphPad Software, Inc.). $P < 0.05$ was considered statistically significant. Dr. Thomas Hielscher from DKFZ biostatistics division used Log-rank test to compare survival curves from *in vivo* experiments. Tumor growth curves were compared between treatments by fitting a linear mixed model for tumor volume with predictor time, treatment and interaction between time and treatment as fixed effects, and random intercept and slope effect for each mouse. The interaction term was tested to compare the growth rate relative to the vehicle group. P-values were adjusted for multiple comparisons using Holm correction. Software R 3.5 was used for analysis.

4. Results

4.1 Partial reprogramming of melanoma cells and induction of de-differentiation.

In order to transform melanoma cells into a more dedifferentiated stage, the method described previously by Knappe N *et al* 2016 was used. Nras-mutant C790 and Braf-mutant 4434 murine melanoma cells were partially reprogrammed for 20 days using a lentiviral vector containing Oct4, Klf4 and Sox2 genes (Figure 10a, b). De-differentiation status was confirmed by morphological changes observed during the process of partial reprogramming (Figure 10c). Additionally, analysis of the expression of markers of stemness and melanocytic lineage differentiation showed that Mitf and Pmel expression was significantly decreased while endogenous expression of Sox2, Oct4 and Ssea-1 increased, confirming that melanoma cells were dedifferentiated (Figure 10d). High ectopic expression of transcription factor Oct4 was also confirmed in reprogrammed cells (Supplementary Figure S1).

Moreover, results from RNA array supported the increment in the expression of stemness related markers in C790 and 4434 partially reprogrammed murine cells (Figure 10e). Enrichment analysis with Ingenuity Pathway Analysis (IPA) predicted activation of mouse embryonic stem cell pluripotency-related genes as well as survival-related pathways (Supplementary Figure S2 and Supplementary Figure S3), supporting the successful de-differentiation of the reprogrammed cells.

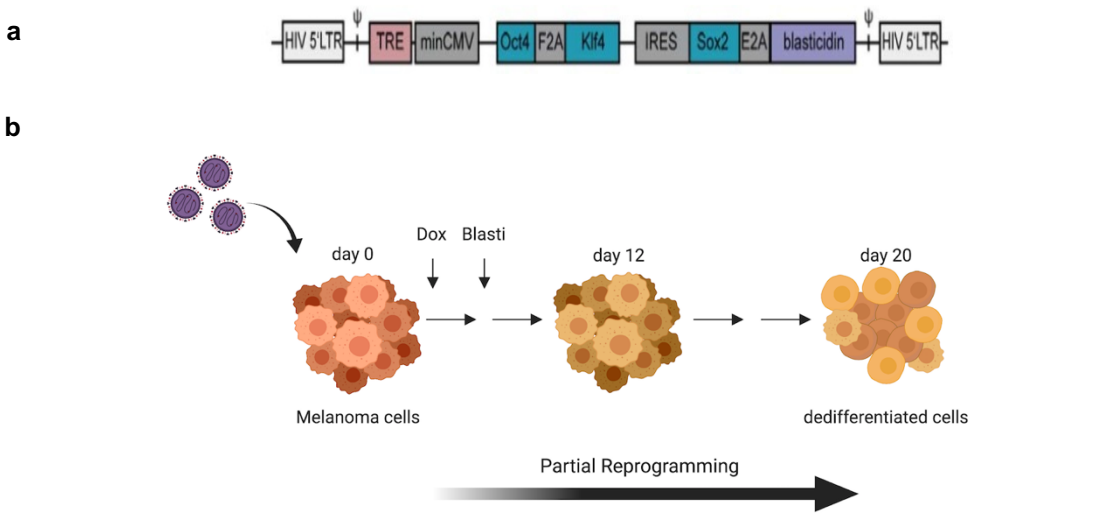
a
HIV 5'LTR
TRE
minCMV
Oct4
F2A
Klf4
IRES
Sox2
E2A
blasticidin
HIV 5'LTR
b
day 0
Dox
Blasti
day 12
day 20
Melanoma cells
dedifferentiated cells
Partial Reprogramming

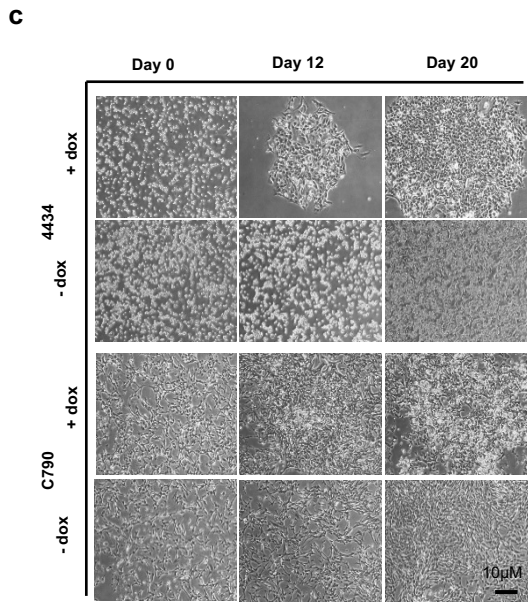
c
Day 0
Day 12
Day 20
4434
+ dox
- dox
C790
+ dox
- dox
10μM

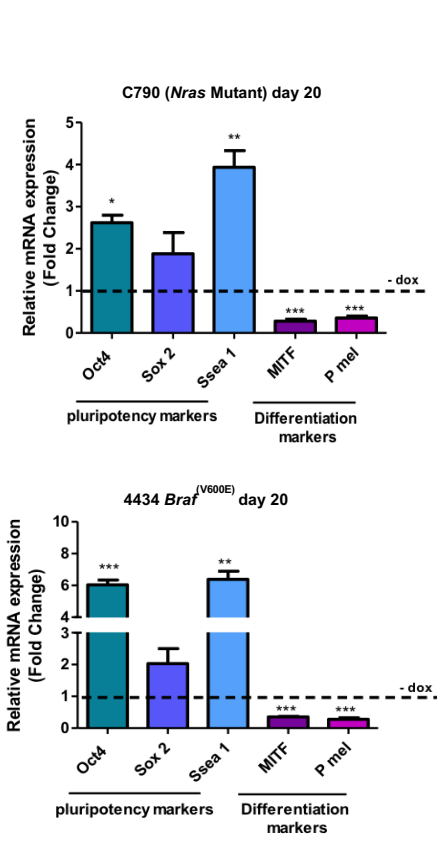
d
C790 (Nras Mutant) day 20
Relative mRNA expression (Fold Change)
- dox
Oct4
Sox 2
Ssea 1
MITF
P mel
pluripotency markers
Differentiation markers
4434 Braf(V600E) day 20
Relative mRNA expression (Fold Change)
- dox
Oct4
Sox 2
Ssea 1
MITF
P mel
pluripotency markers
Differentiation markers

e

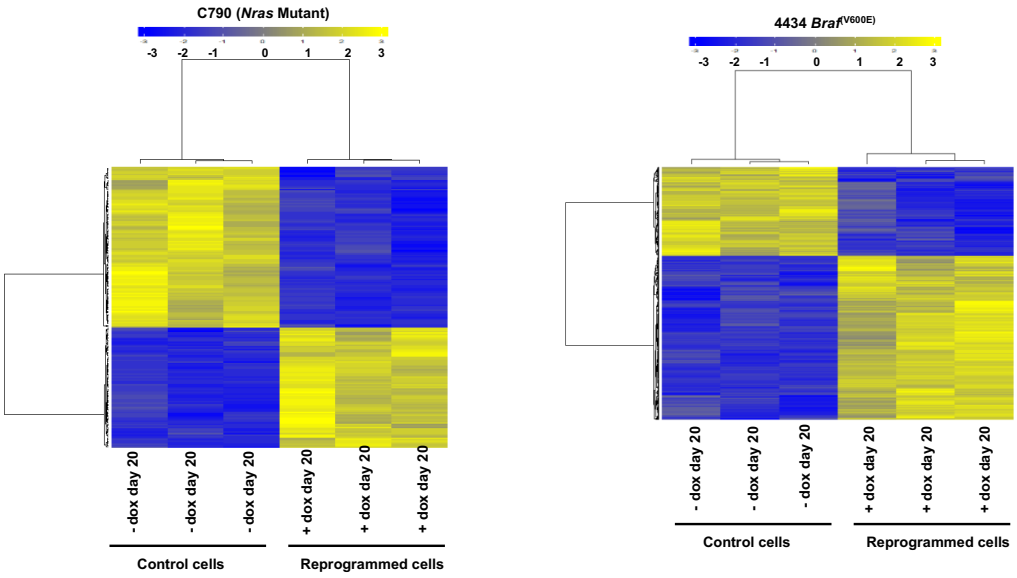

Figure 10. De-differentiation of murine melanoma cells using the partial reprogramming *in vitro* model. a Structure of lentiviral vector used to reprogram cells. Cells were co-infected with a lentiviral vector harboring the reverse tetracycline-controlled transactivator (rtTA) and an expression vector carrying murine genes for Oct4, Klf4 and Sox2 and a blasticidin-resistance gene. Cells not induced with doxycycline but transduced with both vectors were used as a control. **b** Schematic representation of the workflow of partial reprogramming method. After infection, doxycycline was added to the medium to induce transgene expression and on day 3 blasticidin was added to select transduced cells. Cells were reprogrammed for 20 days. Medium without doxycycline was used for control cells during all experiments. c Representative images of morphological changes during partial reprogramming. Scale bars represent 10µm. **d** Real-Time qPCR analysis of the expression of stemness markers *Sox2, Oct4* and *Ssea-1*, as well as melanocytic lineage differentiation markers *Mitf* and *Pmel*, for C790 and 4434 at day 20 of reprogramming. Data was normalized using control cells ("- dox") as reference and GAPDH as housekeeping gene. **e** Differential Gene Expression analysis. Heat map of microarray data showing hierarchical clustering of differentially expressed genes between partially reprogrammed C790 (left) or 4434 (right) cells ("+dox") and control cells ("-dox") at day 20; blue and yellow colors indicate differentially down- or upregulated genes, respectively (FC > 2-fold). All data are represented as mean ± SEM of three or more independent experiments. Statistical analyses were performed with One Way ANOVA and post-hoc test Tukey; *p < 0.05, **p < 0.01 and ***p < 0.001.

4.2 Evaluation of melanoma phenotype switching during partial reprogramming.

During melanoma phenotype switching cells can adopt a more invasive and slow-cycling state[39]. To determine if the *in vitro* model of reprogramming previously described could simulate features of the melanoma phenotype switching and the intermediate stages of tumor progression; proliferation capacity, migration and invasion potential of partially reprogrammed cells were evaluated.

EdU incorporation assay revealed a significant reduction in proliferation of C790 and 4434 partially reprogrammed cells compared to control cells ("- dox") (Figure 11a, b) by reducing percentage of cells in S phase along with an increase of cells in G1 phase at day 20 (Figure 11c). In addition, the reprogrammed cells showed a more aggressive phenotype due to the increment in the number of invading cells (Figure 11d, e) and the enhanced migration capacity ("+ dox") compared with the control cells ("- dox") (Figure 11f, g). Together, these results suggest that partial reprogramming of murine melanoma cells resembles the phenotypic switch that normally occurs during melanoma progression.

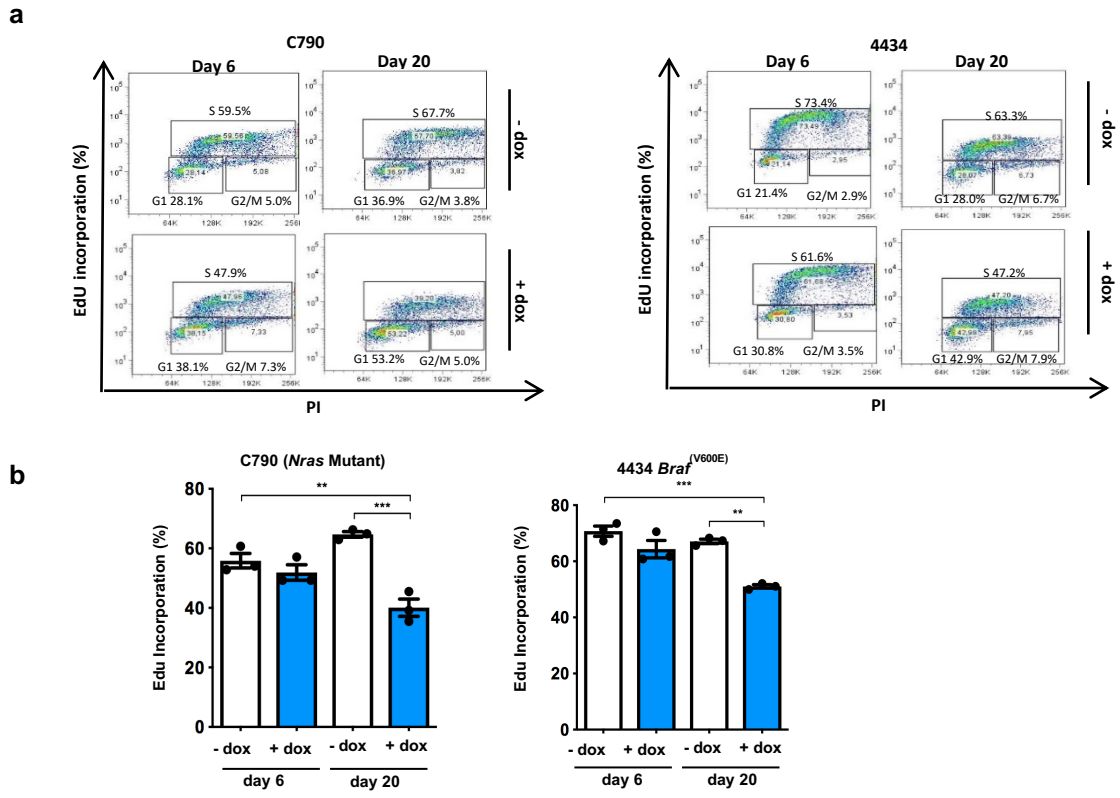

c

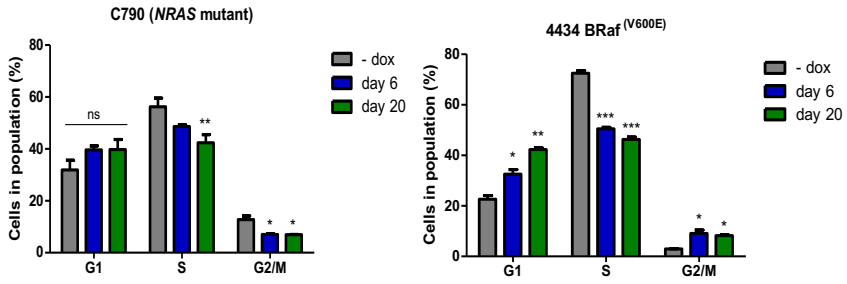
C790 (NRAS mutant)
Cells in population (%)
ns
**
*
*
G1
S
G2/M
- dox
day 6
day 20
4434 BRaf (V600E)
*
**
***
***
*
*

d

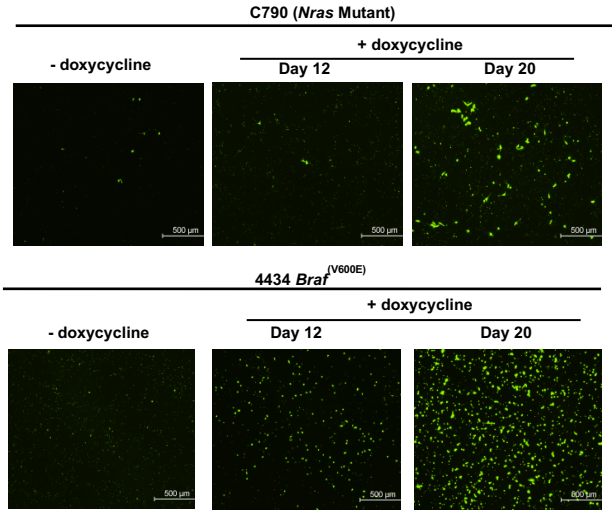
C790 (Nras Mutant)
- doxycycline
+ doxycycline
Day 12
Day 20
500 µm
4434 Braf (V600E)
- doxycycline
+ doxycycline
Day 12
Day 20
500 µm
500 µm
500 µm

e

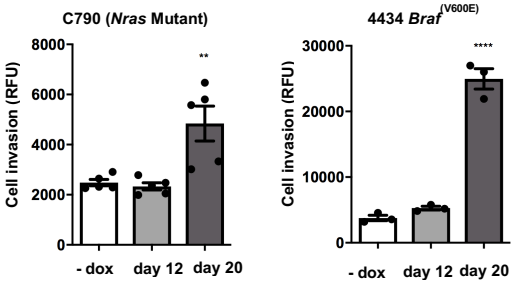
C790 (Nras Mutant)
Cell invasion (RFU)
**
- dox
day 12
day 20
4434 Braf (V600E)
Cell invasion (RFU)
****
- dox
day 12
day 20

f

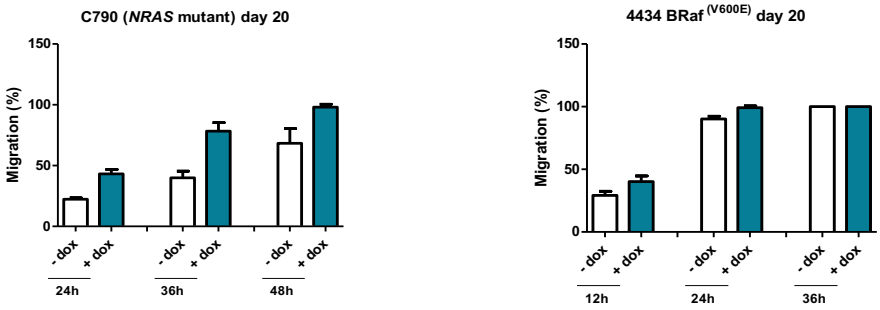
C790 (NRAS mutant) day 20
Migration (%)
- dox
+ dox
24h
36h
48h
4434 BRaf (V600E) day 20
Migration (%)
- dox
+ dox
12h
24h
36h

g

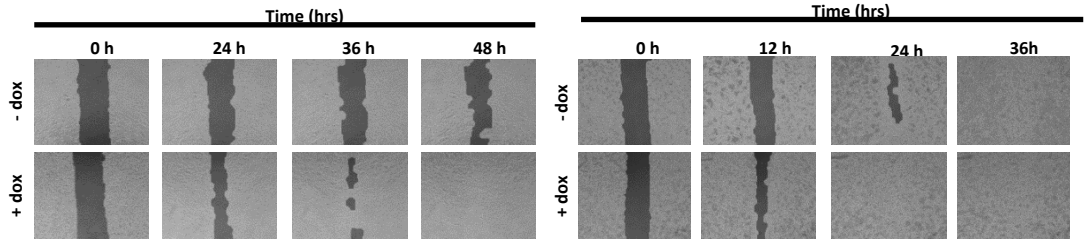
Time (hrs)
0 h
24 h
36 h
48 h
- dox
+ dox
Time (hrs)
0 h
12 h
24 h
36h
- dox
+ dox

Figure 11. Partially reprogrammed melanoma cells acquire characteristics of cancer cells that underwent phenotype switching. a Representative flow cytometry plots showing EdU incorporation in C790 and 4434 reprogrammed cells at day 6 and 20. **b** Percentage of EdU positive cells at day 6 and 20 of partial reprogramming is shown. **c** Quantification of the percentage of reprogrammed C790 and 4434 cells in different cell cycle phases at day 6 and 20 using EdU proliferation assay **d** Representative fluorescence microscopy images of fluorescence microscopy for cell invasion assay in C790 and 4434 reprogrammed cells. **e** Cell invasion assessed by the FluoroBlok invasion assay. Invasion was evaluated at different time points during partial reprogramming. After 20 hours incubation, invading cells were labeled and relative fluorescence units were obtained (RFUs= relative fluorescence units). **f** Scratch assay was used to measured migration capacity in C790 and 4434 reprogrammed cells. Percentage of migration was calculated after 24, 36 ad or 48 hours. **g** A representative image of scratch assay with C790 and 4434 cells. All data represent the mean ± SEM of three or more independent experiments. Statistical analyses were performed with One Way ANOVA and post-hoc test Tukey; *p < 0.05, **p < 0.01 and ***p < 0.001.

4.3 Effect of MAPK inhibitor treatment (MAPKi) on the cell viability of partially reprogrammed C790 and 4434 cells.

Development of resistance to therapies has been associated with the de-differentiation status of tumor cells [117]. I evaluated the effect of the treatment with vemurafenib (BRAF inhibitor) and trametinib (MEK inhibitor) on the cell viability in C790 and 4434 partially reprogrammed cells using the Alamar Blue assay. Cell viability was quantified after 72 hours of treatment with trametinib, vemurafenib or the combination of trametinib and vemurafenib. Cell viability increased in partially reprogrammed cells ("+ dox") throughout day 6, 12 and 20 of reprogramming compared to control cells ("- dox"). Treatment with trametinib alone revealed that C790 control cells were more sensitive (mean IC50=2.09 ± 0.48 μM) compared to C790 reprogrammed cells at day 20 (mean IC50>10 μM) (Figure 12a). Similarly, single treatment with vemurafenib in 4434 reprogrammed cells induced an increment in viability in comparison with the control cells (Figure 12b). In addition, combination treatment of vemurafenib and trametinib in 4434 reprogrammed cells also revealed a higher IC50 value at day 20 (mean IC50=4.38 ± 0.03 μM) compared to 4434 control cells (mean IC50=0.0029 ± 0.0010 μM) (Figure 12c). This increment in the IC50 values after treatment with MAPKi support the development of resistance in dedifferentiated melanoma cells after partial

reprograming. All IC50 values for all treatments are shown in Supplementary Tables S1 and S2.

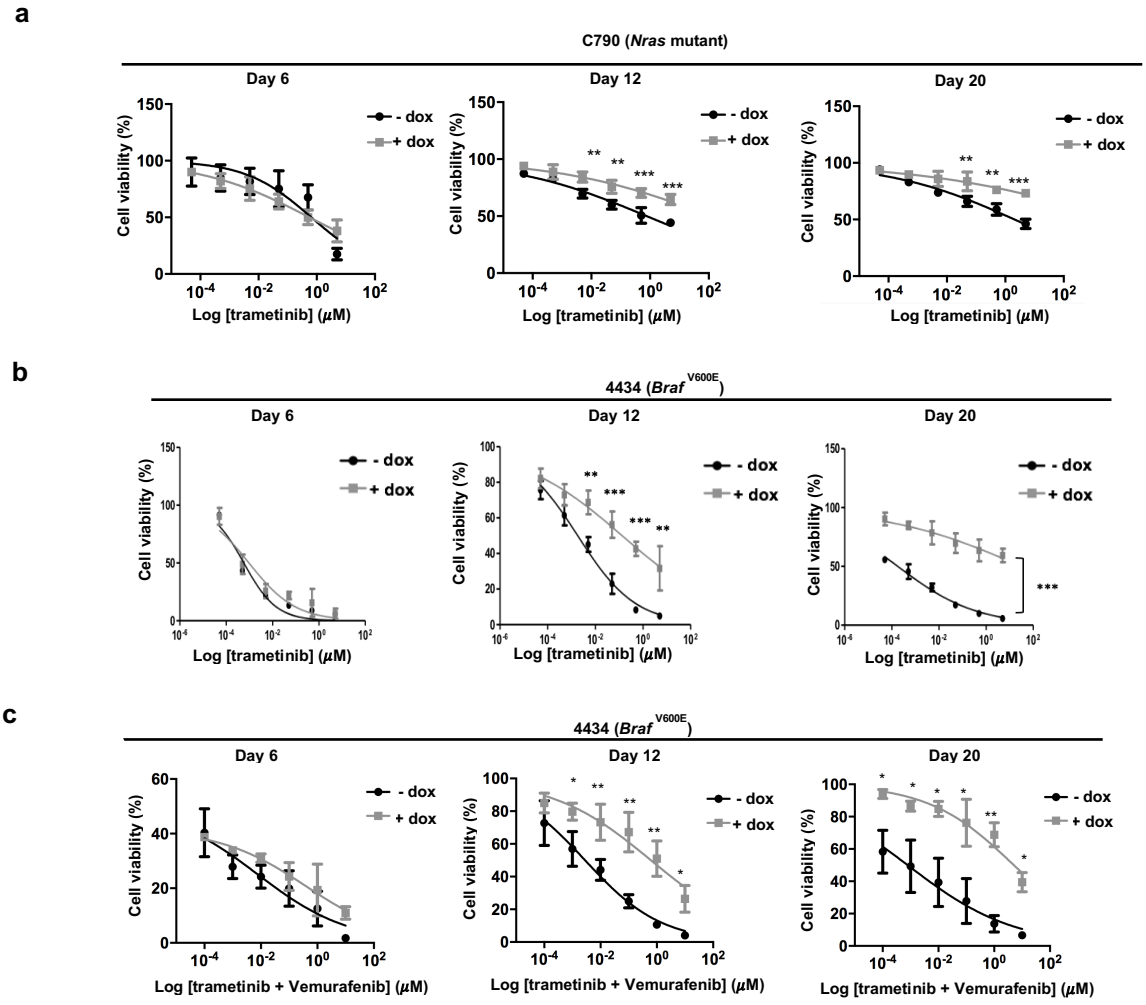

Figure 12. Effect of partial reprogramming on the sensitivity of C790 and 4434 cells to treatment with MAPKi. a *Nras*-mutant cells (C790) were treated with trametinib (10μM to 0.0001μM) for 72 hours. Subsequently, an Alamar blue assay was performed and the fluorescence emission (read at 590nm) was measured. Cell viability was evaluated at days 6, 12 and 20 of reprogramming. Cytotoxicity curves represent as the mean ± SEM (n= 6). **b, c** *BRAF*-mutant cells (4434) were treated with trametinib alone or with the combination of trametinib and vemurafenib (10μM to 0.0001μM) for 72 hours, then alamar blue assay was performed and the fluorescence emission (read at 590 nm) was measured. Cell viability was evaluated at days 6, 12 and 20 of reprogramming. Cytotoxicity curves represent as the mean ± SEM (n= 6). Statistical analyses were performed with One Way ANOVA and post-hoc test Tukey; *p < 0.05, **p < 0.01 and ***p < 0.001.

4.4 Effect of MAPKi treatment on cell death of C790 and 4434 partially reprogrammed cells.

In order to investigate whether cell death was also affected in partially reprogrammed cells after treatment with MAPKi, apoptosis was measured by flow cytometry using Annexin V / PI staining. The percentage of apoptotic cells was significantly reduced upon treatment with trametinib (15 μM), at day 6, 12 and 20 in C790 partially reprogrammed cells ("+ dox") compared to control cells ("- dox"). The percentage of apoptosis was also diminished in C790 reprogrammed cells after treatment with doxorubicin (0.003 μM) (Figure 13a, b). Similar results were obtained at day 12 and 20 for 4434 reprogrammed cells, treated with trametinib (8 μM), vemurafenib (15 μM) or trametinib in combination with vemurafenib (8 μM) (Figure 14a, b). In addition, activation of caspase-3 was suppressed in all reprogrammed cells after treatment with MAPKi compared to control cells (Figure 13c and Figure 14c). Together these findings support that partially reprogrammed cells become less sensitive to MAPKi, due to the decrease of caspase activation and apoptosis.

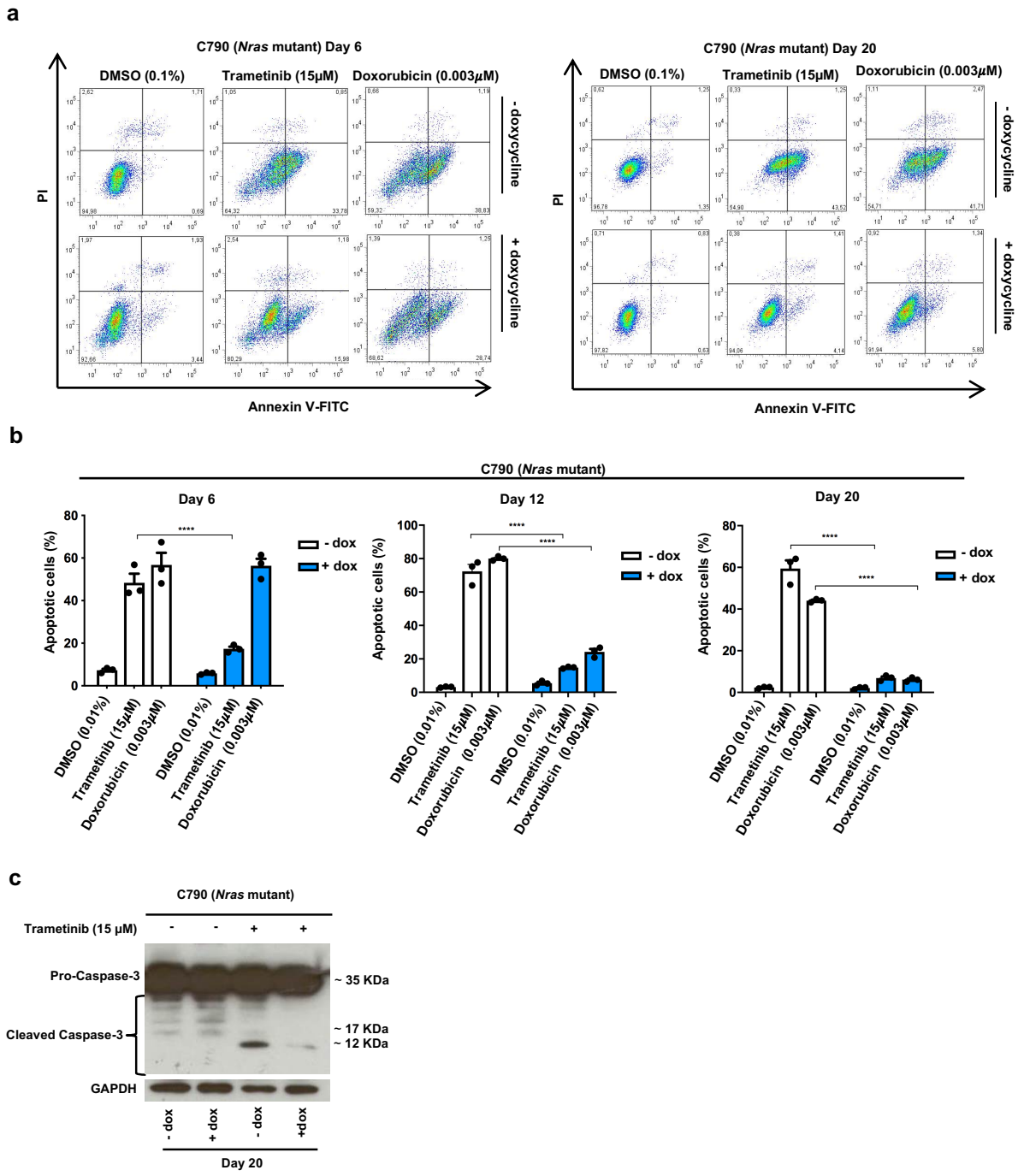

Figure 13. Cell death analysis of C790 partially reprogrammed cells after treatment with MAPKi. a Representative scatter plots of PI (y-axis) vs. annexin V (x-axis) for day 6 and 20 of partial reprogramming of C790 cells. Early apoptotic cells are shown in the lower right quadrant and late apoptotic cells are shown in the upper right quadrant. **b** Apoptosis evaluation after staining with FITC-Annexin V/PI. Cells were treated with trametinib (15 μM) and with doxorubicin (0.003 μM) to induce apoptosis (positive control) during 72 hours. Percentage of apoptotic cells (early and late apoptosis) is shown as mean ± SEM (n=3). **c** Western Blot analysis. Whole cell lysate was immunoblotted with GAPDH and caspase-3 antibodies at day

20 of reprogramming after treatment with trametinib (15 μM). Statistical analyses were performed with One Way ANOVA and post-hoc test Tukey; ***p < 0.001.

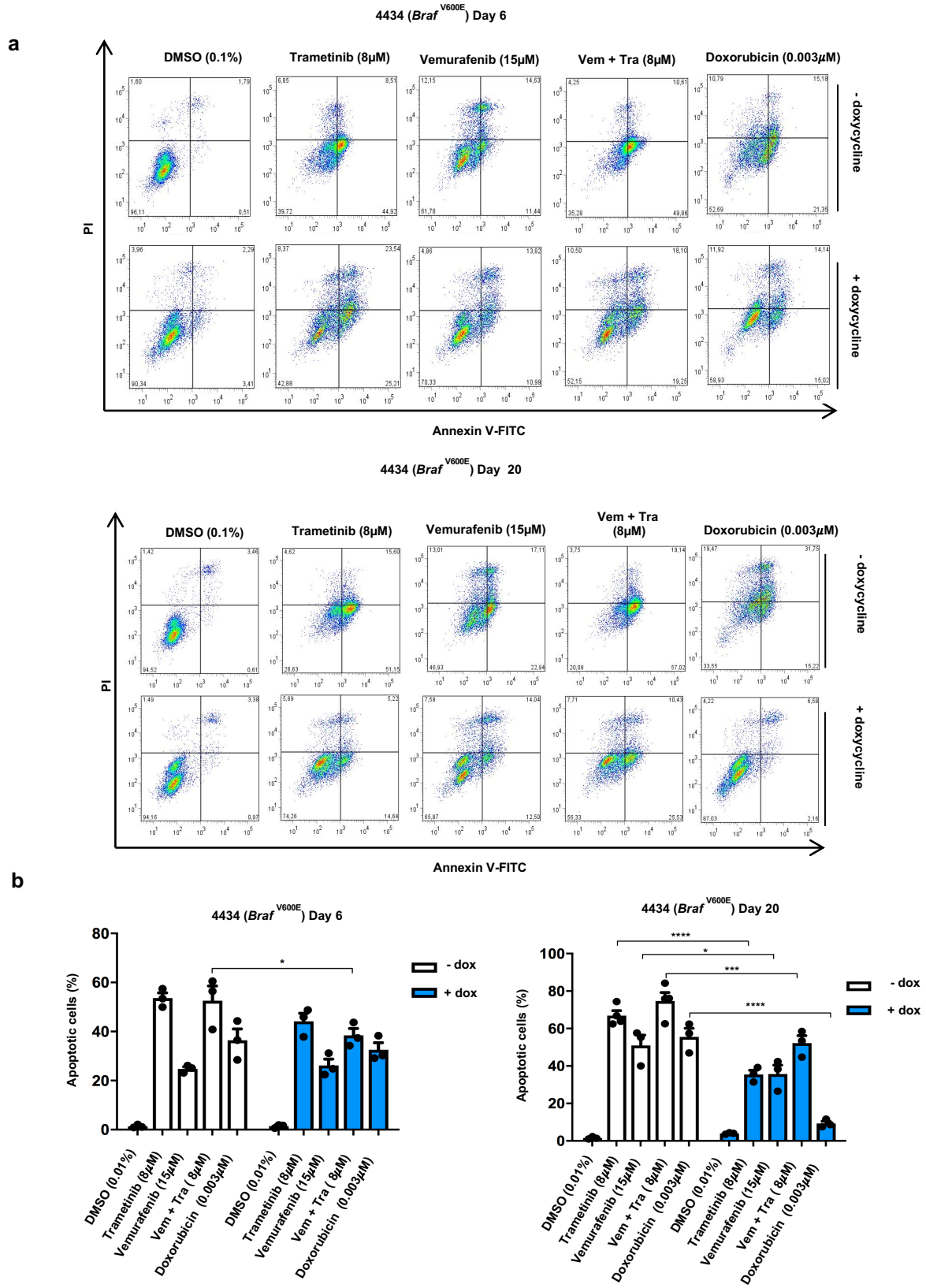

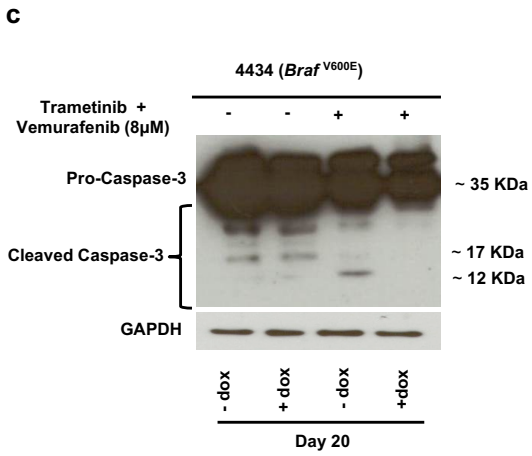

Figure 14. Cell death analysis of 4434 partially reprogrammed cells after treatment with MAPKi. a Representative scatter plots of PI (y-axis) vs. annexin V (x-axis) for day 6 and 20 of partial reprogramming of 4434 cells. Early apoptotic cells are shown in the lower right quadrant and late apoptotic cells are shown in the upper right quadrant. **b** Apoptosis evaluation after staining with FITC-Annexin V/PI. Cells were treated with trametinib, vemurafenib (8 μM) and with doxorubicin (0.003 μM) to induce apoptosis (positive control during 72 hours. Percentage of apoptotic cells (early and late apoptosis) is shown as mean ± SEM (n=3). **c** Western Blot analysis. Whole cell lysate was immunoblotted with GAPDH and caspase-3 antibodies at day 20 of reprogramming after treatment with trametinib and vemurafenib (8 μM). Statistical analyses were performed with One Way ANOVA and post-hoc test Tukey; *p < 0.05, **p < 0.01 and ***p < 0.001.

4.5 The mechanism behind resistance to MAPKi treatment in C790 and 4434 partially reprogrammed cells.

Vemurafenib and trametinib are compounds that can specifically target and inhibit components of the RAS-RAF-MEK-ERK cascade also known as the MAPK pathway[48]. In order to elucidate the mechanism driving the desensitization of partially reprogrammed cells to vemurafenib or trametinib, inhibition of ERK protein from the MAPK pathway was analyzed by western blot (Figure 15a, b). Phosphorylation of ERK protein was impaired in both C790 and 4434 reprogrammed cells as well as in control cells, indicating that the MAPK pathway inhibition is still functional independently from the de-differentiation status of the cells.

To broaden the search for possible resistance mechanisms in C790 partially reprogrammed cells after treatment with MAPKi, gene expression analysis was performed (Figure 15c). The obtained dendrogram showed some of the genes differentially expressed between reprogrammed ("+ dox") and control cells ("- dox")

after treatment with either DMSO or trametinib. Further analysis using IPA software revealed upstream regulators that might be involved in regulation of drug sensitivity after partial reprograming of melanoma cells (Figure 15d).

T-type calcium channels were found to be significantly upregulated in resistant cells, suggesting them as a target to be involved in therapy resistance of melanoma. The expression of the T-type calcium channel CACNA1H was confirmed on the RNA level in both C790 and 4434 partially reprogrammed cells (Figure 15e), highlighting the possible connection of calcium signaling with development of resistance to MAPKi.

The relevance of targeting T-type calcium channels to improve therapy effects in melanoma patients was addressed using the TCGA-SKCM database. TCGA analysis showed that melanoma patients with high expression of CACNA1H have a worse survival outcome compared with those with low CACNA1H expression ($p = 0.029$) (Figure 15f). Based on these data, the role of T-type calcium channels in the resistance to MAPKi of dedifferentiated melanoma cells was further explored.

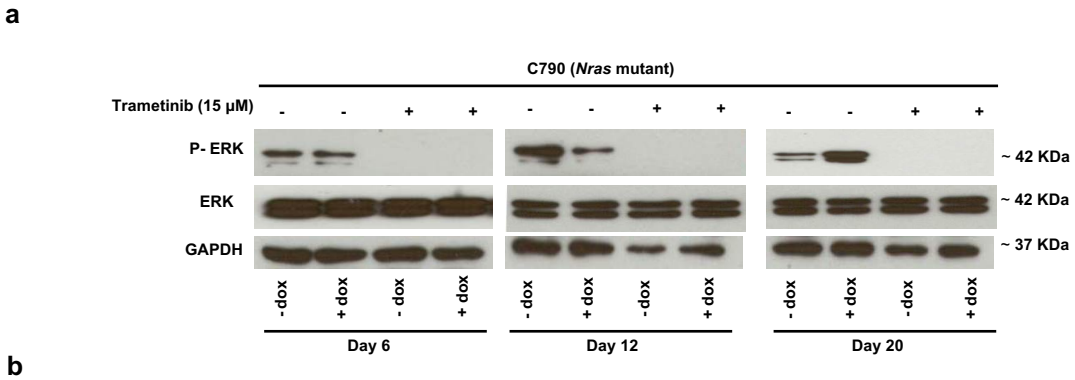

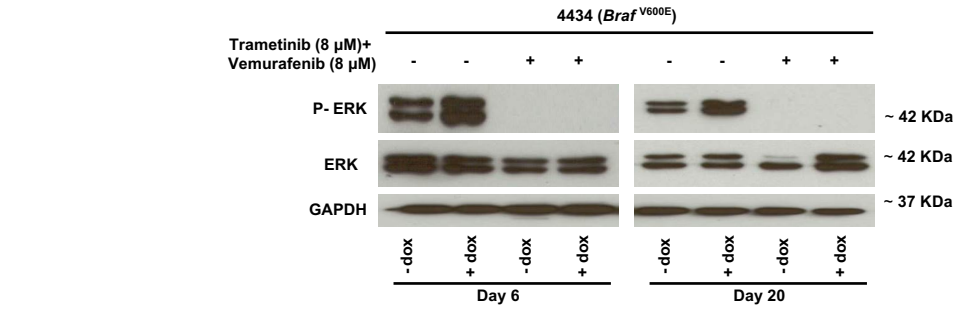

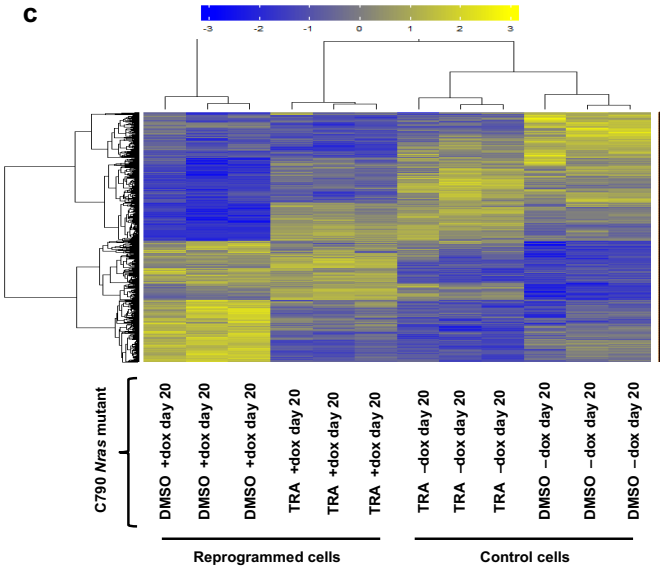

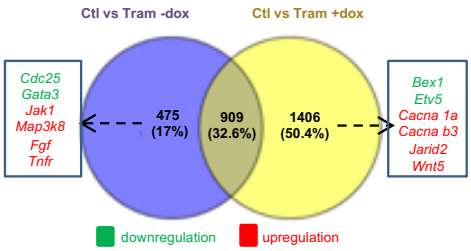

IPA analysis: Top Upstream Regulators

Upstream Regulator	P-value of overlap
T-type Calcium Channels	2.08E-04
SETX	2.08E-04
ALKBH5	2.13E-04
HSD17B1	2.02E-03
PDZK11P1	3.00E-03

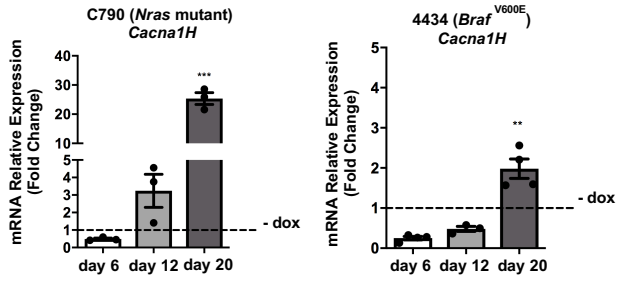

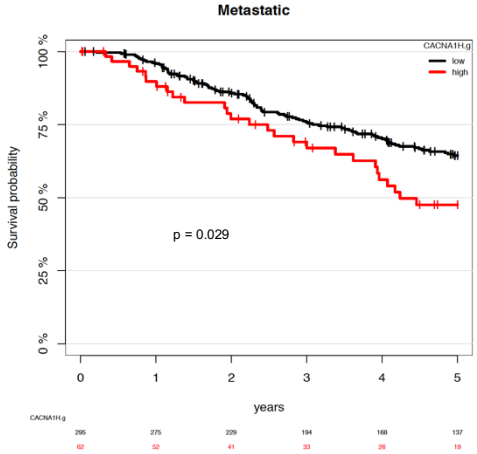

Figure 15. Expression analysis of MAPKi-resistant cells shows an upregulation of T-Type calcium channels. a, b Western blot analysis. Whole cell lysates from C790 and 4434 melanoma cells were immunoblotted with antibodies against GAPDH, ERK and P-ERK. **c** Differential gene expression analysis comparing C790 partially reprogrammed cells with control cells. Heat map of microarray data showing hierarchical clustering of 2700 differentially expressed genes in C790 partially reprogrammed cells after 72 hours treatment with DMSO (control) and trametinib; control ("-dox") and reprogrammed cells ("+dox") were evaluated both at day 20. Blue or yellow colors indicate differentially down- or upregulated genes, respectively (FC > 2-fold). **d** Analysis of gene expression data by a Venn diagram showing the analysis of treatments between control cells and reprogrammed cells (2700 genes). The blue circle (474 genes) indicates the number of genes exclusively expressed in control vs. trametinib ("-dox"); yellow circle (1,406 genes) indicates the number of genes exclusively expressed in control vs. trametinib ("+dox"). Some of the deregulated genes are listed; green and red colors indicate differentially up- or down regulated genes, respectively. Moreover, results from the IPA analysis of upstream regulators from C790 partially reprogrammed cells at day 20 after treatment with trametinib are listed. **e** Real-Time qPCR analysis of *Cacna1h* expression at different days of reprogramming for both C790 and 4434 cells. Data were normalized using control cells as reference and *Gapdh* was used as a housekeeping gene. **f.** Kaplan–Meier curves showing the OS of 357 metastatic melanoma patients depending on the level of CACNA1H expression. The data were obtained from the TCGA database. Expression values for CACNA1H gene were dichotomized into high (red) and low (black) expression using recursive partitioning ($p = 0.02$). Data represent the mean ± SEM of three or more independent experiments. Statistical analyses were performed with One Way ANOVA and post-hoc test; $^{**}p < 0.01$ and $^{***}p < 0.001$.

4.6 The effect of T type calcium channel inhibition on drug sensitivity of reprogrammed and MAPKi-resistant murine melanoma cells.

Reprogrammed cells C790 and 4434 were treated with the calcium channel inhibitors mibefradil or lomerizine for 24 hours to determine whether the inhibition of T-type calcium channels can induce cell death or affect cell viability. My data showed a reduction of cell viability in partially reprogrammed cells ("+ dox") compared to control cells ("- dox") (Figure 16a and Figure 17a). Dedifferentiated cells at day 20 were slightly more sensitive to mibefradil (C790 mean IC50= 5.9 ± 0.74 μM; 4434 mean IC50= 8.87 ± 0.25 μM) than control cells (C790 mean IC50= 6.44 ± 0.66 μM; 4434 mean IC50= 7.82 ± 0.96 μM). Similar results were observed with lomerizine (Supplementary Tables S3 and S4).

In addition, single treatments with mibefradil or lomerizine significantly increased the percentage of apoptotic cells after 24 hours in both C790 (Figure 16b, c) and 4434 partially reprogrammed cells (Figure 17b, c), suggesting that inhibition of T-type calcium channels promoted apoptosis and affected cell viability in dedifferentiated and MAPKi-resistant cells.

Based on the previous results and the high expression of T-type calcium channel in dedifferentiated cells (Figure 15e), the possibility of using these channels as targets to re-sensitize MAPKi-resistant cells was considered. Therefore, C790 and 4434 reprogrammed cells were treated with mibefradil or lomerizine for 24 hours followed by treatment with MAPKi for another 24 hours (sequential treatment) to evaluate their effect on drug sensitivity.

The percentage of apoptotic cells was significantly increased in partially reprogrammed cells after the sequential treatment (Figure 16b, d and Figure 17b, d). Moreover, the capacity of colony formation was significantly reduced in C790 partially reprogrammed cells after sequential treatment, (Figure 16e, f), suggesting that previous sensitization with mibefradil increased cell death and decreased the capacity of unlimited cell reproduction after treatment with MAPKi. Similar results were obtained in 4434 partially reprogrammed cells (Figure 17e, f).

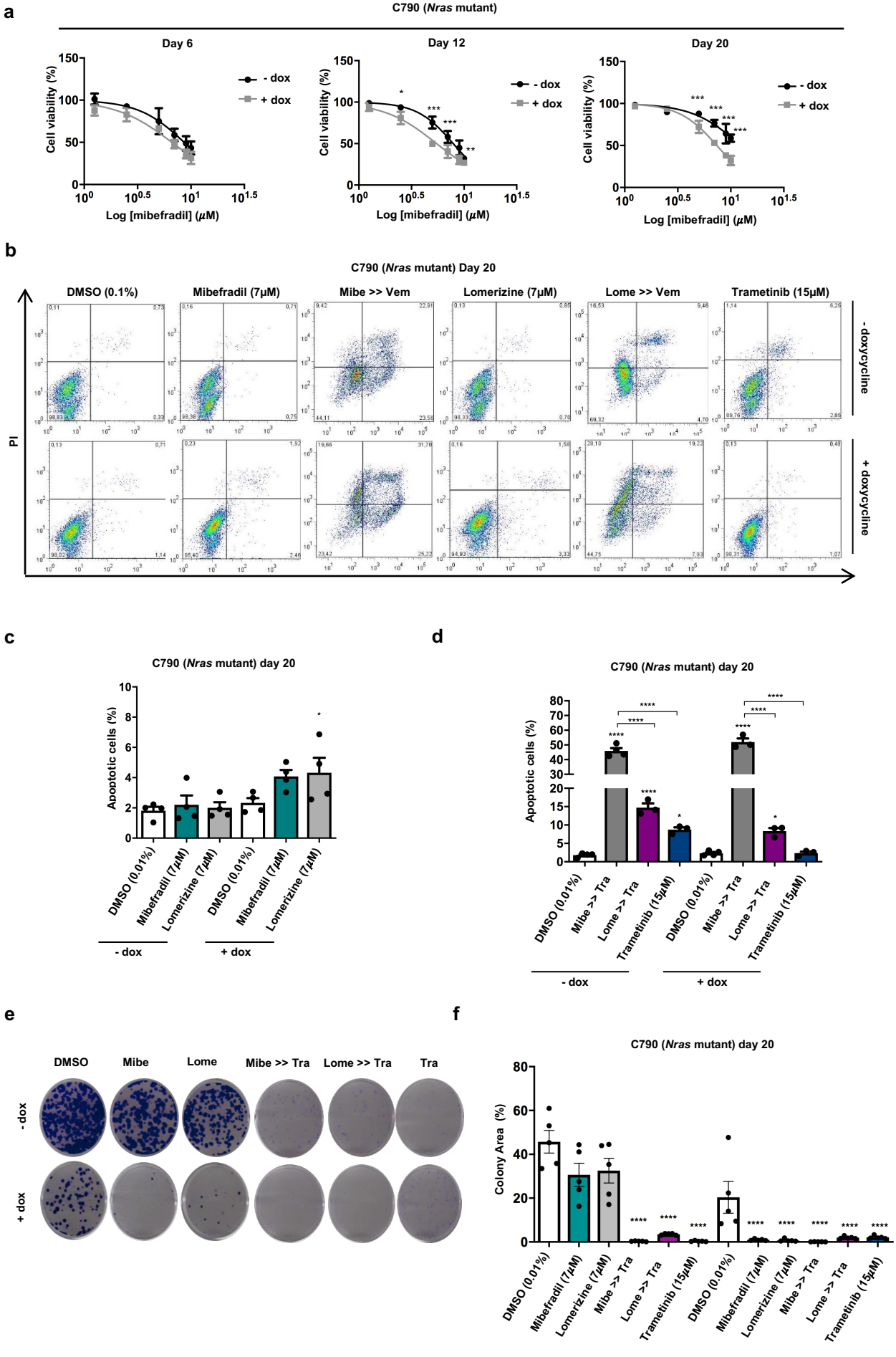
a
C790 (Nras mutant)
Day 6
Day 12
Day 20
Cell viability (%)
Log [mibefradil] (μM)
- dox
+ dox
b
C790 (Nras mutant) Day 20
DMSO (0.1%)
Mibefradil (7μM)
Mibe >> Vem
Lomerizine (7μM)
Lome >> Vem
Trametinib (15μM)
PI
- doxycycline
+ doxycycline
c
C790 (Nras mutant) day 20
Apoptotic cells (%)
DMSO (0.01%)
Mibefradil (7μM)
Lomerizine (7μM)
- dox
+ dox
d
C790 (Nras mutant) day 20
Apoptotic cells (%)
DMSO (0.01%)
Mibe >> Tra
Lome >> Tra
Trametinib (15μM)
- dox
+ dox
e
DMSO
Mibe
Lome
Mibe >> Tra
Lome >> Tra
Tra
- dox
+ dox
f
C790 (Nras mutant) day 20
Colony Area (%)
DMSO (0.01%)
Mibefradil (7μM)
Lomerizine (7μM)
Mibe >> Tra
Lome >> Tra
Trametinib (15μM)

Figure 16. Inhibition of calcium channels increased sensitivity to MAPK inhibitors in C790 partially reprogrammed cells. a Cell viability was performed using alamar blue assay. Partially reprogrammed cells C790 were treated with mibefradil (1.25 - 10 μM) for 24 hours. After alamar blue assay, the fluorescence (at 590 nm) was measured. Cell viability was evaluated at days 6, 12 and 20 of reprogramming. **b** Representative scatter plots of PI (y-axis) vs. annexin V (x-axis) for day 20 of partial reprogramming. Early apoptotic cells are shown in the lower right quadrant and late apoptotic cells are shown in the upper right quadrant. Mibe: mibefradil (7 μM). Lome: lomerizine (7 μM). Mibe (Lome) >>Tra: sequential treatment with mibefradil (lomerizine) for 24 hours, followed by trametinib (15 μM) for another 24 hours. **c** Apoptosis analysis using annexinV/PI staining. Cells were treated with mibefradil (7 μM) and lomerizine (7 μM) for 24 hours. Percentage of apoptotic cells (early and late apoptosis) is shown as mean ± SEM (n= 3). **d**. Apoptosis analysis using sequential treatment with calcium channel blockers and MAPKi. Percentage of apoptotic cells (early and late apoptosis) is shown as mean ± SEM (n= 3). **e** Clonogenic assay of partially reprogrammed cells C790 treated with DMSO (0.01%), mibefradil (7 μM), lomerizine (7 μM), Mibe (Lome) >>Tra: sequential treatment with mibefradil (lomerizine), and trametinib (15 μM) for 24 hours. Representative images of wells stained with crystal violet are shown. **f** Percentage of colony area for all treatments is shown as mean ± SEM (n=5) for partially reprogrammed cells C790. All data represent the mean ± SEM of three or more independent experiments. Statistical analyses were performed with One Way ANOVA and post-hoc test; *$p < 0.05$, **$p < 0.01$ and ***$p < 0.001$.

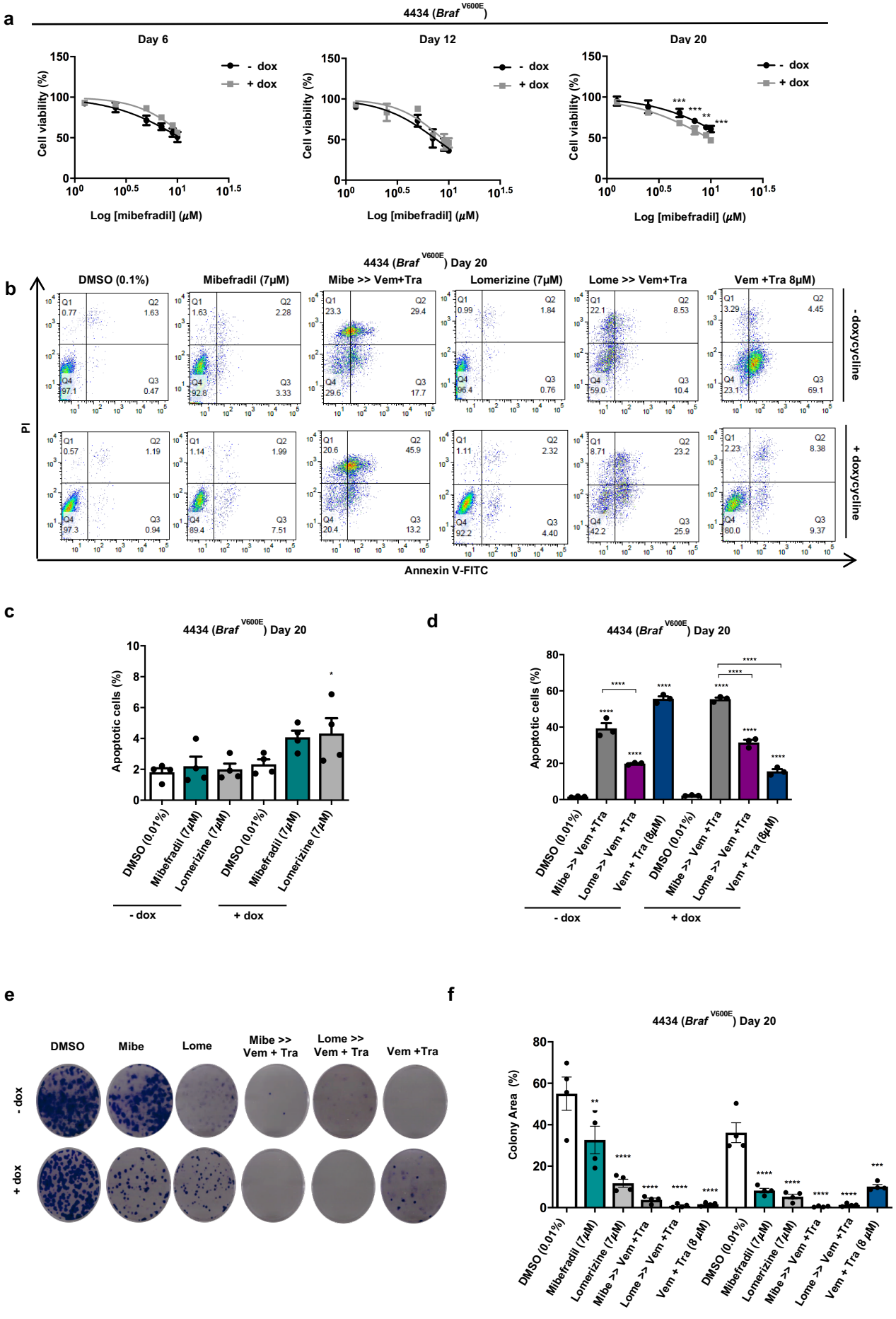
a
4434 (Braf V600E)
Day 6
Day 12
Day 20
- dox
+ dox
Cell viability (%)
Log [mibefradil] (μM)
b
4434 (Braf V600E) Day 20
DMSO (0.1%)
Mibefradil (7μM)
Mibe >> Vem+Tra
Lomerizine (7μM)
Lome >> Vem+Tra
Vem +Tra 8μM)
- doxycycline
+ doxycycline
PI
Annexin V-FITC
c
4434 (Braf V600E) Day 20
Apoptotic cells (%)
DMSO (0.01%)
Mibefradil (7μM)
Lomerizine (7μM)
- dox
+ dox
d
4434 (Braf V600E) Day 20
Apoptotic cells (%)
DMSO (0.01%)
Mibe >> Vem +Tra
Lome >> Vem +Tra
Vem + Tra (8μM)
- dox
+ dox
e
DMSO
Mibe
Lome
Mibe >> Vem + Tra
Lome >> Vem + Tra
Vem +Tra
- dox
+ dox
f
4434 (Braf V600E) Day 20
Colony Area (%)
DMSO (0.01%)
Mibefradil (7μM)
Lomerizine (7μM)
Mibe >> Vem +Tra
Lome >> Vem +Tra
Vem + Tra (8 μM)

Figure 17. Inhibition of calcium channels increases sensitivity to MAPK inhibitors in 4434 partially reprogrammed cells. a Cell viability was performed using alamar blue assay. Partially reprogrammed cells 4434 were treated with mibefradil (1.25 – 10 µM) for 24 hours. After alamar blue assay, the fluorescence (at 590 nm) was measured. Cell viability was evaluated at days 6, 12 and 20 of reprogramming. **b** Representative scatter plots of PI (y-axis) vs. annexin V (x-axis) for day 20 of partial reprogramming. Early apoptotic cells are shown in the lower right quadrant and late apoptotic cells are shown in the upper right quadrant. Mibe: mibefradil (7 µM). Lome: lomerizine (7 µM). Mibe (Lome) >> Vem+Tra: sequential treatment with mibefradil (lomerizine) 24 hours, followed by vemurafenib + trametinib (8 µM) for another 24 hours. **c** Apoptosis analysis using annexinV/PI staining. Cells were treated with mibefradil (7 µM) and lomerizine (7 µM) for 24 hours. Percentage of apoptotic cells (early and late apoptosis) is shown as mean ± SEM (n= 3). **d**. Apoptosis analysis using sequential treatment with calcium channel blockers and MAPKi. Percentage of apoptotic cells (early and late apoptosis) is shown as mean ± SEM (n= 3). **e** Clonogenic assay of partially reprogrammed cells 4434 treated with DMSO (0.01%), mibefradil (7 µM), lomerizine (7 µM), Mibe (Lome) >>Vem+Tra: sequential treatment with mibefradil (lomerizine), and Vem+Tra (8 µM) for 24 hours. Representative images of wells stained with crystal violet are shown. **f** Percentage of colony area for all treatments is shown as mean ± SEM (n= 5) for partially reprogrammed cells 4434. All data represent the mean ± SEM of three or more independent experiments. Statistical analyses were performed with One Way ANOVA and post-hoc test; *$p < 0.05$, **$p < 0.01$ and ***$p < 0.001$.

4.7 Influence of T-type calcium channel inhibition on the differentiation status of reprogrammed and MAPKi-resistant murine melanoma cells.

Although it is well-known that calcium participates as a second messenger in a variety of cellular processes, it remains unclear how calcium can regulate self-renewal capacity and stemness. It is possible that T-type calcium channels can affect the pluripotency status of reprogrammed cells by inducing differentiation. To test this hypothesis, the expression of specific stemness-related markers was evaluated in C790 and 4434 partially reprogrammed cells after treatment with mibefradil and lomerizine.

The expression of the stemness markers *Sox2*, *Ssea-1* and *CD271* was significantly reduced in reprogrammed cells after single treatment with mibefradil and lomerizine in reprogrammed cells ("+ dox") compared to control cells ("- dox") (Figure 18a, b), indicating that they adopted a more differentiated phenotype. Together, these and

previous data suggest that the modulation of calcium influx improved responses to MAPKi-resistant cells by promoting cell death and differentiation.

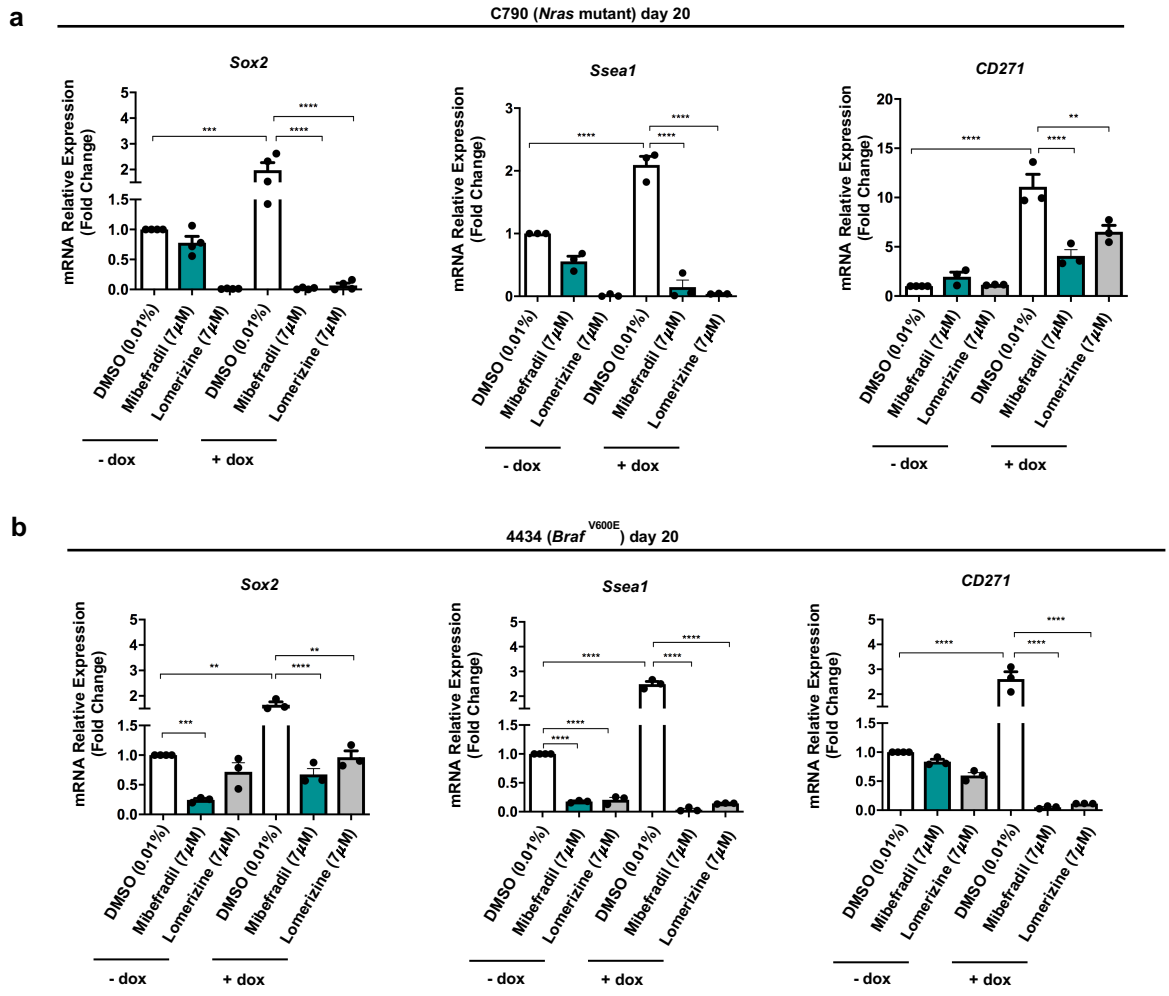

Figure 18. Inhibition of T-type calcium channels induced differentiation of reprogrammed and MAPKi-resistant melanoma cells. a Real-Time qPCR analysis of the expression of the stem cell markers *Sox2*, *Ssea-1* and *CD271*, at day 20 of partial reprogramming of C790 cells, after treatment with mibefradil or lomerizine. Data was normalized using control cells as reference and *Gapdh* as housekeeping gene. **b** Real-Time qPCR analysis of the expression of the stem cell markers *Sox2*, *Ssea-1* and *CD271*, at day 20 of partial reprogramming of 4434 cells, after treatment with mibefradil or lomerizine. Data were normalized using control cells as reference and *Gapdh* as housekeeping gene. All data represent the mean ± SEM of three independent experiments. Statistical analyses were performed with One Way ANOVA and post-hoc test; *$p < 0.05$, **$p < 0.01$ and ***$p < 0.001$.

4.8 Expression of T-type calcium channels in human adaptive BRAFi-resistant melanoma cells.

Adaptive BRAFi-resistance was induced in human A375, SK-MEL-28 and HT144 melanoma cells by treating them for 24 hours with vemurafenib (3 μM). Firstly, mRNA expression of T-type calcium channels was evaluated in all human cell lines. The data showed that expression of Cav3.1 and Cav3.2 genes was enhanced in human resistant cells compared to the parental cells (Figure 19a, b, c).

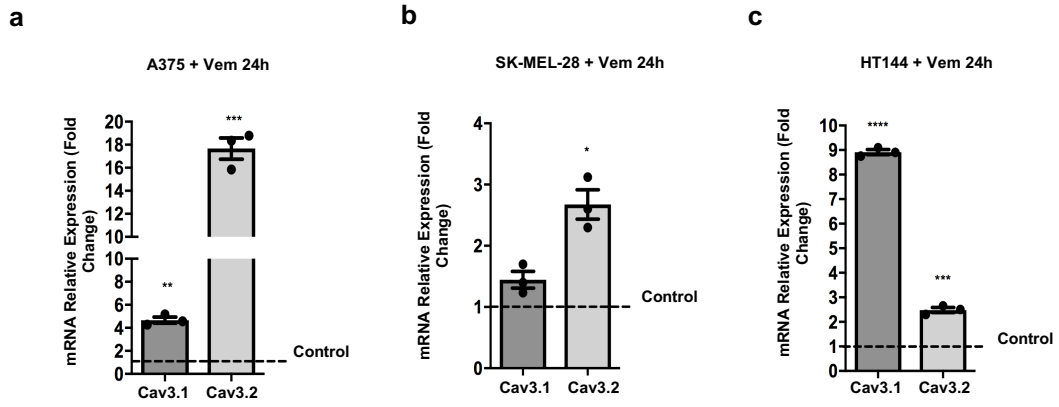

Figure 19. Evaluation of mRNA expression of T-type calcium channels in human adaptive BRAFi-resistant melanoma cells. a,b,c Gene expression analysis of Cav3.1 and Cav3.2 in human melanoma cell lines A375, SK-MEL-28 and HT144 upon 24 hours treatment with vemurafenib (3μM) (adaptive resistance). Data were normalized using control cells as reference and 18S as housekeeping gene. All data represent the mean ± SEM of three independent experiments. Statistical analyses were performed with One Way ANOVA and post-hoc test; *p < 0.05, **p < 0.01 and ***p < 0.001.

4.9 Effect of T-type calcium channel inhibition on cell death in human adaptive BRAFi- resistant melanoma cells.

To determine whether the increment in the expression of calcium channels was associated with a more dedifferentiated and resistant phenotype, in a similar way to reprogrammed murine cells, I tested the effect of mibefradil on cell viability, cell death and colony formation ability in human adaptive BRAFi-resistant cells.

After single treatment for 24 hours with mibefradil, the cell viability of adaptive BRAFi-resistant cells was reduced (A375 mean IC50= 7.43 ± 0.80 μM; SK-MEL-28 mean

IC50= 6.5 ± 0.30 μM; HT144 mean IC50= 2.65 ± 0.14 μM) compared to parental cells (A375 mean IC50= 9.63 ± 0.35 μM; SK-MEL-28 mean IC50= 8.17 ± 0.40 μM; HT144 mean IC50= 5.5 ± 0.41 μM) (Figure 20a and Supplementary Table S5). Single treatment with lomerizine did not have a significant effect on the cell viability of A375 or SK-MEL-28 cells (Supplementary Figure S4a).

Evaluation of my data showed that single treatment with mibefradil did not affect apoptosis in the parental cells but increased apoptosis in all BRAFi-resistant cells ("Vem24h >> Mibe24h"). More importantly, mibefradil increased sensitivity to vemurafenib when used in sequential manner ("Vem24h >> Mibe24h >> Vem24h") (Figure 11b and Supplementary Figure S4b). These results support the use of calcium channel antagonist to re-sensitize resistant cells to BRAFi.

In addition to these findings, colony formation capacity was impaired in A375 and SK-MEL-28 BRAFi-resistant cells after treatment with mibefradil ("Vem24h >> Mibe24h") in comparison to single treatment with vemurafenib or DMSO but, the capacity of colony formation was completely suppressed in all BRAFi-resistant cells after sequential treatment ("Vem24h >> Mibe24h >> Vem24h") (Figure 20c, d). These results are consistent with observations obtained on partially reprogrammed murine cells and suggest the possibility of using calcium channels blockers to increase drug sensitivity to MAPK inhibitors in resistant cells.

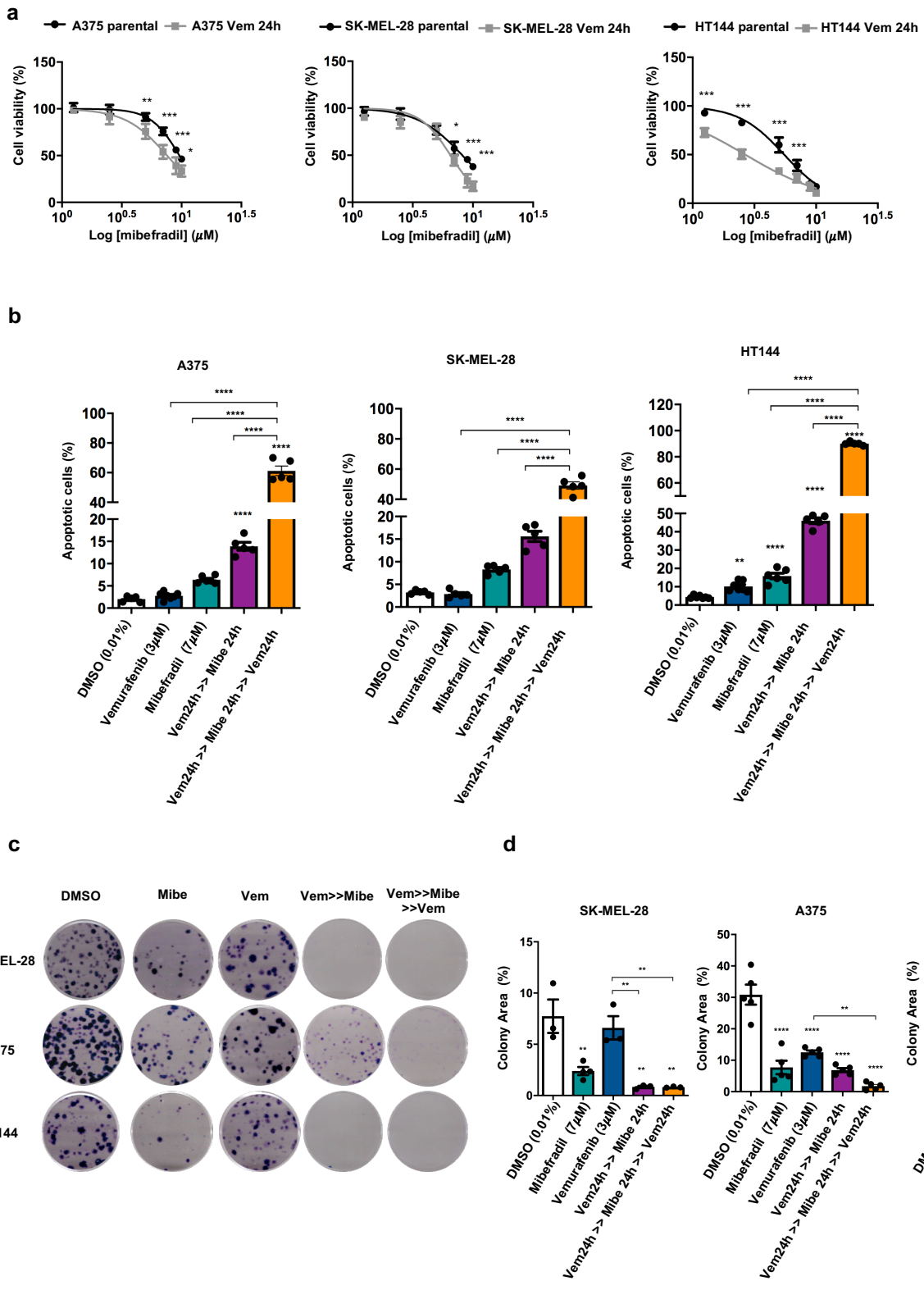
a
A375 parental
A375 Vem 24h
SK-MEL-28 parental
SK-MEL-28 Vem 24h
HT144 parental
HT144 Vem 24h
Cell viability (%)
Log [mibefradil] (μM)
b
A375
SK-MEL-28
HT144
Apoptotic cells (%)
DMSO (0.01%)
Vemurafenib (3μM)
Mibefradil (7μM)
Vem24h >> Mibe 24h
Vem24h >> Mibe 24h >> Vem24h
c
DMSO
Mibe
Vem
Vem>>Mibe
Vem>>Mibe >>Vem
SK-MEL-28
A375
HT144
d
SK-MEL-28
A375
HT144
Colony Area (%)
DMSO (0.01%)
Mibefradil (7μM)
Vemurafenib (3μM)
Vem24h >> Mibe 24h
Vem24h >> Mibe 24h >> Vem24h

Figure 20. Mibefradil increases sensitivity of human adaptive BRAF-resistant melanoma cells to MAPK inhibitors. a Human melanoma cells were treated with mibefradil and lomerizine (10,9,7,5,2.5 and 1.25 μM) for 24 hours (only mibefradil treatment is shown). After alamar blue assay, the fluorescence (590 nm) was measured. **b** Apoptosis analysis of human melanoma, cells were treated with vemurafenib (3 μM) for 24 hours, followed by mibefradil (7 μM) for 24 hours; after this period cells were re-treated with vemurafenib (3μM) for another 24 hours ("Vem 24h >> Mibe 24h >> Vem 24h"). Cells were stained and analyzed by flow cytometry. Percentage of apoptotic cells (early and late apoptosis) is shown as mean ± SEM (n= 5). **c** Clonogenic assay with human cells A375, SK-MEL-28 and HT144 cells treated for 24 hours with DMSO (0.01%), mibefradil (7 μM), vemurafenib (3 μM) and sequential treatment (Vem 24h >> Mibe 24h >> Vem 24h). Representative images of wells stained with crystal violet are shown. **d** Percentage of colony area for all treatments is shown as mean ± SEM (n= 3) in all human melanoma cell lines. All data represent the mean ± SEM of three or more independent experiments. Statistical analyses were performed with One Way ANOVA and post-hoc test; *p < 0.05, **p < 0.01, ***p < 0.001 and ****p < 0.0001.

4.10 Effect of T-type calcium channel inhibition on differentiation status in human adaptive BRAFi-resistant melanoma cells.

In order to establish a connection between the blockage of calcium influx and the differentiation status of resistant cells, expression of differentiation markers associated with adaptive resistance in melanoma, such as ID1, ID3[118] and SOX2[75], were evaluated.

In agreement with earlier results obtained in murine reprogrammed cells, treatment with mibefradil significantly reduced the expression of differentiation markers related to adaptive resistance, in both parental and resistant cells (Figure 21a, b, c). Even after sequential treatment ("Vem24h >> Mibe24h >> Vem24h"), expression of SOX2 was suppressed in resistant SK-MEL-28 and HT144 cells on the mRNA (Figure 21a, b) and protein level (Figure 21d), supporting a potential role of calcium signaling in stemness maintenance.

a

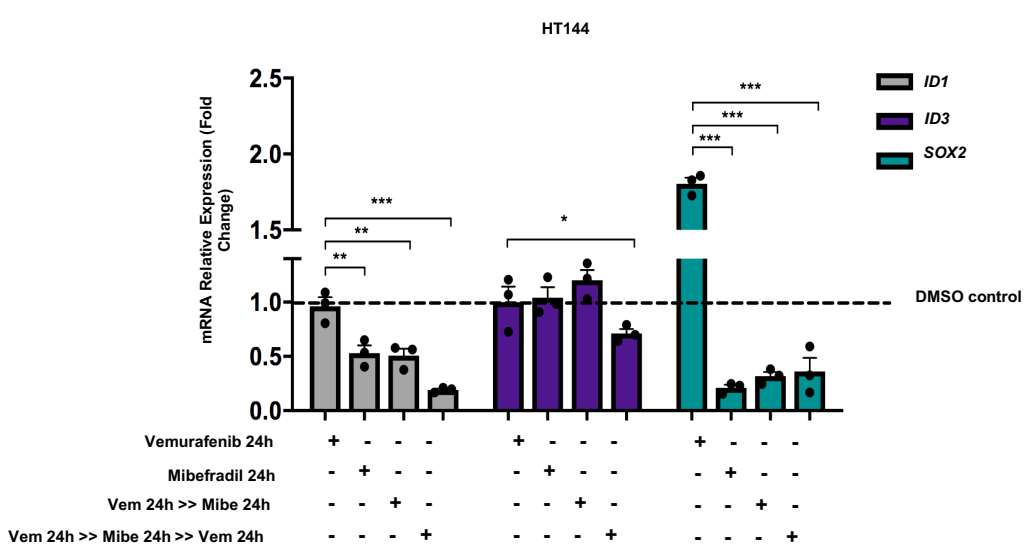
HT144
mRNA Relative Expression (Fold Change)
2.5
2.0
1.5
1.0
0.5
0.0
ID1
ID3
SOX2
DMSO control
Vemurafenib 24h
Mibefradil 24h
Vem 24h >> Mibe 24h
Vem 24h >> Mibe 24h >> Vem 24h

b

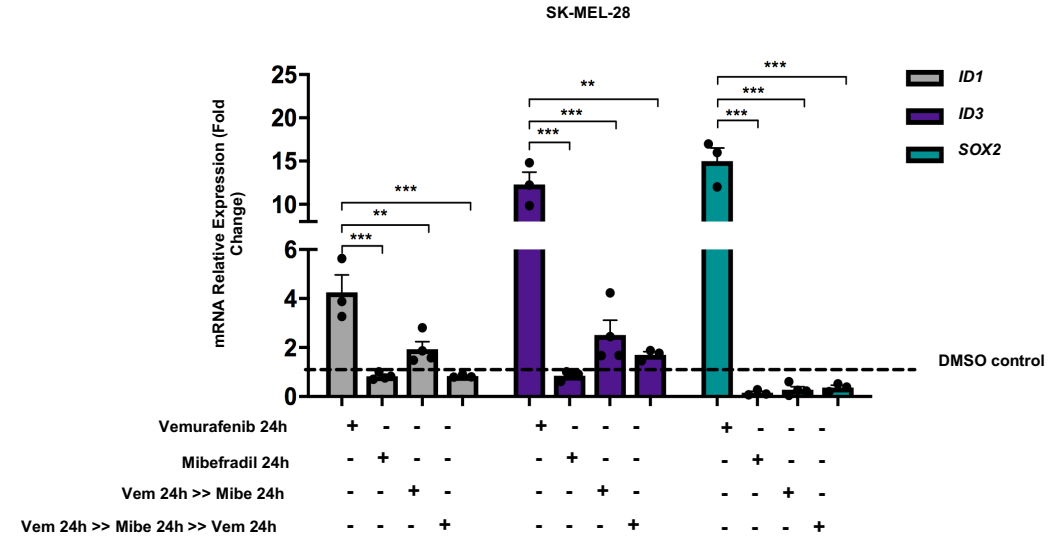
SK-MEL-28
mRNA Relative Expression (Fold Change)
25
20
15
10
6
4
2
0
ID1
ID3
SOX2
DMSO control
Vemurafenib 24h
Mibefradil 24h
Vem 24h >> Mibe 24h
Vem 24h >> Mibe 24h >> Vem 24h

c

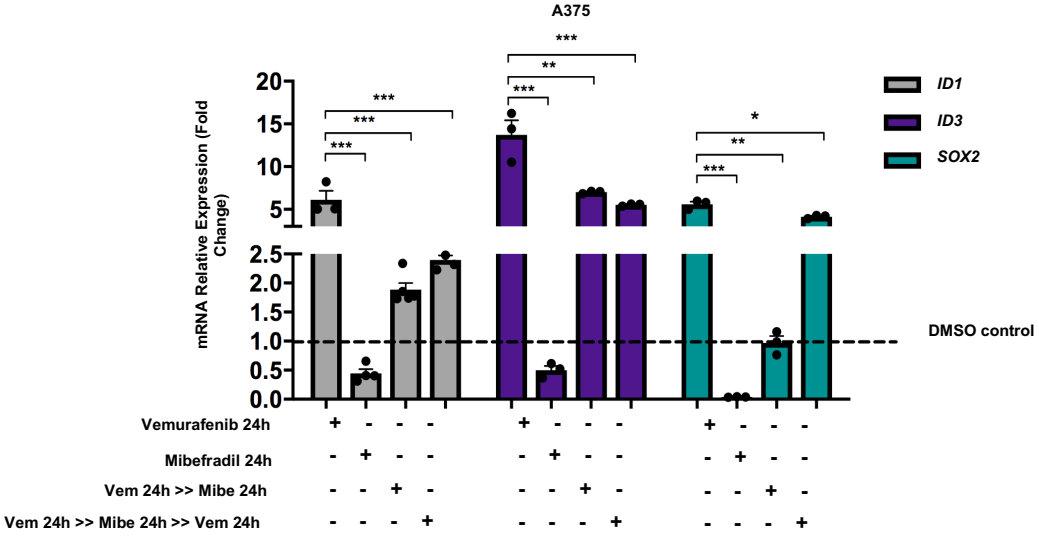
A375
mRNA Relative Expression (Fold Change)
20
15
10
5
2.5
2.0
1.5
1.0
0.5
0.0
ID1
ID3
SOX2
DMSO control
Vemurafenib 24h
Mibefradil 24h
Vem 24h >> Mibe 24h
Vem 24h >> Mibe 24h >> Vem 24h

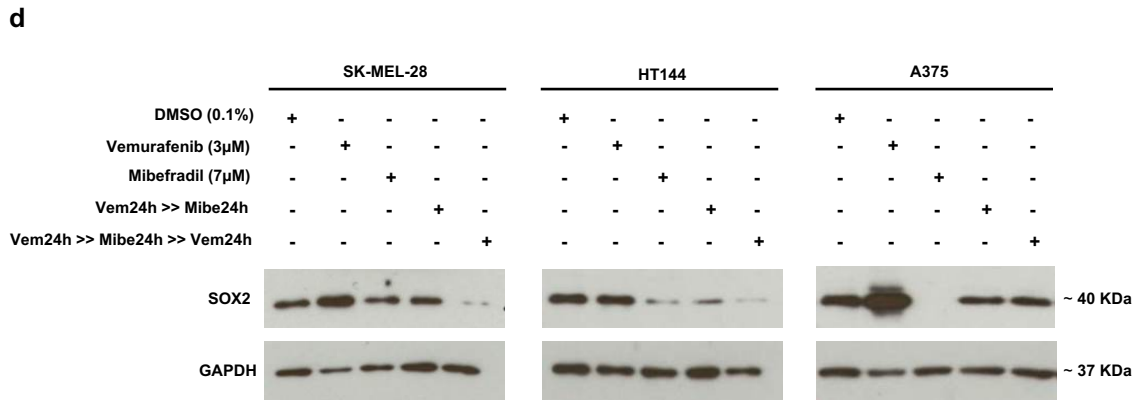

Figure 21. Mibefradil induces differentiation in human adaptive BRAF-resistant melanoma cells. a,b,c qPCR analysis of the expression of markers of adaptive resistance *SOX2*, *ID1* and *ID3* in HT144, SK-MEL-28a and A375 cells respectively, after treatment with mibefradil alone or sequential treatment with vemurafenib and mibefradil ("Vem24h>>Mibe24h>>Vem24h"). Data were normalized using control cells as reference and 18S as housekeeping gene. **d** Western Blot analysis. Whole cell lysates from HT144, SK-MEL-28 and A375 cells were immunoblotted with antibodies against GAPDH and SOX2. All data represent the mean ± SEM of three or more independent experiments. Statistical analyses were performed with One Way ANOVA and post-hoc test; *$p < 0.05$, **$p < 0.01$, ***$p < 0.001$ and ****$p < 0.0001$.

4.11 Silencing of Cav3.2 and cell death in human adaptive BRAFi-resistant melanoma cells.

T-type calcium channel Cav3.2 was silenced in human melanoma cells A375, SK-MEL-28 and HT144 to test whether it is responsible for the increment in apoptosis and sensitization in human adaptive resistant cells. Once verification by qPCR (Figure 22a) and western Blot (Figure 22b) of Cav3.2 knockdown in the human cell lines was performed, the effect on cell death and differentiation after treatment with vemurafenib or with the combination of vemurafenib and trametinib was evaluated.

Cav3.2 knockdown increased apoptosis in A375 and SK-MEL-28 knockdown cell lines compared to the scramble control (Figure 22c and Supplementary Figure S5), thereby confirming that induction of apoptosis in BRAFi-adaptive resistant cells was driven by inhibition of Cav3.2 calcium channel. Due to limited efficiency of the Cav3.2 knockdown (Figure 22a, b), HT144 cells showed a lower percentage of apoptotic cells compared

to scramble control. Moreover, colony formation capacity was impaired in Cav3.2 knockdown cells lines A375 and SK-MEL-28 after treatment with vemurafenib (Figure 22d, e), supporting that Cav3.2 calcium channel knockdown increased sensitivity of resistant cells to BRAFi. These results support the conclusion that the T-type calcium channel Cav3.2 plays a role in resistance and survival of melanoma cells.

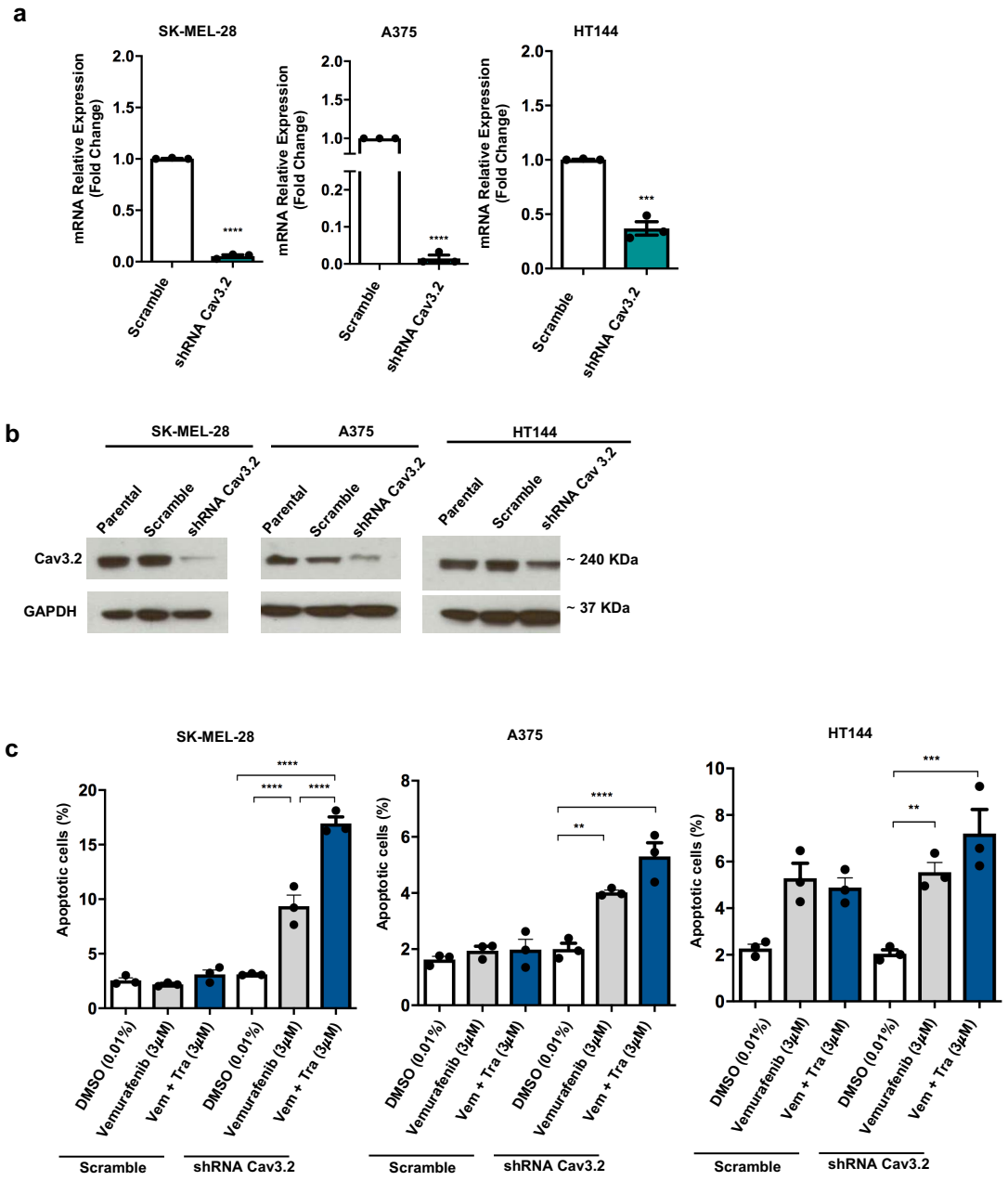

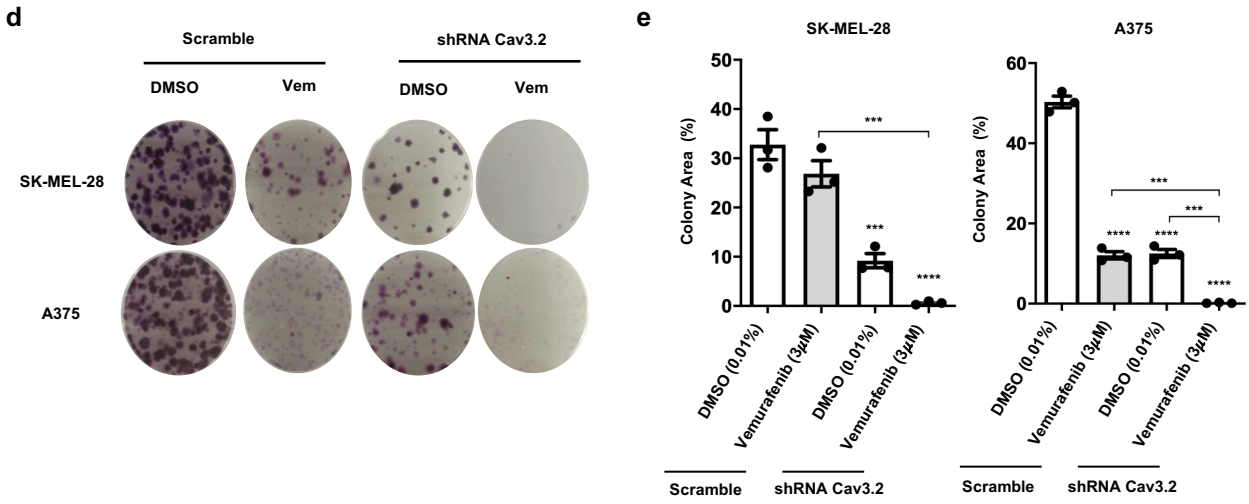

Figure 22. Knockdown of the calcium channel Cav3.2 induces cell death of human melanoma cells. a Human melanoma cells A375, SK-MEL-28 and HT144 were transfected with sh-Cav3.2 or sh-control (Scramble). After 48 hours selection with puromycin (0.8 µg/mL), cells were collected and analyzed by qPCR and western Blot. Analysis of Cav3.2 gene expression confirmed the silencing of the gene in all cell lines. **b** Western blot analysis. Protein lysates of human melanoma cells were immunoblotted with antibodies against GAPDH and Cav3.2. **c** Apoptosis assay with A375, SK-MEL-28 and HT144 cells. After treatment with sh-Cav3.2, cells were stained with annexinV/PI to analyze apoptosis by flow cytometry. Percentage of apoptotic cells (early and late apoptosis) is shown as mean ± SEM (n=3). **d** Clonogenic assay with human cells A375 and SK-MEL-28 transfected with sh-Cav3.2 or sh-control (Scramble), treated for 24 hours with DMSO (0.01%) and vemurafenib (3 µM). Representative images of wells stained with crystal violet are shown. **e** Percentage of colony area for all treatments is shown as mean ± SEM (n=3) in A375 and SK-MEL-28 cell lines. All data represent the mean ± SEM of three or more independent experiments. Statistical analyses were performed with One Way ANOVA and post-hoc test; *$p < 0.05$, **$p < 0.01$, ***$p < 0.001$ and ****$p < 0.0001$.

4.12 The effect of knockdown of Cav3.2 on the differentiation status of human adaptive BRAFi-resistant melanoma cells.

To determine if the knockdown of Cav3.2 was involved in the observed changes of the differentiation status of human melanoma cells, SOX2 expression was evaluated. The mRNA (Figure 23a) and protein level (Figure 23b) were substantially reduced in A375 and SK-MEL-28 knockdown cell lines, indicating a decreased in the stemness phenotype. There was no significant difference in SOX2 expression in HT144 Cav3.2

knockdown cells compared to scramble control most probably due to the low efficiency of the Cav3.2 knockdown.

Considering these data and the previous results, Cav3.2 silencing had a similar effect on cell death and differentiation as the pharmacological inhibition of calcium channels with mibefradil, confirming the role of T-type calcium channels on drug sensitivity of murine and human MAPKi-resistant melanoma cells.

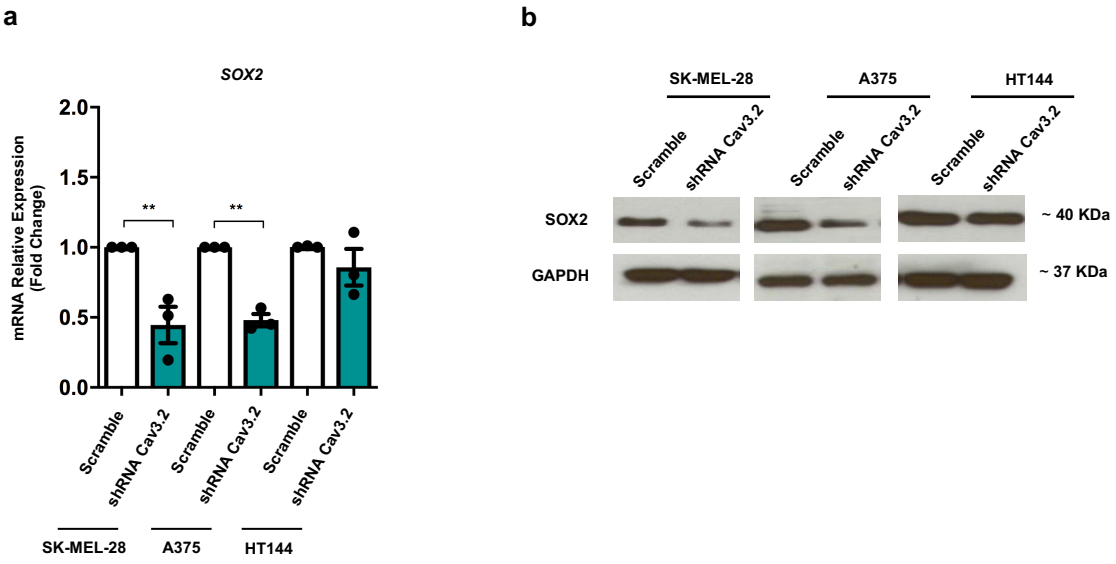

Figure 23. Knockdown of the calcium channel Cav3.2 induced differentiation of human melanoma cells. a qPCR analysis of SOX2 after silencing Cav3.2 in SK-MEL-28, A375 and HT144 human cells. Data were normalized using control cells (scramble) as reference and 18S as housekeeping gene. **e** Western Blot analysis. Whole cell lysates of SK-MEL-28, A375 and HT144 human cells with Cav3.2-knockdown were immunoblotted with antibodies against GAPDH and SOX2. All data represent the mean ± SEM of three independent experiments. Statistical analyses were performed with One Way ANOVA and post-hoc test; *$p < 0.05$, **$p < 0.01$, ***$p < 0.001$ and ****$p < 0.0001$.

4.13 The effect of mibefradil treatment on tumor growth *in vivo* and the survival of mice injected with human melanoma cells.

A xenograft mouse model was used to evaluate the antitumor effect of the sequential treatment (“Vem24h >> Mibe24h >> Vem24h”) *in vivo*. Mice were inoculated subcutaneously with A375 or HT144 cells, which were beforehand treated for 24h with

vemurafenib. After the tumor volume reached 100-300 mm3, the animals (n= 40) were randomly separated into 4 different treatment groups. Sequential treatment consisted of oral administration of vemurafenib for 5 days, follow by mibefradil for another 5 days. This workflow was repeated until 2 cycles were completed and finally, vemurafenib was applied for the last 5 days of the experiment (Figure 24a, Figure 25a). In parallel, single treatments with vemurafenib, mibefradil or vehicle were tested.

HT144 xenografts showed that single treatments with vemurafenib (p = 0.013) and mibefradil (p = 0.025) significantly reduce tumor growth compared to control group (vehicle), however, the sequential treatment (p < 0.001) showed the most significant and stronger effect on tumor volume compared to control mice (vehicle) (Figure 24b). Moreover, survival data showed a better outcome for mice treated with sequential treatment compared with control group (p < 0.001) (Figure 24c). Single treatments of vemurafenib (p = 0.001) and mibefradil (p < 0.001) showed a significant difference in survival compared with vehicle group. These results support the use of mibefradil to enhance the antitumor effects of vemurafenib *in vivo*.

Regarding A375 xenografts, single treatment with vemurafenib alone led to a slight reduction in tumor growth compared to control group (vehicle). In contrast, mice treated with mibefradil (p = 0.013) or sequential treatment (p = 0.019) had a significant reduction in tumor volume compared to control mice (vehicle) (Figure 25b). Considering the survival data, mice treated with sequential treatment showed a better outcome, compared with control group (p < 0.001), similar to the effect observed in HT144 xenografts (Figure 25c). Single treatments of vemurafenib (p = 0.053) and mibefradil (p = 0.063) did not show significant difference in survival compared with vehicle group.

These effects *in vivo* are consistent with my previous *in vitro* data on resistant human cells and reprogrammed mouse cells, suggesting that the inhibition of T-type calcium channels is a promising strategy to sensitize dedifferentiated and resistant melanoma cells to MAPKi.

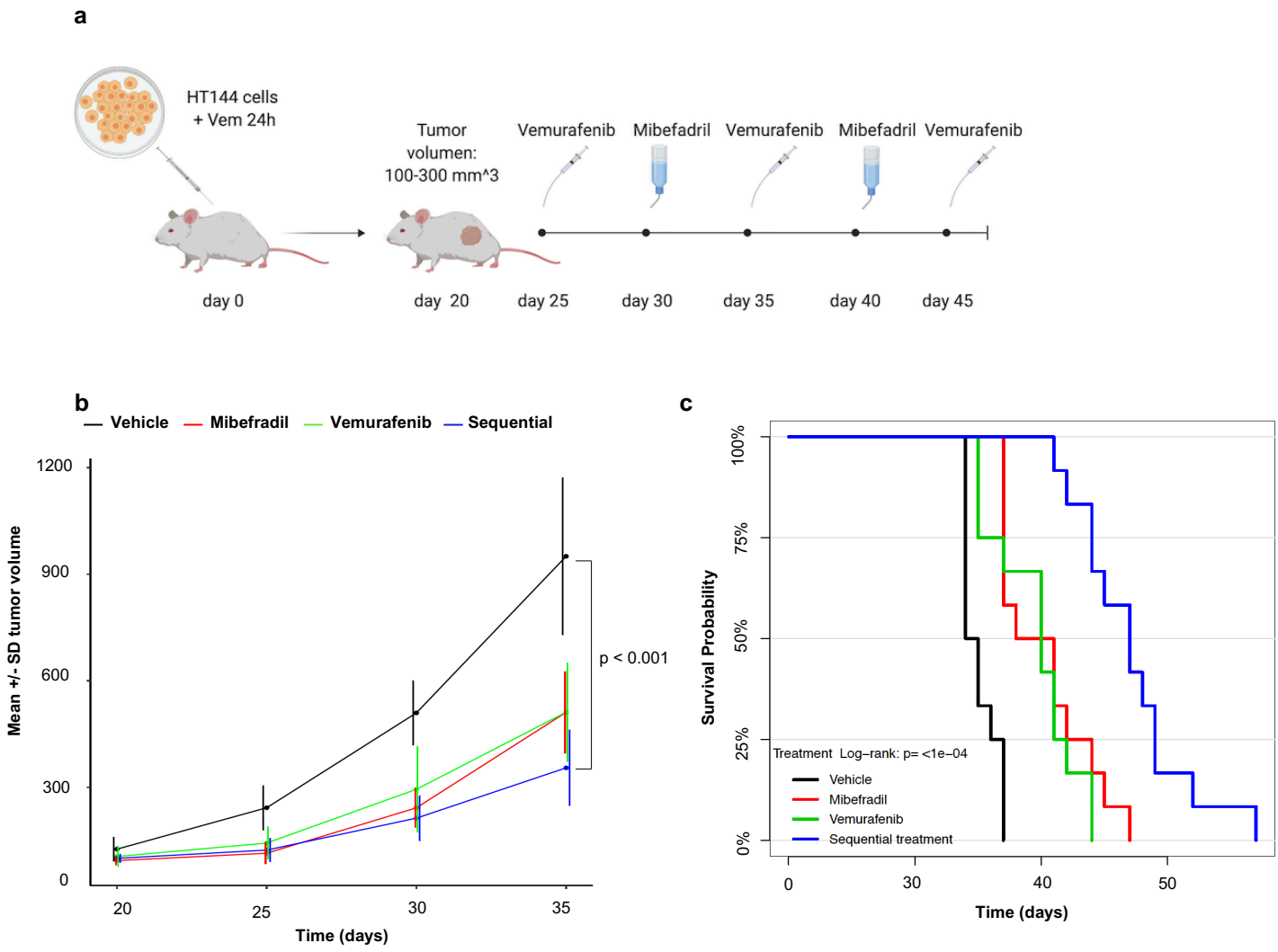

Figure 24. Inhibition of tumor growth *in vivo* and increased survival in HT144 human adaptive BRAFi-resistant melanoma xenografts. a Workflow of *in vivo* evaluation of sequential treatment (Vem >> Mibe >> Vem) in adaptive-resistant human cells. HT144 cells treated with vemurafenib for 24 hours were injected subcutaneously in female NGS mice. Once tumor volume reached 100-300 mm^3, animals were randomly divided into 4 groups (n=12), and treatments were administered daily as depicted. **b** Effect of sequential treatment on tumor growth in HT144 xenografts, shown as mean and standard deviation of tumor volume over time following treatment initiation. Tumor growth curves were compared based on a linear mixed model with predictors time, treatment and interaction between time and treatments as fixed effects, and random intercept/slope effect. The interaction term was tested to compare the growth rate relative to the vehicle group. P-values were adjusted for multiple testing. **c** Kaplan-Meier curves representing survival of HT144 xenografts mice treated with vehicle (black line), mibefradil (red line), vemurafenib (green line) and sequential treatment (blue line). Survival end point was defined as tumor volume reaching 1000 mm^3. The survival curves were analyzed with pairwise treatment comparison using log-rank test with adjustment of p-values for multiple testing.

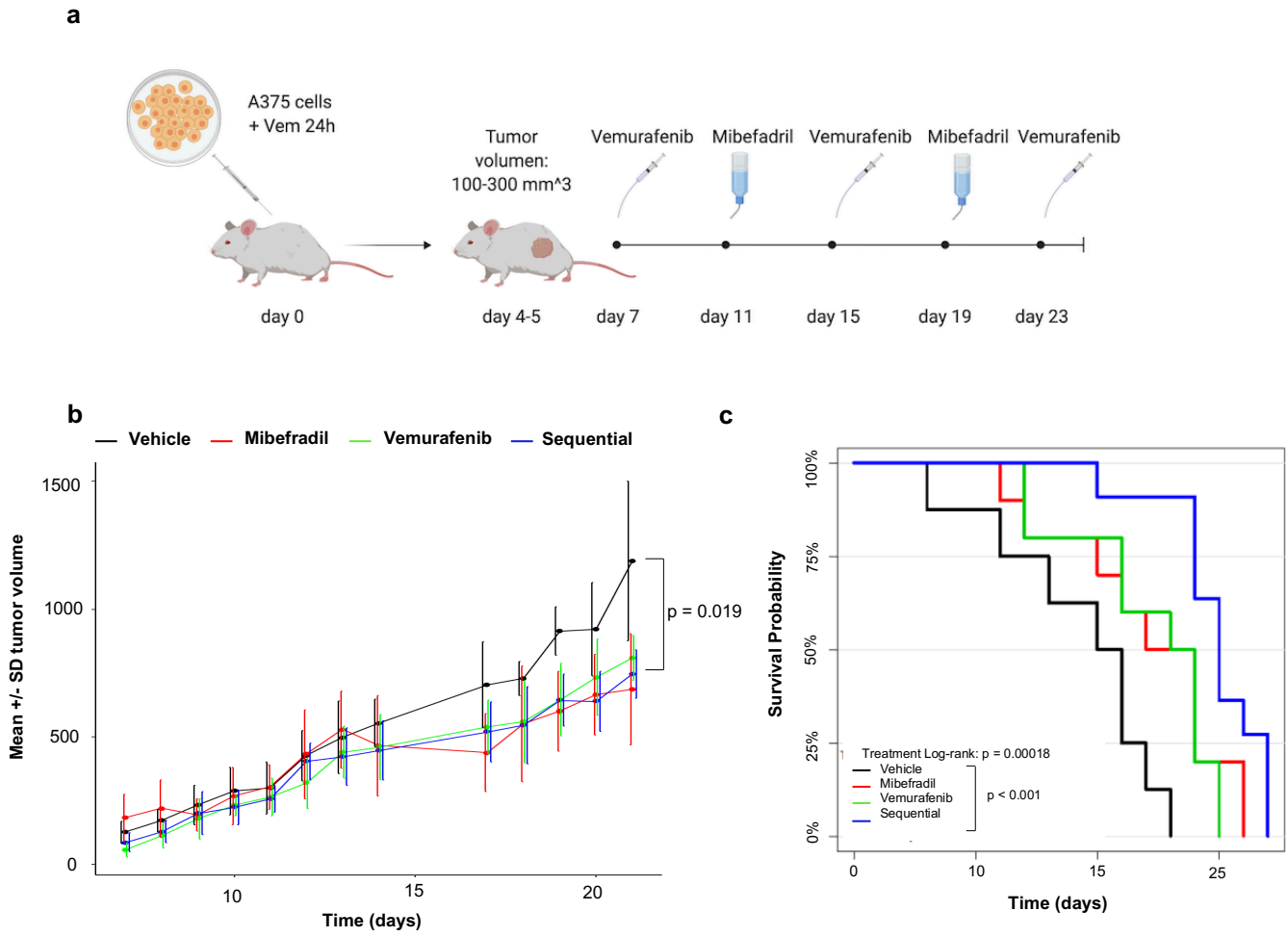

Figure 25. Inhibition of tumor growth *in vivo* and increased survival in A375 human adaptive BRAFi-resistant melanoma xenografts. a Workflow of *in vivo* evaluation of sequential treatment (Vem >> Mibe >> Vem) in adaptive-resistant human cells. A375 cells treated with vemurafenib for 24 hours were injected subcutaneously in female NGS mice. Once tumor volume reached 100-300 mm^3, animals were randomly divided into 4 groups (n=12), and treatments were administered daily as depicted. **b** Effect of sequential treatment on tumor growth in A375 xenografts, shown as mean and standard deviation of tumor volume over time following treatment initiation. Tumor growth curves were compared based on a linear mixed model with predictors time, treatment and interaction between time and treatments as fixed effects, and random intercept/slope effect. The interaction term was tested to compare the growth rate relative to the vehicle group. P-values were adjusted for multiple testing. **c** Kaplan-Meier curves representing survival of A375 xenografts mice treated with vehicle (black line), mibefradil (red line), vemurafenib (green line) and sequential treatment (blue line). Survival end point was defined as tumor volume reaching 1000 mm^3. The survival curves were analyzed with pairwise treatment comparison using log-rank test with adjustment of p-values for multiple testing.

5. Discussion

Therapy resistance remains an unsolved problem in the treatment of many types of cancer. Since melanoma patients have a high risk of developing resistance to current treatments, tumor recurrence is still very common[5]. Understanding the mechanisms behind resistance and finding new targets is essential in order to improve treatment response and patient survival.

A dedifferentiated status of cancer cells has been associated with a higher risk of acquiring drug resistance[117]. For this reason, many studies on cancer plasticity and cancer stem cells aim at discovering new targets for anticancer drugs that would enhance the efficacy of cancer treatments. In vitro reprogramming of cancer cells to a less differentiated state mimics the phenotypic and functional changes that occur *in vivo* during cancer progression and that are responsible for the heterogeneity observed among cancer cells[105]. Hence, nuclear reprogramming of cancer cells represents a suitable approach to investigate the development of drug resistance in cancer cells.

In the present work, I used the technique of reprogramming cancer cells to a less differentiated state in order to investigate the role of a stem cell-like cancer cell population in melanomas that is responsible for the development of resistances to BRAF and MEK inhibitors, which are currently used as a standard treatment for melanoma patients. Here, it has been demonstrated that partial reprogramming of melanoma cells induced a dedifferentiated and aggressive phenotype along with an increment in resistance to MAPKi. Moreover, genome expression analysis showed that T-type calcium channels were overexpressed in human and murine MAPKi-resistant melanoma cells. Inhibition of T-type calcium channels enhanced cell death and differentiation in C790 and 4434 murine partially reprogrammed cells as well as in human adaptive BRAFi-resistant melanoma cells. Moreover, the efficiency of the treatment with the calcium channel blocker, mibefradil, in a sequential manner along with vemurafenib was confirmed by the increment in apoptosis and suppression of colony formation capacity, which strongly suggest that the use of the calcium channel antagonists re-sensitizes resistant melanoma cells to MAPKi. Finally, based on the reduction of tumor growth and the increment in overall survival after sequential treatment *in vivo*, it is possible to conclude that T-type calcium channels are potential targets to eliminate adaptive resistance of melanoma cells by restoring sensitivity to MAPKi.

5.1 Melanoma cells adopted a dedifferentiated and aggressive phenotype that is highly resistant to MAPK inhibitors upon partial reprogramming.

When differentiated and somatic cells undergo de-differentiation, this is usually associated with disease progression and particularly with cancer development. Based on this, cellular reprogramming of cancer cells represents a suitable platform to study features of tumor progression and to identify factors that contribute to the development of resistance to cancer therapies. *In vitro* de-differentiation or direct reprogramming of melanoma cells has been described previously [12,109,119,120]. In this work, murine *Nras* and *Braf*-mutated melanoma cells have been partially reprogrammed to study genetic and phenotypic changes that occur during the intermediate stages of melanoma progression. A switch in gene expression was observed in C790 and 4434 partially reprogrammed cells by increasing the expression of stemness-related genes and reducing levels of melanocytic-specific markers, along with a decreased proliferation and enhanced invasiveness, which was consistent with the classical features observed during phenotype switching in melanoma[121,122].

During development, melanocyte progenitors undergo phenotype switching which is necessary for normal melanocyte lineage differentiation. However, the reversion of this phenotypic change plays a role in initiating malignant transformation and metastasis[121]. MITF plays a pivotal role during phenotype switching in melanoma and its expression level can be used to distinguish between proliferative and invasive melanoma cells. Low expression of MITF usually correlates with more invasion, senescence, stem-like properties and drug resistance[44,123–125], while higher expression leads to an increment in proliferation and increased expression of differentiation-related genes that are involved in melanin production and melanosome biogenesis[125].

During melanogenesis, additional enzymatic and structural proteins participate in the melanosome maturation process, including: tyrosinase (Tyr), tyrosinase-related protein 1or 2 (Tyrp1,2), ocular albinism type 1 protein (OA1) and pre-melanosomal protein (Pmel). From all the structural proteins, Pmel, a melanocyte-specific type I transmembrane glycoprotein, is essential to initiate melanin synthesis and to culminate melanosome maturation[126]. After partial reprogramming of C790 and 4434 murine cells for 20 days, cell populations showed a significant reduction in the expression of these lineage specific-markers, *Mitf* and *Pmel,* together with a higher expression of

pluripotency-related genes in mouse (*Sox2*, *Ssea1* and *Oct4*), indicating a reversion of the melanocytic phenotype into a more dedifferentiated stage.

Considering that cellular de-differentiation has been correlated with development of resistance to therapies[6,121,127], and that progressive de-differentiation status of melanoma cells has been observed in patient samples under standard treatments with MAPKi[117], I tested the hypothesis that partially reprogrammed cells would be less sensitive to BRAF or MEK inhibitors. Consistent with other reports showing that de-differentiation of human melanoma cells conveyed increased resistance to MAPKi[119], my results indicate that partially reprogrammed murine melanoma cells had improved survival after treatment with trametinib, vemurafenib or with a combination of both drugs.

Although BRAF and MEK inhibitors can efficiently inhibit the MAPK pathway by impeding ERK activation, still the most common mechanism of resistance is the reactivation of ERK protein[48,128]. This suggest that tumor cells can rapidly adjust to maintain the MAPK cascade active through different mechanisms, assuring an elevated cell proliferation and survival. For instance, BRAFi-resistant tumors show activation of the MAP3K8 kinase, also known as COT, that can directly activate ERK signaling independently of RAF[48].

Moreover, several alternative signaling pathways[2,5,74,128] have been implicated either in acquired, adaptive or intrinsic resistance in melanoma. The PI3K-mTOR pathway is the most frequently activated in resistant tumors, due mainly to deletion of PTEN or activation of receptor tyrosine kinases (RTK)[129]. Additionally, certain genes such as MITF, AXL and WNT5A have been associated with development of resistance to targeted therapies and melanoma phenotype switching[48,130].

In this study, reactivation of ERK was tested in MAPKi-resistant cells by western blot. My data showed that the inhibition of MAPK pathway in partially reprogrammed cells altered the phosphorylation status of ERK protein in both C790 and 4434 melanoma cells, independently of the dedifferentiated state of the cells. Based on these results and the quantity of possible mechanisms responsible of the MAPKi-resistance in murine reprogrammed cells, a broader analysis was performed using a gene expression array in order to identify new candidate genes that might be involved in the development of MAPKi resistance in dedifferentiated cancer cells.

5.2. Dedifferentiated and MAPKi-resistant cells overexpressed T-type calcium channels.

To identify new candidate genes that might drive possible mechanisms of resistance, gene expression analysis of C790 partially reprogrammed cells after treatment with trametinib was performed. The obtained data revealed an upregulation of T-type calcium channels suggesting a relation between them and de-differentiation and resistance.

T-type calcium channels belong to a big family of voltage gated calcium channels (VGCCs). Each subfamily contains several isoforms (Cav1, Cav2 or Cav3) that display different electrophysiological properties[131]. Low voltage-activated and transient currents calcium channels are known as T-type channels, which are expressed in numerous cell types including non-excitable cells[132]. Alterations in the expression of any of the VGCCs are associated with neurological diseases, such as absence seizures[133], epilepsies[134], neuropathic pain[135]; or cardiac conditions like arrhythmias[136]. Since T-type calcium channels were reported to be upregulated in cancer cells[137], growing evidence has shown that VGCCs are widely expressed in many types of cancer with a particularly significant increase in the expression of T-type calcium channels[138–140]. This overexpression has been confirmed in glioblastoma[141,142], ovarian cancer[143], breast cancer[144], leukemia[145] and melanoma[146].

In this study, results confirmed upregulation of T-type calcium channels in MAPKi-resistant melanoma cells along with an increase in sensitivity of mouse and human MAPKi-resistant cells with mibefradil treatment, which led to increased apoptosis and a reduction in the capacity of the colony formation capacity of these cells.

Mibefradil was introduced as a novel calcium channel antagonist for treatment of hypertension and angina pectoris in 1997 by Roche Laboratories Inc.[147]. The mechanism of action of mibefradil consists in a selective blockage of transient, low-voltage-activated T-type calcium channels. Although mibefradil was withdrawn from the market in 1998 because of potential risk of interactions with other drugs[148], currently mibefradil has been repurposed as an anticancer drug and it has been already evaluated in clinical trials for glioblastoma treatment.

Since the role of T-type calcium channels in cancer proliferation was reported by Tau Therapeutics LLC[149], more studies have indicated that calcium channel blocking agents not only affect calcium signaling into the cells but also proliferation and survival

of cancer cells. Calcium is a key molecule that participates in many cellular processes, including cell proliferation, differentiation and cell cycle control[150,151]. Targeting T-type calcium channels is one strategy to eliminate proliferating cells during the G1-S transition in the cell cycle[150,152]. Previous reports have shown that administration of T-type calcium channel antagonists (mibefradil or NNC-55-0396) inhibits proliferation and induces apoptosis in several cancer cells[153], such as U87MG glioma [154,155] , colon cancer[156], human lung adenocarcinoma (A549), pancreatic cancer (MiaPaCa2) [157], melanoma [158] and leukemia cells[145]. In addition, biopsies from melanoma patients have shown a gradual increase in T-type calcium channel expression, which relates to poor prognosis[159]. Based on the analysis, of data from the TCGA, it was possible to correlate high expression of the calcium channel subunit CACNA1H with a poor survival outcome for melanoma patients compared to patients with low expression of CACNA1H.

In congruence with these previous studies, mibefradil increased apoptosis and reduced cell viability and colony formation capacity of both murine MAPKi-resistant cells and human adaptive BRAFi-resistant cells. However, this effect was moderated and therefore the use of mibefradil was reconsidered as a potentiator of MAPKi effect by increasing drug sensitivity of resistant cells. This approach has been proposed for brain tumor treatment, and is known as Interlaced Therapy™, which consists in a synergistic cancer therapy using mibefradil in a sequential manner with another anticancer drug, for instance chemotherapy[155]. Hence, the potential use of mibefradil in a sequential manner with vemurafenib for the treatment of human adaptive BRAFi-resistant melanoma cells was addressed in the present study.

5.3 *In vitro* and *in vivo* inhibition of T-type calcium channels re-sensitized resistant melanoma cells to MAPK inhibitors.

In order to assess whether mibefradil is capable of sensitizing resistant melanoma cells to MAPK inhibitors, a similar sequential treatment as previously described was tested. The sequential treatment Interlaced Therapy™ consists first in the administration of a T-type calcium channel antagonist, like mibefradil, to arrest cancer cells at the G1/S checkpoint of the cell cycle, then mibefradil is withdrawn and the administration of chemotherapy begins. In this way, mibefradil can synchronize the cell cycle of the cells and increase the number of cancer cells entering S phase at the same time. As a

consequence, the number of sensitive cancer cells increases which makes them more vulnerable to the lethal effect of the chemotherapy[155].

This approach has not been described before for treatment of resistant cell populations in melanoma, using inhibitors of the MAPK pathway. Therefore, considering the overexpression of T-type calcium channels and the effect of mibefradil on MAPKi-resistant melanoma cells, a sequential treatment using mibefradil and vemurafenib was evaluated in this study.

Inhibition of T-type calcium channels has been used to sensitize other types of resistant cancer cells to specific therapies or conventional chemotherapy, in a sequential treatment manner. In ovarian cancer, mibefradil enhances antitumor activity of carboplatin *in vitro* and *in vivo*[143,160]. In a similar way, in glioblastoma, mibefradil treatment enhances the anti-tumor effects of ionizing radiation[161], and the combination of mibefradil with temozolomide has shown a stronger therapeutic effect and increased patient survival[142]. Consistent with these findings, my results showed that mibefradil potentiates the lethal effect of MAPKi when it is administered sequentially to MAPKi-resistant cells *in vitro* and *in vivo*.

Sequential treatments with mibefradil and either trametinib, vemurafenib or a combination of both, effectively increased cell death and completely suppressed the colony formation capacity of resistant murine and human melanoma cells. Moreover, *in vivo* data from mouse xenograft experiments not only showed a significant reduction of tumor volume after treatment with mibefradil (single treatment) or with the sequential treatment, but also mice treated in a sequential manner showed increased survival compared to the control group, while single treatments with mibefradil or vemurafenib did not result in significant differences in survival. These results were further supported through the silencing of Cav3.2 transcript in BRAFi-adaptive human resistant cells. Based on the data obtained with the Cav3.2 knockdown, it is possible to conclude that Cav3.2 was played an important role for colony formation and cell viability.

Taking together, *in vitro* and *in vivo* data suggest that the inhibition of T-type calcium channels is a promising strategy to enhance the response of resistant melanoma cells to MAPKi.

5.4 Inhibition of t-type calcium channels induced differentiation in murine MAPKi-resistant and dedifferentiated melanoma cells.

The role of T-type calcium channels in de-differentiation and drug resistance remains unclear. Zang *et al.* (2017) showed that T-type calcium channels are enriched in glioblastoma stem-like cells, which are resistant to temozolomide. They demonstrated that blockade of calcium channels can re-sensitize resistant cells to treatments but also induce differentiation[142].

Resistant and dedifferentiated cancer cells display many features that are also found in the classical stem cells like self-renewal capacity, and are responsible for generating heterogeneous tumor cell population. It has been reported that BRAFi-resistant melanoma cells develop a metastatic phenotype along with an upregulation of certain cancer stem cells-markers like CD271[36,162,163].

CD271 marker is also known as low-affinity nerve growth factor receptor (LNGFR) and belongs to a family of receptors for neurotrophins, proteins that stimulate survival and differentiation in neuronal cells. CD271 has been reported to be expressed in many different types of cells, from mesenchymal stem cells[164] to even tumor initiating cells[165]. Moreover, several reports have shown that knockdown of CD271 induced apoptosis[166], reduced migration[167] and tumorigenicity, and abolished stemness-related features in melanoma cells[168]. These properties qualify CD271 as a suitable factor to establish de-differentiation and resistance in melanoma cells.

Besides CD271, dedifferentiated cells also express other markers, including the stage specific embryonic antigens (SSEA): SSEA1, SSEA3 and SSEA4. SSEA1 is a marker exclusively expressed on the surface of murine ESCs and is absent in human ESCs[169,170]. Expression of SSEA1 increases upon differentiation of human cells, but decreases during differentiation of mouse cells[170], therefore, SSEA1 is indeed a proper marker to evaluate differentiation status of murine cells.

To elucidate the effect of the inhibition of T-type calcium channels on the de-differentiation status of MAPKi-resistant cells, expression levels of stemness-markers in murine reprogrammed melanoma cells were evaluated. After single treatment with mibefradil or lomerizine, a significant decrease of the stemness-related markers *Sox2*, *Ssea1* and *CD271* at the mRNA level in C790 and 4434 dedifferentiated cells was observed. These results are in line with the reduction of *Oct3/4* and *Nanog* expression

in mouse ESCs reported in another study, after pharmacological blockage of T-type calcium channels or knockdown with Cav 3.2 siRNA[171].

Although it is well known that calcium can regulate different pathways that are involved in differentiation, little is known about the role of calcium in the maintenance of pluripotency of dedifferentiated cells. Calcium currents have been detected in G1 to S transition during cell cycle progression in diverse cell lines, including dedifferentiated cells [172–174], indicating that calcium is also a key regulator during stem cells proliferation. In addition, dedifferentiated mouse ESCs have been reported to show voltage-dependent Ca^+ and/or Na^+ currents, which influence cell cycle progression and maintenance of self-renewal in murine ESCs[171]. All these data confirmed that calcium blockage affects the de-differentiation status of resistant melanoma cells by reducing expression of stemness-related genes, making them more vulnerable to treatment.

5.5 Inhibition of T-type calcium channels induced differentiation of human adaptive vemurafenib-resistant melanoma cells.

As mentioned before, resistant cancer cells display a more dedifferentiated phenotype that provides them a survival advantage during treatment. In order to find out whether inhibition of T-type calcium channels also induces differentiation in adaptive resistant cells, an analysis of the expression levels of stemness-related genes in human adaptive BRAFi-resistant melanoma cells was performed after inhibition of T-type calcium channels.

Studies on glioblastoma stem-like cells (GSC) have reported differentiation of GSC induced upon treatment with mibefradil, which was confirmed by downregulation of stemness markers, CD133, nestin, Bmi1 and SOX2[142]. SOX2 is a well-known transcription factor that participates in many processes during mammalian development, including: self-renewal maintenance of pluripotency, germ cell differentiation, hematopoiesis, and more[175]. Due to the variety of functions, SOX2 is highly involved in many developmental disorders and cancer progression. High expression of SOX2 has been connected with a more stem cell-like phenotype in cancer cells and with an increase of drug resistance in different tumors[75,176].

Among the types of drug resistance in melanoma, the adaptive resistance to BRAF inhibitors involved critical mechanisms at the very early stage of treatment. During initial response to treatment, certain cancer cells are able to adapt and tolerate the

effects of the anti-cancer drugs, this generates clones with adaptive resistance that can survive and proliferate. This type of resistance it develops a few hours after the onset of treatment and is driven by different mechanisms. Factors like SOX2[75], LNGFR[74], ID1 and ID3[118] are not only highly expressed in melanoma cells with an adaptive resistance to targeted therapy, but also their expression correlates with a more dedifferentiated phenotype, making them appropriate markers to evaluate de-differentiation in therapy-resistant melanoma cells.

Inhibition of T-type calcium channels with mibefradil in human adaptive resistant melanoma cells decreased the expression of markers SOX2, ID1 and ID3. Reduction of SOX2 expression was also confirmed upon Cav3.2 knockdown in human melanoma cells at the mRNA and protein level, supporting the role of Cav3.2 in maintenance of the dedifferentiated status.

Taking together all results, it is possible to conclude that the inhibition of T-type calcium channels induces differentiation in human adaptive resistant cells, suggesting that calcium signaling might be involved in the maintenance of de-differentiation status and in the development of resistance in melanoma.

6. Conclusions

The present work has demonstrated that partial reprogramming of melanoma cells *in vitro* provides a suitable platform to study MAPKi-resistance in melanoma and to identify new potential targets that can improve current therapies. Using this model, it was possible to confirm that treatment with T-type calcium antagonists induced differentiation and increase apoptosis in resistant melanoma cells (Figure 26). In addition, results corroborated that single treatment with mibefradil was capable of eliminating cancer cells. However, applying mibefradil in a sequential treatment together with BRAFi was more effective against MAPKi-resistant cells *in vitro* and *in vivo*, reducing tumor growth and increasing OS of mice.

Noteworthy, a phase I study has determined the maximum permissible dose of mibefradil when given sequentially with temozolomide in patients with recurrent high-grade gliomas[177], supporting the safety and therapeutic use of mibefradil in humans. This approach of sequential administration not only enhances the effects of conventional anticancer treatments but also reduces exposure time for the patients to chemotherapy, reducing their burden.

The results showed in this work, highlight the possibility of using T-type calcium channel antagonists to restore sensitivity to MAPKi and achieve successful melanoma tumor remission without relapse.

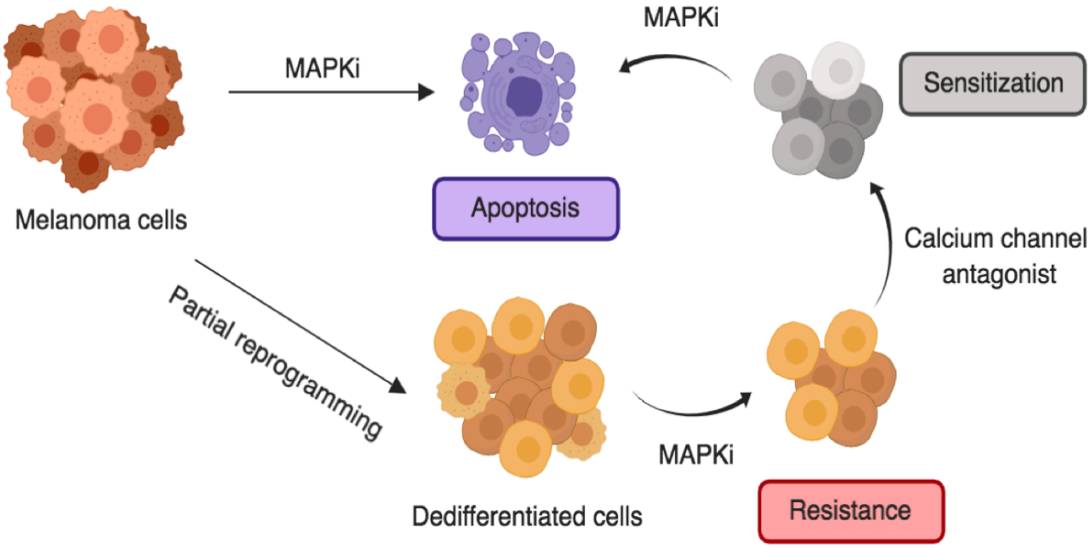

Figure 26. Schematic overview of the main effects on dedifferentiated and MAPKi-resistant melanoma cells induced by the inhibition of T-type calcium channels. Partial reprogramming of melanoma cells induced de-differentiation and increased resistance to MAPK inhibitors. Blockage of calcium channels, using mibefradil, could sensitize resistant cells to MAPK inhibitors resulting in increased cell death and differentiation.

7. References

1. McArthur, G. A. & Ribas, A. Targeting oncogenic drivers and the immune system in melanoma. *J. Clin. Oncol.* **31**, 499–506 (2013).
2. Muñoz-Couselo, E., García, J. S., Pérez-García, J. M., Cebrián, V. O. & Castán, J. C. Recent advances in the treatment of melanoma with BRAF and MEK inhibitors. *Ann. Transl. Med.* **3**, 207 (2015).
3. Stadler, S., Weina, K., Gebhardt, C. & Utikal, J. New therapeutic options for advanced non-resectable malignant melanoma. *Adv. Med. Sci.* **60**, 83–88 (2015).
4. Long, G. V. *et al.* Dabrafenib plus trametinib versus dabrafenib monotherapy in patients with metastatic BRAF V600E/K-mutant melanoma: long-term survival and safety analysis of a phase 3 study. *Ann. Oncol. Off. J. Eur. Soc. Med. Oncol.* **28**, 1631–1639 (2017).
5. Manzano, J. L. *et al.* Resistant mechanisms to BRAF inhibitors in melanoma. *Ann. Transl. Med.* **4**, 237–237 (2016).
6. Konieczkowski, D. J. *et al.* A melanoma cell state distinction influences sensitivity to MAPK pathway inhibitors. *Cancer Discov.* **4**, 816–827 (2014).
7. Ahmed, F. & Haass, N. K. Microenvironment-Driven Dynamic Heterogeneity and Phenotypic Plasticity as a Mechanism of Melanoma Therapy Resistance. *Front. Oncol.* **8**, 1–7 (2018).
8. Vandamme, N. & Berx, G. Melanoma Cells Revive an Embryonic Transcriptional Network to Dictate Phenotypic Heterogeneity. *Front. Oncol.* **4**, 1–6 (2014).
9. Woods, K., Pasam, A., Jayachandran, A., Andrews, M. C. & Cebon, J. Effects of Epithelial to Mesenchymal Transition on T Cell Targeting of Melanoma Cells. *Front. Oncol.* **4**, 1–7 (2014).

10. Kim, J. E., Leung, E., Baguley, B. C. & Finlay, G. J. Heterogeneity of expression of epithelial-mesenchymal transition markers in melanocytes and melanoma cell lines. *Front. Genet.* **4**, 1–8 (2013).
11. Maik-Rachline, G. & Seger, R. The ERK cascade inhibitors: Towards overcoming resistance. *Drug Resist. Updat.* **25**, 1–12 (2016).
12. Knappe, N. *et al.* Directed Dedifferentiation Using Partial Reprogramming Induces Invasive Phenotype in Melanoma Cells. *Stem Cells* **34**, 832–846 (2016).
13. Guy, G. P. *et al.* Vital signs: Melanoma incidence and mortality trends and projections — United States, 1982–2030. *Morb. Mortal. Wkly. Rep.* **64**, 591–596 (2015).
14. Feigelson, H. S. *et al.* Melanoma incidence, recurrence, and mortality in an integrated healthcare system: A retrospective cohort study. *Cancer Med.* **8**, 4508–4516 (2019).
15. Chattopadhyay, S. *et al.* Familial Risks and Mortality in Second Primary Cancers in Melanoma. *JNCI Cancer Spectr.* **2**, 1–7 (2018).
16. Forsea, A. M., Del Marmol, V., De Vries, E., Bailey, E. E. & Geller, A. C. Melanoma incidence and mortality in Europe: New estimates, persistent disparities. *Br. J. Dermatol.* **167**, 1124–1130 (2012).
17. Aitken, J. F. *et al.* Generational shift in melanoma incidence and mortality in Queensland, Australia, 1995–2014. *Int. J. Cancer* **142**, 1528–1535 (2018).
18. Douki, T., von Koschembahr, A. & Cadet, J. Insight in DNA Repair of UV-induced Pyrimidine Dimers by Chromatographic Methods. *Photochem. Photobiol.* **93**, 207–215 (2017).
19. Alberts, B. et al. *Molecular Biology of the cell*. (Garland Science Taylor & Francis, 2008).
20. Davies, H. *et al.* Mutations of the BRAF gene in human cancer. *Nature* **417**, 949–

954 (2002).

21. Reddy, B. Y., Miller, D. M. & Tsao, H. Somatic driver mutations in melanoma. *Cancer* **123**, 2104–2117 (2017).

22. Garman, B. *et al.* Genetic and Genomic Characterization of 462 Melanoma Patient-Derived Xenografts, Tumor Biopsies, and Cell Lines. *Cell Rep.* **21**, 1936–1952 (2017).

23. Hodis, E. *et al.* A landscape of driver mutations in melanoma. *Cell* **150**, 251–263 (2012).

24. Heppt, M. V. *et al.* Prognostic significance of BRAF and NRAS mutations in melanoma: a German study from routine care. *BMC Cancer* **17**, 536 (2017).

25. Casula, M. *et al.* Germline and somatic mutations in patients with multiple primary melanomas: a next generation sequencing study. *BMC Cancer* **19**, 1–10 (2019).

26. Vinagre, J. *et al.* Frequency of TERT promoter mutations in human cancers. *Nat. Commun.* **4**, 1–6 (2013).

27. Lawrence, M. S. *et al.* Comprehensive genomic characterization of head and neck squamous cell carcinomas. *Nature* **517**, 576–582 (2015).

28. Vultur, A. & Herlyn, M. SnapShot: Melanoma. *Cancer Cell* **23**, 706–706 (2013).

29. Paraiso, K. H. T., Der Kooi, K. Van, Messina, J. L. & Smalley, K. S. M. Measurement of constitutive MAPK and PI3K/AKT signaling activity in human cancer cell lines. *Methods Enzymol.* **484**, 549–567 (2010).

30. De Luca, A., Maiello, M. R., D'Alessio, A., Pergameno, M. & Normanno, N. The RAS/RAF/MEK/ERK and the PI3K/AKT signalling pathways: Role in cancer pathogenesis and implications for therapeutic approaches. *Expert Opin. Ther. Targets* **16**, 517–527 (2012).

31. Mendoza, M. C., Er, E. E. & Blenis, J. The Ras-ERK and PI3K-mTOR pathways:

Cross-talk and compensation. *Trends Biochem. Sci.* **36**, 320–328 (2011).

32. Bettum, I. J. *et al.* Metabolic reprogramming supports the invasive phenotype in malignant melanoma. *Cancer Lett.* **366**, 71–83 (2015).
33. O'Connell, M. P. & Weeraratna, A. T. Change is in the air: The hypoxic induction of phenotype switching in melanoma. *J. Invest. Dermatol.* **133**, 2316–2317 (2013).
34. Widmer, D. S. *et al.* Hypoxia contributes to melanoma heterogeneity by triggering HIF1α-dependent phenotype switching. *J. Invest. Dermatol.* **133**, 2436–2443 (2013).
35. Monaghan-Benson, E. & Burridge, K. Mutant B-RAF regulates a Rac-dependent cadherin switch in melanoma. *Oncogene* **32**, 4836–4844 (2013).
36. Roesch, A. *et al.* Phenotypic tumour cell plasticity as a resistance mechanism and therapeutic target in melanoma. *Eur. J. Cancer* **59**, 109–112 (2016).
37. Wellbrock, C. & Arozarena, I. The Complexity of the ERK/MAP-Kinase Pathway and the Treatment of Melanoma Skin Cancer. *Front. Cell Dev. Biol.* **4**, 1–9 (2016).
38. Chapman, A. *et al.* Heterogeneous tumor subpopulations cooperate to drive invasion. *Cell Rep.* **8**, 688–695 (2014).
39. Hoek, K. S. *et al.* In vivo switching of human melanoma cells between proliferative and invasive states. *Cancer Res.* **68**, 650–656 (2008).
40. Goding, C. R. A picture of Mitf in melanoma immortality. *Oncogene* **30**, 2304–2306 (2011).
41. Kemper, K., De Goeje, P. L., Peeper, D. S. & Van Amerongen, R. Phenotype switching: Tumor cell plasticity as a resistance mechanism and target for therapy. *Cancer Res.* **74**, 5937–5941 (2014).
42. Landsberg, J. *et al.* Melanomas resist T-cell therapy through inflammation-

induced reversible dedifferentiation. *Nature* **490**, 412–416 (2012).

43. Tsoi, J. *et al.* Multi-stage Differentiation Defines Melanoma Subtypes with Differential Vulnerability to Drug-Induced Iron-Dependent Oxidative Stress. *Cancer Cell* **33**, 890–904 (2018).
44. Müller, J. *et al.* Low MITF/AXL ratio predicts early resistance to multiple targeted drugs in melanoma. *Nat. Commun.* **5**, 1–15 (2014).
45. Bhatia, S., Tykodi, S. S. & Thompson, J. A. Treatment of metastatic melanoma: An overview. *Oncology* **23**, 488–496 (2009).
46. Kaufman, H. & Mehnert, J. *Melanoma*. (Springer International Publishing, 2016).
47. Johnstone, T. C., Wilson, J. J. & Lippard, S. J. Understanding and Improving Platinum Anticancer Drugs. *Inorg. Chem.* **52**, 12234–12249 (2013).
48. Kozar, I., Margue, C., Rothengatter, S., Haan, C. & Kreis, S. Many ways to resistance: How melanoma cells evade targeted therapies. *Biochim. Biophys. Acta - Rev. Cancer* **1871**, 313–322 (2019).
49. Chapman, P. B. *et al.* Improved survival with vemurafenib in melanoma with BRAF V600E mutation. *N. Engl. J. Med.* **364**, 2507–2516 (2011).
50. Hatzivassiliou, G. *et al.* RAF inhibitors prime wild-type RAF to activate the MAPK pathway and enhance growth. *Nature* **464**, 431–435 (2010).
51. Kim, K. B. *et al.* Phase II study of the MEK1/MEK2 inhibitor trametinib in patients with metastatic BRAF-mutant cutaneous melanoma previously treated with or without a BRAF inhibitor. *J. Clin. Oncol.* **31**, 482–489 (2013).
52. Flaherty, K. T. *et al.* Combined BRAF and MEK inhibition in melanoma with BRAF V600 mutations. *N. Engl. J. Med.* **367**, 1694–1703 (2012).
53. Larkin, J. *et al.* Combined vemurafenib and cobimetinib in BRAF-mutated melanoma. *N. Engl. J. Med.* **371**, 1867–1876 (2014).
54. Ascierto, P. A. *et al.* Cobimetinib combined with vemurafenib in advanced

BRAFV600-mutant melanoma (coBRIM): updated efficacy results from a randomised, double-blind, phase 3 trial. *Lancet Oncol.* **17**, 1248–1260 (2016).

55. Greger, J. G. *et al.* Combinations of BRAF, MEK, and PI3K/mTOR inhibitors overcome acquired resistance to the BRAF inhibitor GSK2118436 dabrafenib, mediated by NRAS or MEK mutations. *Mol. Cancer Ther.* **11**, 909–920 (2012).
56. Atefi, M. *et al.* Reversing melanoma Cross-Resistance to BRAF and MEK inhibitors by Co-Targeting the AKT/mTOR pathway. *PLoS One* **6**, 1–12 (2011).
57. Klinac, D., Gray, E. S., Millward, M. & Ziman, M. Advances in personalized targeted treatment of metastatic melanoma and non-invasive tumor monitoring. *Front. Oncol.* **3**, 1–16 (2013).
58. Tran, K. A. *et al.* MEK inhibitors and their potential in the treatment of advanced melanoma: The advantages of combination therapy. *Drug Des. Devel. Ther.* **10**, 43–52 (2015).
59. Seidel, J. A., Otsuka, A. & Kabashima, K. Anti-PD-1 and anti-CTLA-4 therapies in cancer: Mechanisms of action, efficacy, and limitations. *Front. Oncol.* **8**, 1–14 (2018).
60. Wolchok, J. D. *et al.* Overall Survival with Combined Nivolumab and Ipilimumab in Advanced Melanoma. *N. Engl. J. Med.* **377**, 1345–1356 (2017).
61. Leach, D. R., Krummel, M. F. & Allison, J. P. Enhancement of antitumor immunity by CTLA-4 blockade. *Science (80-.).* **271**, 1734–1736 (1996).
62. Hodi, F. S. *et al.* Biologic activity of cytotoxic T lymphocyte-associated antigen 4 antibody blockade in previously vaccinated metastatic melanoma and ovarian carcinoma patients. *Proc. Natl. Acad. Sci. U. S. A.* **100**, 4712–4717 (2003).
63. Robert, C. *et al.* Ipilimumab plus dacarbazine for previously untreated metastatic melanoma. *N. Engl. J. Med.* **364**, 2517–2526 (2011).
64. Lugowska, I., Teterycz, P. & Rutkowski, P. Immunotherapy of melanoma.

Wspolczesna Onkol. **2**, 61–67 (2017).

65. Topalian, S. L. *et al.* Survival, durable tumor remission, and long-term safety in patients with advanced melanoma receiving nivolumab. *J. Clin. Oncol.* **32**, 1020–1030 (2014).
66. Robert, C. *et al.* Nivolumab in previously untreated melanoma without BRAF mutation. *N. Engl. J. Med.* **372**, 320–330 (2015).
67. Robert, C. *et al.* Anti-programmed-death-receptor-1 treatment with pembrolizumab in ipilimumab-refractory advanced melanoma: A randomised dose-comparison cohort of a phase 1 trial. *Lancet* **384**, 1109–1117 (2014).
68. Hunder, N. N. *et al.* Treatment of metastatic melanoma with autologous CD4+ T cells against NY-ESO-1. *N. Engl. J. Med.* **358**, 2698–2703 (2008).
69. Brentjens, R. *et al.* CD19-targeted T cells rapidly induce molecular remissions in adults with chemotherapy-refractory acute lymphoblastic leukemia. *Sci Transl Med.* **5**, (2013).
70. Beard, R. E. *et al.* Multiple chimeric antigen receptors successfully target chondroitin sulfate proteoglycan 4 in several different cancer histologies and cancer stem cells. *J. Immunother. Cancer* **2**, 1–11 (2014).
71. O'Donoghue, C., Doepker, M. P. & Zager, J. S. Talimogene laherparepvec: overview, combination therapy and current practices. *Melanoma Manag.* **3**, 267–272 (2016).
72. Hu, J. C. C. *et al.* A phase I study of OncoVEX GM-CSF , a second-generation oncolytic herpes simplex virus expressing granulocyte macrophage colony-stimulating factor. *Clin. Cancer Res.* **12**, 6737–6747 (2006).
73. Mandalá, M. & Romano, E. *Mechanisms of drug resistance in cancer therapy*. **1249**, (Springer International Publishing, 2018).
74. Fallahi-Sichani, M. *et al.* Adaptive resistance of melanoma cells to RAF inhibition

via reversible induction of a slowly dividing de-differentiated state. *Mol. Syst. Biol.* **13**, 905 (2017).

75. Hüser, L. *et al.* SOX2-mediated upregulation of CD24 promotes adaptive resistance towards targeted therapy in melanoma. *IJC* **00**, 1–12 (2018).
76. Kugel, C. H. & Aplin, A. E. Adaptive resistance to RAF inhibitors in melanoma. *Pigment Cell Melanoma Res.* **27**, 1032–1038 (2014).
77. Alcalá, A. M. & Flaherty, K. T. BRAF inhibitors for the treatment of metastatic melanoma: Clinical trials and mechanisms of resistance. *Clin. Cancer Res.* **18**, 33–39 (2012).
78. Hartsough, E., Shao, Y. & Aplin, A. E. Resistance to RAF inhibitors revisited. *J. Invest. Dermatol.* **134**, 319–325 (2014).
79. Lito, P. *et al.* Relief of Profound Feedback Inhibition of Mitogenic Signaling by RAF Inhibitors Attenuates Their Activity in BRAFV600E Melanomas. *Cancer Cell* **22**, 668–682 (2012).
80. Abel, E. V *et al.* Melanoma adapts to RAF/MEK inhibitors through FOXD3-mediated upregulation of ERBB3. **123**, 2155–2168 (2013).
81. Waddington, C. . *The strategy of the genes*. (George Allen & Unwin LTD, 1957).
82. Karagiannis, P. & Yamanaka, S. The fate of cell reprogramming. *Nat. Methods* **11**, 1006–1008 (2014).
83. Jopling, C., Boue, S. & Belmonte, J. C. I. Dedifferentiation, transdifferentiation and reprogramming: Three routes to regeneration. *Nat. Rev. Mol. Cell Biol.* **12**, 79–89 (2011).
84. Friedmann-Morvinski, D. & Verma, I. M. Dedifferentiation and reprogramming: Origins of cancer stem cells. *EMBO Rep.* **15**, 244–253 (2014).
85. Ben-Porath, I. *et al.* An embryonic stem cell-like gene expression signature in poorly differentiated aggressive human tumors. *Nat. Genet.* **40**, 499–507 (2008).

86. Schwitalla, S. *et al.* Intestinal tumorigenesis initiated by dedifferentiation and acquisition of stem-cell-like properties. *Cell* **152**, 25–38 (2013).

87. Dulak, J., Szade, K., Szade, A., Nowak, W. & Józkowicz, A. Adult stem cells: Hopes and hypes of regenerative medicine. *Acta Biochim. Pol.* **62**, 329–337 (2015).

88. Wyles, S. P., Brandt, E. B. & Nelson, T. J. Stem cells: The pursuit of genomic stability. *Int. J. Mol. Sci.* **15**, 20948–20967 (2014).

89. Daley, G. Q. Stem cells and the evolving notion of cellular identity. *Philos. Trans. R. Soc. B Biol. Sci.* **370**, 1–5 (2015).

90. Gurdon, J. B. Sexually mature individuals of xenopus laevis from the transplantation of single somatic nuclei. *Nature* **182**, 800–801 (1958).

91. Takahashi, K. & Yamanaka, S. Induction of Pluripotent Stem Cells from Mouse Embryonic and Adult Fibroblast Cultures by Defined Factors. *Cell* **126**, 663–676 (2006).

92. Utikal, J., Maherali, N., Kulalert, W. & Hochedlinger, K. Sox2 is dispensable for the reprogramming of melanocytes and melanoma cells into induced pluripotent stem cells. *J. Cell Sci.* **122**, 3502–3510 (2009).

93. Yu, J. *et al.* Induced pluripotent stem cell lines derived from human somatic cells. *Science (80-.).* **318**, 1917–1920 (2007).

94. Kim, J. B. *et al.* Pluripotent stem cells induced from adult neural stem cells by reprogramming with two factors. *Nature* **454**, 646–650 (2008).

95. Cimmino, L., Neel, B. G. & Aifantis, I. Vitamin C in Stem Cell Reprogramming and Cancer. *Trends Cell Biol.* **28**, 698–708 (2018).

96. Ma, X., Kong, L. & Zhu, S. Reprogramming cell fates by small molecules. *Protein Cell* **8**, 328–348 (2017).

97. Smith, O. K. *et al.* Distinct epigenetic features of differentiation-regulated

replication origins. *Epigenetics Chromatin* **9**, 1–17 (2016).

98. Soufi, A. Mechanisms for enhancing cellular reprogramming. *Curr. Opin. Genet. Dev.* **25**, 101–109 (2014).
99. Prieto, J. *et al.* MYC Induces a Hybrid Energetics Program Early in Cell Reprogramming. *Stem Cell Reports* **11**, 1479–1492 (2018).
100. Nishimura, K., Fukuda, A. & Hisatake, K. Mechanisms of the metabolic shift during somatic cell reprogramming. *Int. J. Mol. Sci.* **20**, 1–16 (2019).
101. Jaenisch, R. & Young, R. Stem Cells, the Molecular Circuitry of Pluripotency and Nuclear Reprogramming. *Cell* **132**, 567–582 (2008).
102. Takata, C., Albright, J. F. & Yamada, T. Lens fiber differentiation and gamma crystallins: Immunofluorescent study of wolffian regeneration. *Science (80-.).* **147**, 1299–1301 (1965).
103. Donati, G. *et al.* Wounding induces dedifferentiation of epidermal Gata6 + cells and acquisition of stem cell properties. *Nat. Cell Biol.* **19**, 603–613 (2017).
104. Tata, P. R. *et al.* Dedifferentiation of committed epithelial cells into stem cells in vivo. *Nature* **503**, 218–223 (2013).
105. Xiong, S., Feng, Y. & Cheng, L. Cellular Reprogramming as a Therapeutic Target in Cancer. *Trends Cell Biol.* **20**, 1–12 (2019).
106. O'Brien, C. A., Kreso, A. & Jamieson, C. H. M. Cancer stem cells and self-renewal. *Clin. Cancer Res.* **16**, 3113–3120 (2010).
107. Kahn, M. *Wnt Signaling in Stem Cells and Cancer Stem Cells: A Tale of Two Coactivators*. *Progress in Molecular Biology and Translational Science* **153**, (Elsevier Inc., 2018).
108. Câmara, D. A. D., Mambelli, L. I., Porcacchia, A. S. & Kerkis, I. Advances and challenges on cancer cells reprogramming using induced pluripotent stem cells technologies. *J. Cancer* **7**, 2296–2303 (2016).

109. Bernhardt, M., Galach, M., Novak, D. & Utikal, J. Mediators of induced pluripotency and their role in cancer cells - current scientific knowledge and future perspectives. *Biotechnol. J.* **7**, 810–821 (2012).

110. Carette, J. E. *et al.* Generation of iPSCs from cultured human malignant cells. *Blood* **115**, 4039–4042 (2010).

111. Miyoshi, N. *et al.* Defined factors induce reprogramming of gastrointestinal cancer cells. *Proc. Natl. Acad. Sci. U. S. A.* **107**, 40–45 (2010).

112. Choong, P. F. *et al.* Heterogeneity of osteosarcoma cell lines led to variable responses in reprogramming. *Int. J. Med. Sci.* **11**, 1154–1160 (2014).

113. Kim, J. *et al.* An iPSC Line from Human Pancreatic Ductal Adenocarcinoma Undergoes Early to Invasive Stages of Pancreatic Cancer Progression. *Cell Rep.* **3**, 2088–2099 (2013).

114. Franken, N. A. P., Rodermond, H. M., Stap, J., Haveman, J. & Bree, C. Van. Clonogenic assay of cells in vitro. *Nat. Protoc.* **1**, 2315–2319 (2006).

115. Hothorn, T., Hornik, K. & Zeileis, A. Unbiased recursive partitioning: A conditional inference framework. Research Report Series 8, Department of Statistics and Mathematics, WU Wien, 2004. *Comb. Tradit. Graph. Grid Graph.* **289**, 31 (2006).

116. Garolini, D. *et al.* TCGAbiolinks : an R/Bioconductor package for integrative analysis of TCGA data . *Nucleic Acids Res.* **44**, e71–e71 (2015).

117. Tsoi, J. *et al.* Multi-stage Differentiation Defines Melanoma Subtypes with Differential Vulnerability to Drug-Induced Iron-Dependent Oxidative Stress. *Cancer Cell* **33**, 890-904.e5 (2018).

118. Sachindra *et al.* New role of ID3 in melanoma adaptive drug-resistance. *Oncotarget* **8**, 110166–110175 (2017).

119. Bernhardt, M. *et al.* Melanoma-Derived iPCCs Show Differential Tumorigenicity and Therapy Response. *Stem Cell Reports* **8**, 1379–1391 (2017).

120. Utikal, J., Maherali, N., Kulalert, W. & Hochedlinger, K. Sox2 is dispensable for the reprogramming of melanocytes and melanoma cells into induced pluripotent stem cells. *J. Cell Sci.* **122**, 3502–3510 (2009).

121. Sáez-Ayala, M. *et al.* Directed Phenotype Switching as an Effective Antimelanoma Strategy. *Cancer Cell* **24**, 105–119 (2013).

122. Clark, W. H. *et al.* A study of tumor progression: The precursor lesions of superficial spreading and nodular melanoma. *Hum. Pathol.* **15**, 1147–1165 (1984).

123. Falletta, P. *et al.* Translation reprogramming is an evolutionarily conserved driver of phenotypic plasticity and therapeutic resistance in melanoma. *Genes Dev.* **31**, 18–33 (2017).

124. Kong, X. *et al.* Cancer drug addiction is relayed by an ERK2-dependent phenotype switch. *Nature* **550**, 270–274 (2017).

125. Carreira, S. *et al.* Mitf regulation of Dia1 controls melanoma proliferation and invasiveness. *Genes Dev.* **20**, 3426–3439 (2006).

126. Sun, L. *et al.* Silencing of PMEL attenuates melanization via activating lysosomes and degradation of tyrosinase by lysosomes. *Biochem. Biophys. Res. Commun.* **503**, 2536–2542 (2018).

127. Sellerio, A. L. *et al.* Overshoot during phenotypic switching of cancer cell populations. *Sci. Rep.* **5**, 1–14 (2015).

128. Lito, P., Rosen, N. & Solit, D. B. Tumor adaptation and resistance to RAF inhibitors. *Nat. Med.* **19**, 1401–1409 (2013).

129. Zuo, Q. *et al.* AXL/AKT axis mediated-resistance to BRAF inhibitor depends on PTEN status in melanoma. *Oncogene* **37**, 3275–3289 (2018).

130. Shaffer, S. M. *et al.* Rare cell variability and drug-induced reprogramming as a mode of cancer drug resistance. *Nature* **546**, 431–435 (2017).

131. Buchanan, P. J. & McCloskey, K. D. CaVchannels and cancer: canonical functions indicate benefits of repurposed drugs as cancer therapeutics. *Eur. Biophys. J.* **45**, 621–633 (2016).

132. Schlick, B., Flucher, B. E. & Obermair, G. J. Voltage-Activated Calcium Channel Expression Profiles in Mouse Brain and Cultured Hippocampal Neurons. *Neuroscience* **167**, 786–798 (2012).

133. Masicampo, M. L., Shan, H. Q., Xu, V., Speagle, M. & Godwin, D. W. Selective Blockade of T-Type Ca2+ Channels is Protective Against Alcohol-Withdrawal Induced Seizure and Mortality. *Alcohol Alcohol.* **53**, 526–531 (2018).

134. Bezençon, O. *et al.* Discovery of a Potent, Selective T-type Calcium Channel Blocker as a Drug Candidate for the Treatment of Generalized Epilepsies. *J. Med. Chem.* **60**, 9769–9789 (2017).

135. Kang, X.-J. *et al.* Increased expression of Ca V 3.2 T-type calcium channels in damaged DRG neurons contributes to neuropathic pain in rats with spared nerve injury. *Mol. Pain* **14**, 1–11 (2018).

136. Mesirca, P., Torrente, A. G. & Mangoni, M. E. Functional role of voltage gated Ca2+ channels in heart automaticity. *Front. Physiol.* **6**, 1–13 (2015).

137. Densmore, J. J., Szabo, G. & Gray, L. S. A voltage-gated calcium channel is linked to the antigen receptor in Jurkat T lymphocytes. **312**, 161–164 (1992).

138. Wang, C. Y., Lai, M. D., Phan, N. N., Sun, Z. & Lin, Y. C. Meta-analysis of public microarray datasets reveals voltage-gated calcium gene signatures in clinical cancer patients. *PLoS One* **10**, 1–21 (2015).

139. Su, A. I. *et al.* Molecular classification of human carcinomas by use of gene expression signatures. *Cancer Res.* **61**, 7388–93 (2001).

140. Antal, L. & Martin-Caraballo, M. T-type calcium channels in cancer. *Cancers (Basel).* **11**, 1–18 (2019).

141. Zhang, Y. *et al.* Inhibition of T-type Ca^{2+} channels by endostatin attenuates human glioblastoma cell proliferation and migration. *Br. J. Pharmacol.* **166**, 1247–1260 (2012).

142. Zhang, Y. *et al.* Targetable T-type calcium channels drive glioblastoma. *Cancer Res.* **77**, 3479–3490 (2017).

143. Dziegielewska, B. *et al.* T-Type Ca2+ Channel Inhibition Sensitizes Ovarian Cancer to Carboplatin. *Mol. Cancer Ther.* **15**, 460–70 (2016).

144. Pera, E. *et al.* The voltage gated Ca2+-channel Cav3.2 and therapeutic responses in breast cancer. *Cancer Cell Int.* **16**, 1–15 (2016).

145. Huang, W., Lu, C., Wu, Y., Ouyang, S. & Chen, Y. T-type calcium channel antagonists, mibefradil and NNC-55-0396 inhibit cell proliferation and induce cell apoptosis in leukemia cell lines. *J. Exp. Clin. Cancer Res.* **34**, 1–15 (2015).

146. Das, A. *et al.* Functional expression of voltage-gated calcium channels in human melanoma. *Pigment Cell Melanoma Res.* **25**, 200–212 (2012).

147. Clozel, J.-P., Ertel, E. A. & Ertel, S. I. Discovery and main pharmacological properties of mibefradil (Ro 40-5967), the first selective T-type calcium channel blocker. *J. Hypertens.* **15**, S17–S26 (1997).

148. Bradbury, J. Posicor withdrawn voluntarily from market by Roche. *Lancet* **351**, 1791 (1998).

149. Krouse, A. J., Gray, L., Macdonald, T. & McCray, J. Repurposing and Rescuing of Mibefradil, an Antihypertensive, for Cancer: A Case Study. *Drug Repurposing, Rescue, Repositioning* **1**, 36–39 (2016).

150. Gray, L. S. *et al.* The role of voltage gated T-type Ca2+channel isoforms in mediating ‘capacitative’ Ca2+ entry in cancer cells. *Cell Calcium* **36**, 489–497 (2004).

151. Hao, B., Webb, S. E., Miller, A. L. & Yue, J. The role of Ca2+signaling on the

self-renewal and neural differentiation of embryonic stem cells (ESCs). *Cell Calcium* **59**, 67–74 (2016).

152. Sallan, M. C. *et al.* T-type Ca2+Channels: T for targetable. *Cancer Res.* **78**, 603–609 (2018).
153. Panner, A. & Wurster, R. D. T-type calcium channels and tumor proliferation. *Cell Calcium* **40**, 253–259 (2006).
154. Panner, A. *et al.* Variation of T-type calcium channel protein expression affects cell division of cultured tumor cells. *Cell Calcium* **37**, 105–119 (2005).
155. Keir, S. T., Friedman, H. S., Reardon, D. A., Bigner, D. D. & Gray, L. A. Mibefradil, a novel therapy for glioblastoma multiforme: Cell cycle synchronization and interlaced therapy in a murine model. *J. Neurooncol.* **111**, 97–102 (2013).
156. Dziegielewska, B., Brautigan, D. L., Larner, J. M. & Dziegielewski, J. T-Type Ca2+ Channel Inhibition Induces p53-Dependent Cell Growth Arrest and Apoptosis through Activation of p38-MAPK in Colon Cancer Cells. *Mol. Cancer Res.* **12**, 348–358 (2014).
157. Choi, D. L. *et al.* Inhibition of cellular proliferation and induction of apoptosis in human lung adenocarcinoma A549 cells by T-type calcium channel antagonist. *Bioorganic Med. Chem. Lett.* **24**, 1565–1570 (2014).
158. Das, A. *et al.* T-type calcium channel blockers inhibit autophagy and promote apoptosis of malignant melanoma cells. *Pigment Cell Melanoma Res.* **26**, 874–885 (2013).
159. Maiques, O. *et al.* Immunohistochemical analysis of T-type calcium channels in acquired melanocytic naevi and melanoma. *Br. J. Dermatol.* **176**, 1247–1258 (2017).
160. Jang, S. J. *et al.* In vitro cytotoxicity on human ovarian cancer cells by T-type

calcium channel blockers. *Bioorganic Med. Chem. Lett.* **23**, 6656–6662 (2013).

161. Valerie, N. C. K. *et al.* Inhibition of T-type calcium channels disrupts Akt signaling and promotes apoptosis in glioblastoma cells. *Biochem. Pharmacol.* **85**, 888–897 (2013).
162. Boiko, A. D. *et al.* Human melanoma-initiating cells express neural crest nerve growth factor receptor CD271. *Nature* **466**, 133–137 (2010).
163. Zubrilov, I. *et al.* Vemurafenib resistance selects for highly malignant brain and lung-metastasizing melanoma cells. *Cancer Lett.* **361**, 86–96 (2015).
164. Álvarez-Viejo, M. CD271 as a marker to identify mesenchymal stem cells from diverse sources before culture. *World J. Stem Cells* **7**, 470–476 (2015).
165. Murillo-Sauca, O. *et al.* CD271 is a functional and targetable marker of tumor-initiating cells in head and neck squamous cell carcinoma. *Oncotarget* **5**, 6854–6866 (2014).
166. Redmer, T. *et al.* The role of the cancer stem cell marker CD271 in DNA damage response and drug resistance of melanoma cells. *Oncogenesis* **6**, 1–13 (2017).
167. Radke, J., Roßner, F. & Redmer, T. CD271 determines migratory properties of melanoma cells. *Sci. Rep.* **7**, 1–14 (2017).
168. Redmer, T. *et al.* The nerve growth factor receptor CD271 is crucial to maintain tumorigenicity and stem-like properties of melanoma cells. *PLoS One* **9**, 1–16 (2014).
169. Zhao, W., Ji, X., Zhang, F., Li, L. & Ma, L. Embryonic stem cell markers. *Molecules* **17**, 6196–6236 (2012).
170. Ginis, I. *et al.* Differences between human and mouse embryonic stem cells. *Dev. Biol.* **269**, 360–380 (2004).
171. Rodríguez-Gómez, J. A., Levitsky, K. L. & López-Barneo, J. T-type Ca $^{2+}$ channels in mouse embryonic stem cells: modulation during cell cycle and

contribution to self-renewal. *Am. J. Physiol. Physiol.* **302**, C494–C504 (2012).

172. Resende, R. R., da Costa, J. L., Kihara, A. H., Adhikari, A. & Lorençon, E. Intracellular Ca 2+ Regulation During Neuronal Differentiation of Murine Embryonal Carcinoma and Mesenchymal Stem Cells . *Stem Cells Dev.* **19**, 379–394 (2008).
173. Resende, R. R. *et al.* Influence of spontaneous calcium events on cell-cycle progression in embryonal carcinoma and adult stem cells. *Biochim. Biophys. Acta - Mol. Cell Res.* **1803**, 246–260 (2010).
174. Korkka, I. *et al.* Functional Voltage-Gated Calcium Channels Are Present in Human Embryonic Stem Cell-Derived Retinal Pigment Epithelium. *Stem Cells Transl. Med.* **8**, 179–193 (2019).
175. Julian, L. M., McDonald, A. C. & Stanford, W. L. Direct reprogramming with SOX factors: masters of cell fate. *Curr. Opin. Genet. Dev.* **46**, 24–36 (2017).
176. Sim, B. M. *et al.* Sox 2 promotes tamoxifen resistance in breast cancer cells. *EMBO Mol. Med.* **6**, 66–79 (2014).
177. Holdhoff, M. *et al.* Timed sequential therapy of the selective T-type calcium channel blocker mibefradil and temozolomide in patients with recurrent high-grade gliomas. *Neuro. Oncol.* **19**, 845–852 (2017).

8. Supplemental material

8.1 Supplementary Figures

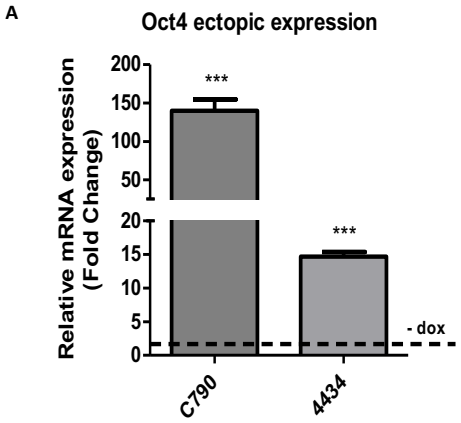

Supplementary Figure S1. Real-Time qPCR analysis of the exogenous expression of the reprogramming factor *Oct4* in C790 and 4434 at day 20 of reprogramming. Data were normalized using control cells ("- dox") as reference and GAPDH as a housekeeping gene.

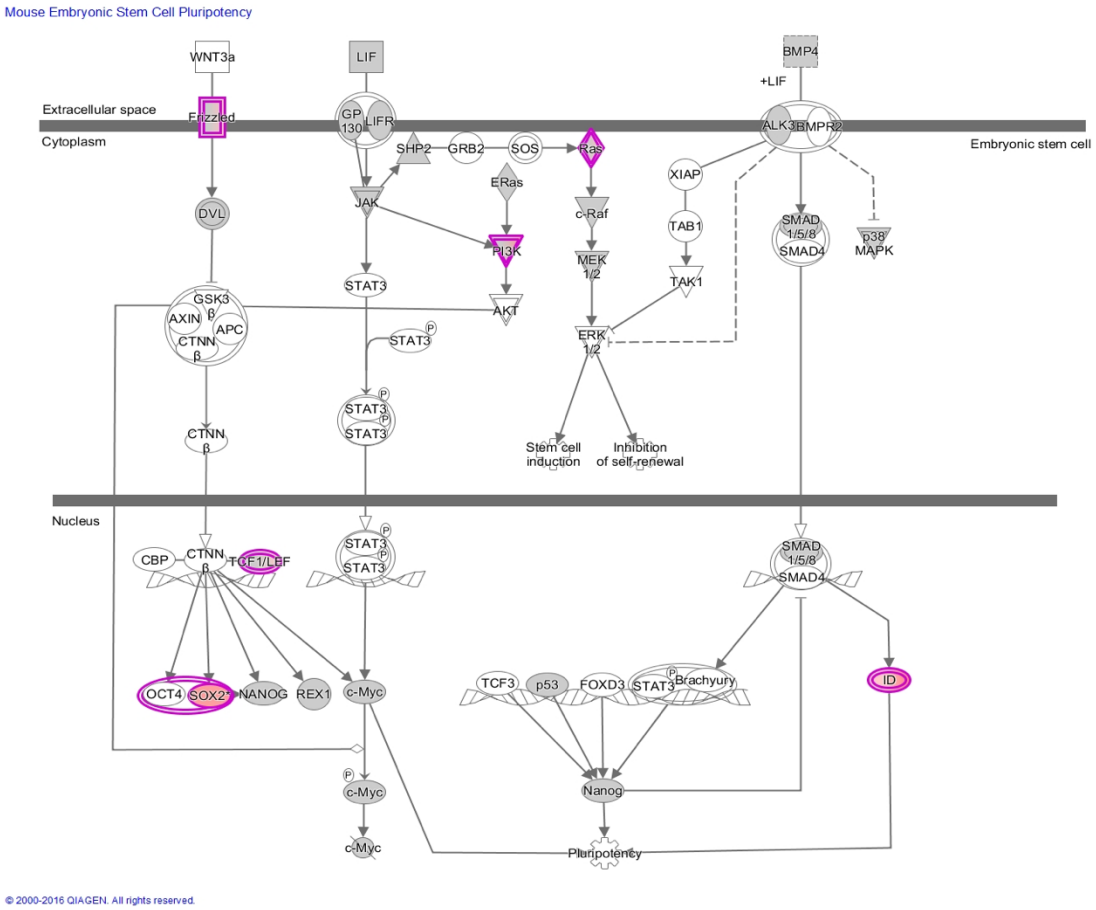

Supplementary Figure S2. IPA Analysis for pathways deregulated in C790 reprogrammed cells at day 20. Genes related to mouse embryonic stem cell pluripotency were predicted to be activated (Oct4, Sox2, ID, Frizzled, PI3K and Ras).

a

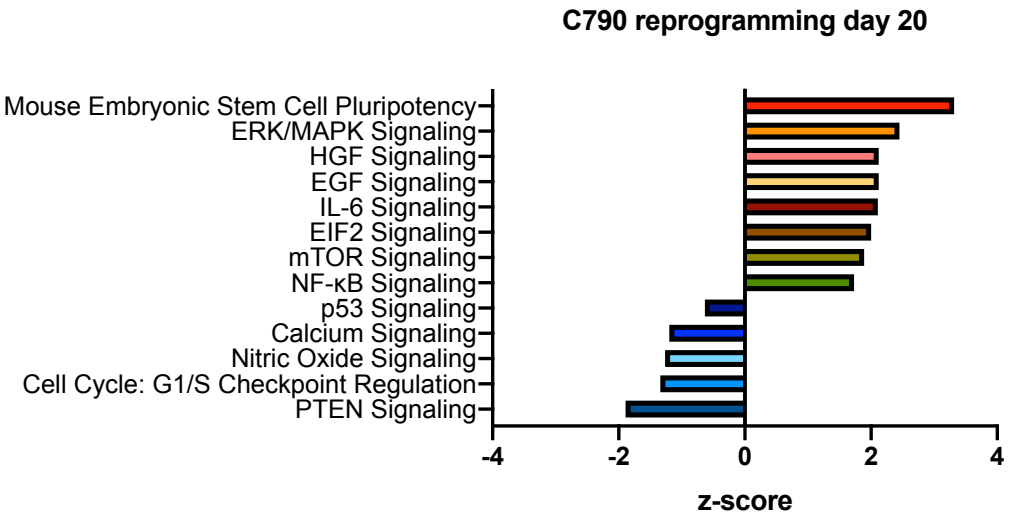

b

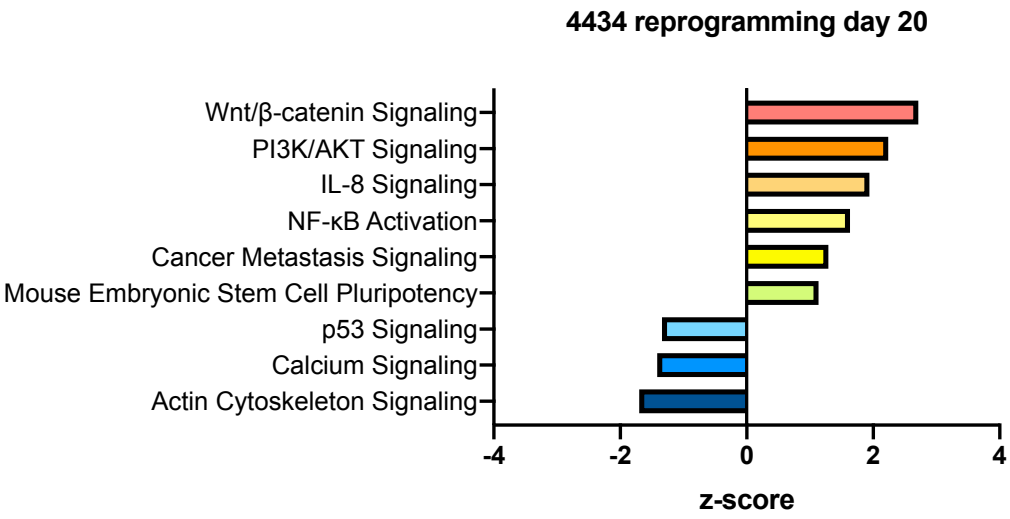

Supplementary Figure S3. IPA Analysis for canonical pathways activated or inhibited in C790 and 4434 reprogrammed cells at day 20. Pathways associated with pluripotency and survival were activated in dedifferentiated reprogrammed cells.

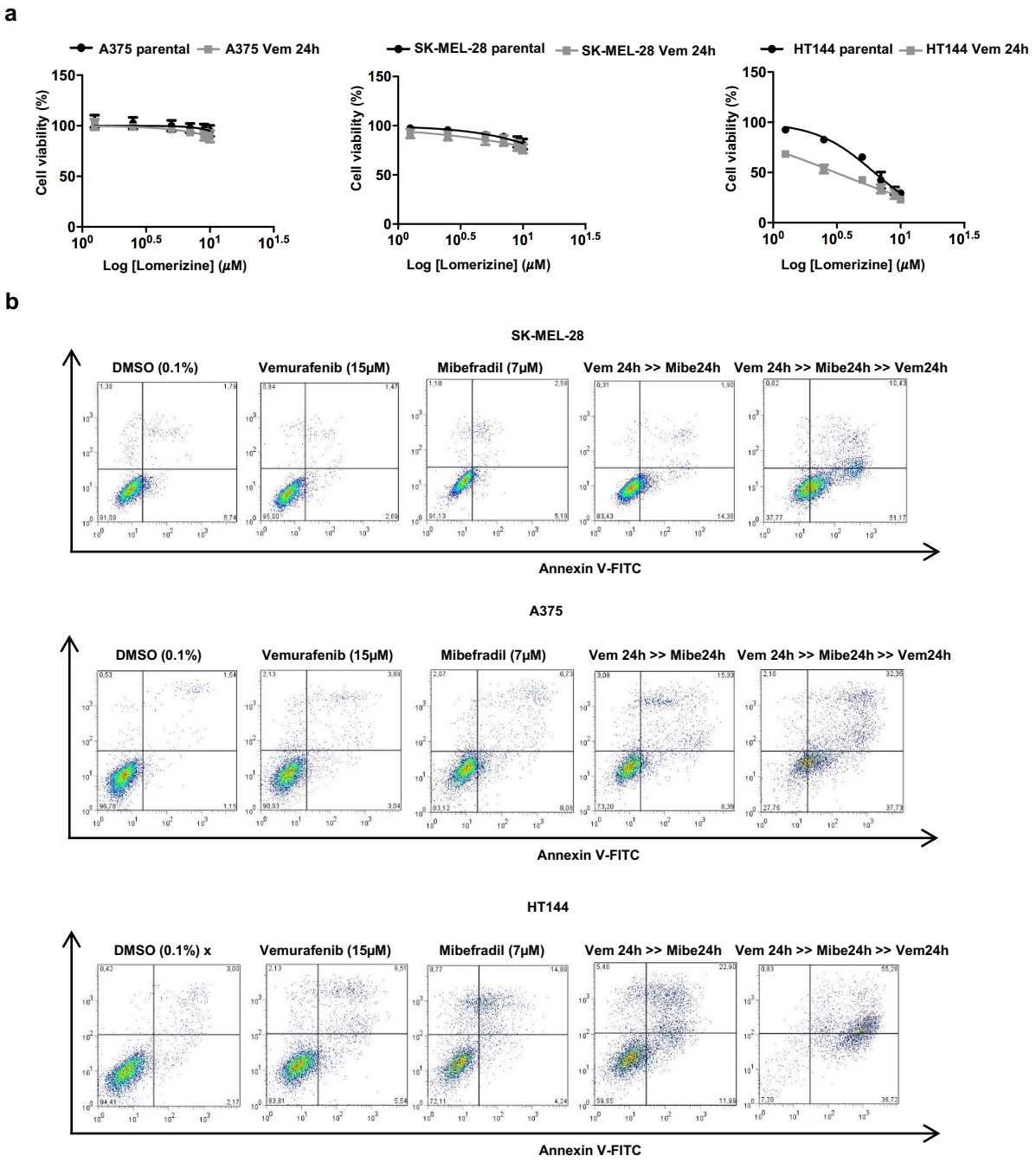

Supplementary Figure S4. Effect of mibefradil and lomerizine in human adaptive BRAF-resistant melanoma cells. a Cell viability assay. After 24 hours treatment with vemurafenib, cells were treated with lomerizine (1.25 – 10 μM) for 24 hours. **b** Representative scatter plots of PI (y-axis) vs. annexin V (x-axis) for human melanoma cells after single treatment with vemurafenib (15 μM), mibefradil (7 μM), and sequential treatment with vemurafenib and mibefradil ("Vem24h>>Mibe24h>>Vem24h"). Early apoptotic cells are shown in the lower right quadrant and late apoptotic cells are shown in the upper right quadrant.

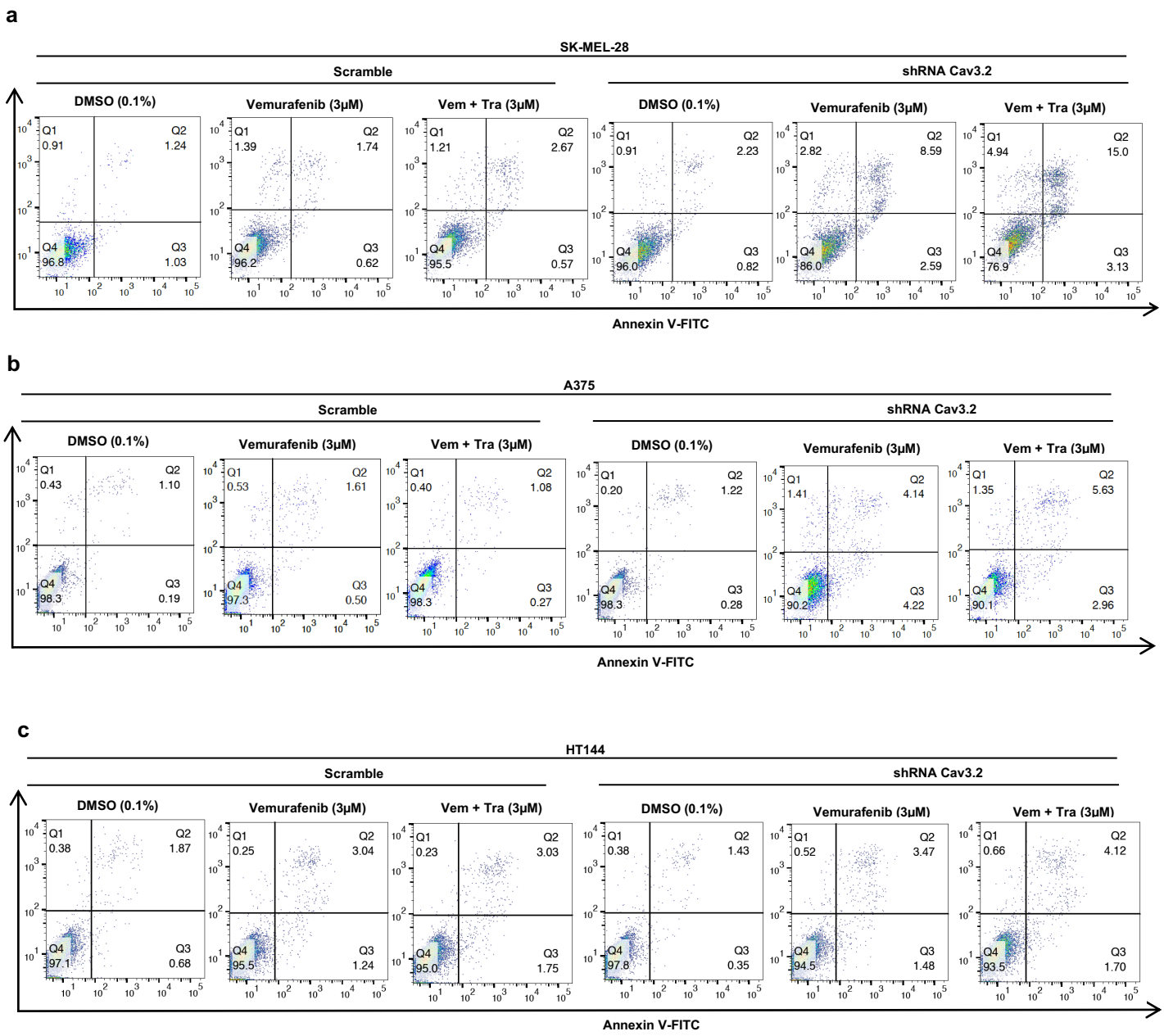

Supplementary Figure S5. Apoptosis analysis after Cav3.2 knockdown in human melanoma cells. a,b,c Representative scatter plots of PI (y-axis) vs. annexin V (x-axis) for all human Cav3.2 knockdown melanoma cells and scramble control, after single treatment with vemurafenib (3 μM) and combination treatment with vemurafenib and trametinib (3 μM). Early apoptotic cells are shown in the lower right quadrant and late apoptotic cells are shown in the upper right quadrant.

8.2 Supplementary Tables

Table S1. IC50 values of trametinib for C790 partially reprogrammed cells.

C790 (NRAS mutant)	IC50 values	
	trametinib (μM)	
	- doxycycline	+ doxycycline
day 6	1.71 ± 0.99	0.20 ± 0.02
day 12	2.16 ± 1.42	> 10μM
day 20	2.09 ± 0.48	> 10μM

Table S2. IC50 values of vemurafenib, trametinib and a combination of both drugs for 4434 partially reprogrammed cells.

4434 (Braf V600E)	IC50 values					
	trametinib (μM)		vemurafenib (μM)		trametinib + vemurafenib (μM)	
	- doxycycline	+ doxycycline	- doxycycline	+ doxycycline	- doxycycline	+ doxycycline
day 6	0.0009 ± 0.0003	0.0008 ± 0.0002	5.40 ± 0.67	1.01 ± 0.05	0.0002 ± 0.0001	0.000007 ± 0.000001
day 12	0.0026 ± 0.0005	0.24 ± 0.06	4.94 ± 1.06	> 10μM	0.0038 ± 0.0053	0.0008 ± 0.0002
day 20	0.0025 ± 0.0001	> 10μM	5.05 ± 0.35	> 10μM	0.0029 ± 0.0020	4.38 ± 0.03

Supplementary Table S3. IC50 values of calcium channel inhibitors for C790 cells (Nras mutant) during partial reprograming at days 6, 12 and 20.

C790 (Nras mutant)	IC50 values			
	lomerizine (μM)		mibefradil (μM)	
	- doxycycline	+ doxycycline	- doxycycline	+ doxycycline
day 6	10.60 ± 0.01	5.59 ± 0.83	6.16 ± 0.25	3.70 ± 0.28
day 12	8.49 ± 0.16	7.18 ±0.25	5.75 ± 0.35	5.39 ± 0.01
day 20	10.02 ± 1.69	7.05 ± 0.49	6.44 ± 0.66	5.09 ± 0.74

Supplementary Table S4. IC50 values of calcium channels inhibitors for 4434 cells (BrafV600E) during reprograming at day 20.

4434 (Braf V600E)	IC50 values			
	mibefradil (μM)		lomerizine (μM)	
	- doxycycline	+ doxycycline	- doxycycline	+ doxycycline
day 20	7.82 ± 0.96	8.87 ± 0.25	> 10μM	> 10μM

Supplementary Table S5. IC50 values of vemurafenib and calcium channel inhibitors for human melanoma cell lines during adaptive resistance.

Cell line	IC50 Values		
	vemurafenib (μM)	mibefradil (μM)	lomerizine(μM)
A375 parental	0.54 ± 0.58	9.63 ± 0.35	> 10 μM
A375 + Vem 24h	> 10 μM	7.43 ± 0.80	> 10 μM
SK-MEL-28 parental	1.3 ± 0.24	8.17 ± 0.40	> 10 μM
SK-MEL-28 + Vem 24h	> 10 μM	6.5 ± 0.30	> 10 μM
HT144 parental	0.7 ± 0.24	5.5 ± 0.41	6.24 ± 0.15
HT144 + Vem 24h	> 10 μM	2.65 ± 0.14	3.07 ± 0.14

9. Acknowledgments

I am genuinely grateful for the opportunity of carried out my doctorate in Germany during the last 4 years, surrounded by many people and friends whom in some way or another have helped me to conclude this journey and for which I am highly grateful. First, I would like to thank the University of Costa Rica (OAICE-CAB-09-133-2015) and the Ministry of Science, Technology and Telecommunications of Costa Rica (MICITT, PINN, PED-054-2015-2) for the financial support for my PhD studies.

My deepest gratitude goes to **Prof. Dr. Jochen Utikal**. First, for the opportunity of being as a PhD student in his research group and for believing in my personal skills and competencies to carry out a doctorate. Also, for all the support and guidance throughout the development of my research project and to let me grow at the personal and professional level over all these years. Furthermore, I really appreciated working in the laboratory at the German Cancer Research Center, where I could learn many techniques and improved my knowledge, which will help me continue my career in the research field.

I also would like to thank **Prof. Dr. Viktor Umansky** for all the significant contributions to my research project and all the advices given. Thank you for considering me as a candidate during the PhD selection rounds, because that moment defined the beginning of this incredible experience. Moreover, I am very grateful to my TAC committee members **Prof. Dr. Jonathan Sleeman** and **Dr. Mike Milson** for their support and feedback during my TAC meetings.

An especial thanks to **Sachindra, Laura** and **Nello** for all the nice memories, you were my closer friends during my PhD. I am happy that I have met you and spent good, funny, sad and stressful moments. All the best years of my doctorate were next to you guys. Now all of us are on the other side!

Another big thanks to **Daniel** not only for his help in the laboratory and feedback but more important for all the memorable moments that we shared, this made my PhD life easier and now I can say: I survived the Snap!

Another super thanks to **Jenny** for her friendship over these years, for all the help in the laboratory and the support. I also would like to thank all former and current lab mates, especially to **Nathalie, Huizi, Sunee, Juliane, Tamara, James, Marlene, Lionel, Ke** and **Ze**; for all the nice moments I have shared with you guys.

The biggest thanks for my parents and my sisters for all their love and support over this time, no matter the distance or the time difference, you were always there for me. Muchas gracias por todo, los amo. And last but not least, I will always be grateful for having **Luis** next to me during all these years, he is my best friend, best colleague and best boyfriend that I could ever imagine. Thank you for everything.

My deepest gratitude goes to each of you.